Microgravity Compatible Reagentless Instrumentation for Detection of Dissolved Organic Acids and Alcohols in Potable Water.

Final Report

James R. Akse, Ph. D.
Principle Investigator

April 2002

Advanced Human Support Technology Program:
Advanced Environmental Monitoring and Control
Grant Number: NAG9-1081

Submitted to:

Darrell L. Jan, Ph. D.
Advanced Environmental Monitoring and Control Manager
Jet Propulsion Laboratory
M/S 180-604
4800 Oak Grove Drive
Pasadena, CA 91109-8099

TABLE OF CONTENTS

LIST OF FIGURES

LIST OF TABLES

PROJECT SUMMARY

The Organic Acid and Alcohol Monitor (OAAM) program has resulted in the successful development of a computer controlled prototype analyzer capable of accurately determining aqueous organic acids and primary alcohol concentrations over a large dynamic range with high sensitivity. Formic, acetic, and propionic acid were accurately determined at concentrations as low as 5 to 10 μg/L in under 20 minutes, or as high as 10 to 20 mg/L in under 30 minutes. Methanol, ethanol, and propanol were determined at concentrations as low as 20 to 100 μg/L, or as high as 10 mg/L in under 30 minutes. Importantly for space based application, the OAAM requires no reagents or hazardous chemicals to perform these analyses needing only power, water, and CO_2 free purge gas. The OAAM utilized two membrane processes to segregate organic acids from interfering ions. The organic acid concentration was then determined based upon the conductiometric signal. Separation of individual organic acids was accomplished using a chromatographic column. Alcohols are determined in a similar manner after conversion to organic acids by sequential biocatalytic and catalytic oxidation steps. The OAAM was designed to allow the early diagnosis of under performing or failing sub-systems within the Water Recovery System (WRS) baselined for the International Space Station (ISS). To achieve this goal, several new technologies were developed over the course of the OAAM program.

The new technologies developed during this program included; 1) a Solid Phase Acidification Module (SPAM) based upon sequential layers of $CaSO_4$ granules and strong acid ion exchange resin beads in the hydrogen ion form capable of lowering the pH of a flowing water stream to less than 1.75; 2) a counter-flow, polydimethylsiloxane membrane based CO_2 Degassing Module (CDM) capable of rapidly separating carbon dioxide from an acidified solution containing volatile organic acids without loss of organic acids; 3) an efficient microporous polypropylene membrane based Organic Acid Transfer Module (OATM) capable of rapidly transfering volatile organic acids from an acidified carrier stream to a deionized water analytical stream; 4) a bed containing robust and highly active alcohol oxidase immobilized on a diatomaceous earth support for the conversion of primary organic acids to the corresponding aldehyde at ambient temperature without retention of the aldehyde product, and; 5) an ambient temperature noble metal catalyst supported on a novel mesocellular foam (MCF) carrier capable of oxidizing aldehydes to organic acids without retention of organic acids. The OAAM was configured as a Flow Injection Analyzer (FIA) using these basic components. Software programs which control pump speeds, acquire data, and analyze data were interfaced with the OAAM to view, store, and analyze data for the determination of organic acid and alcohol concentrations in water.

The computer controlled, prototype OAAM developed during this program is capable of rapidly determing alcohols and organic acids in water with great sensitivity and a wide dynamic range. The attributes of this enabling technology fit well with a potential role as an analytical instrument that will characterize sub-system performance in the WRS that has been baselined for the ISS. Full development of this technology will allow a real time evaluation of WRS performance and the diagnosis of incipient and evident sub-system malfunctions. This technology also has the potential for expansion to other analytes of interest including nitrate, nitrite, and ammonia with minor modification of the basic components. The results from the OAAM development program have been reported in *Life Support and Biosphere Science*.[36] In addition, a synopsis of the operation principles used by the OAAM as well as some analytical results is presented on the UMPQUA Research Company webpage at http://www.urc.cc/oam.htm.

1.0 INTRODUCTION.

The 'reagentless' microgravity compatible organic acid and alcohol monitor for the determination of these contaminants at various points in the Water Recovery System (WRS) aboard the International Space Station (ISS) was developed to insure potable water quality by allowing better process control and providing diagnostic data useful for the identification of potential problems. An overview of the significance of organic acids and alcohols in the reclamation of waste water as well as the Organic Acid and Alcohol Monitor (OAAM) operation principles are summarized below to facilitate the description of the achievements during the third year of this program.

Organic acids and alcohols occur in humidity condensate, urine distillate, and composite waste waters, which consitute a significant fraction of all contaminated water streams aboard spacecraft such as ISS.[1-4] The WRS that is designed to produce potable water from such waste waters is shown schematically in Figure 1.[5,6] The WRS removes contaminant species using a combination of processes. Ionic contaminants such as organic acids and inorganic salts are removed by ion exchange (IX), while the majority of organic species are removed by sorption media within the multifiltration (MF) subsystem. Highly polar, low molecular weight organic contaminants such as alcohols are not efficiently removed by MF, and therefore, must be catalytically oxidized in the Volatile Removal Assembly (VRA).[7-11] Oxidation of alcohols forms organic acids which are removed by a post-treatment IX bed. The concentration of organic acids and alcohols at the outlets to MF, VRA, and post-treatment IX beds indicates process effectiveness at elimination or conversion of the corresponding contaminant fraction. The ability to quantify alcohols and organic acids at various points within the WRS will provide a means for verification of proper operation of MF, VRA, or post-treatment IX processes and for diagnoses of developing problems.

Currently, the only WRS on-line sensor determines conductivity, which provides limited diagnostic information with which to trace sub-system failures or potential problems. The ability to accurately quantify both organic acids and alcohols significantly enhances and refines such capabilities. For example, the initial MF process is expected to eliminate all ionic and most organic contaminants. Detection of organic acids at the MF outlet, strongly indicates failure of the IX components within the MF train. At the same time, alcohols will be present at a concentration that depends on alcohol generation and useage rates within the spacecraft. The VRA oxidizes these alcohols and other low molecular weight, highly polar organics. The chief oxidation by-products are organic acids and carbon dioxide. Consequently, the presence of alcohols

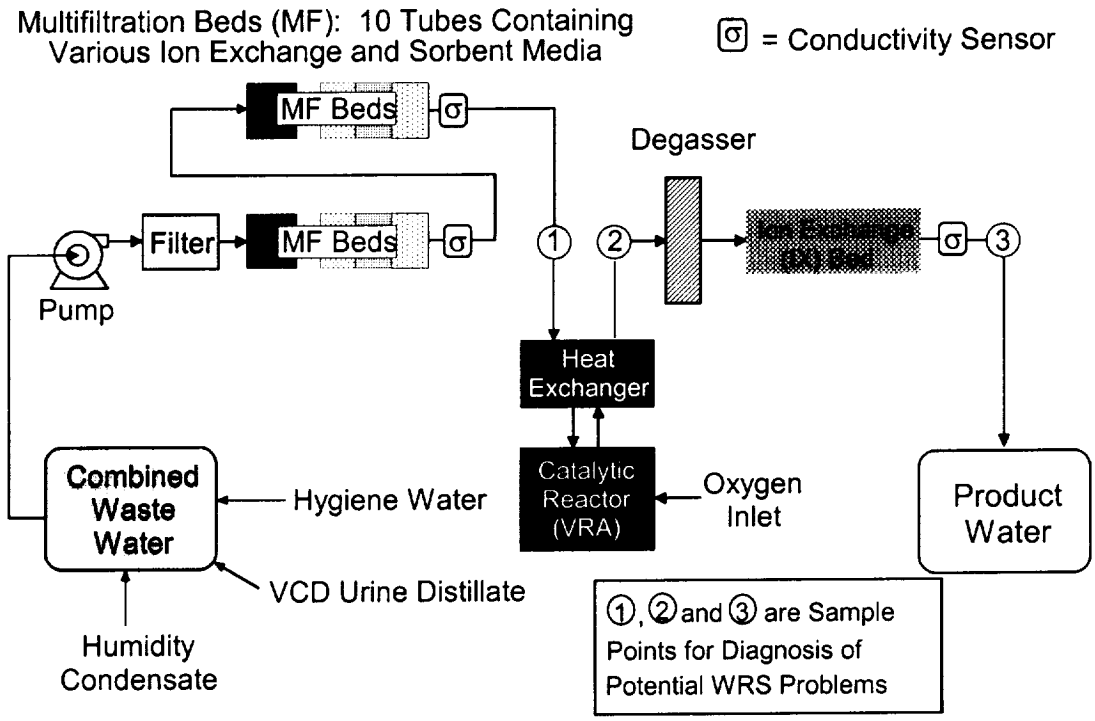

Figure 1. International Space Station Water Recovery System (WRS) Schematic.

at the VRA outlet indicates less than optimal oxidation conditions within the VRA. If organic acids are not detected at the VRA outlet, then either the VRA catalyst or oxygen supply has failed. The detection of organic acids confirms proper VRA operation. The post-treatment IX beds remove organic acids from the VRA effluent. If organic acids are present at the WRS outlet, then the post-treatment IX beds have failed. In short, the addition of organic acid and alcohol analytical capability provides an essential tool for rapid on-line diagnosis of water processor problems. Response to such problems as they become evident will facilitate maintenance of each process and result in the production of high quality potable water.

A schematic of the OAAM is shown in Figure 2. The prototype OAAM is configured as a flow injection analyzer (FIA). A stopped flow version of the OAAM was also tested during the program. Although the stopped flow version provided lower detection limits, a number of factors favored the FIA design. These included a faster response, a nearly equivalent sensitivity, ease of use, and design flexibility. Only power, water, carbon dioxide free purge gas, and solid phase reagent producing beds are required to operate the OAAM, which minimizes storage and handling of hazardous

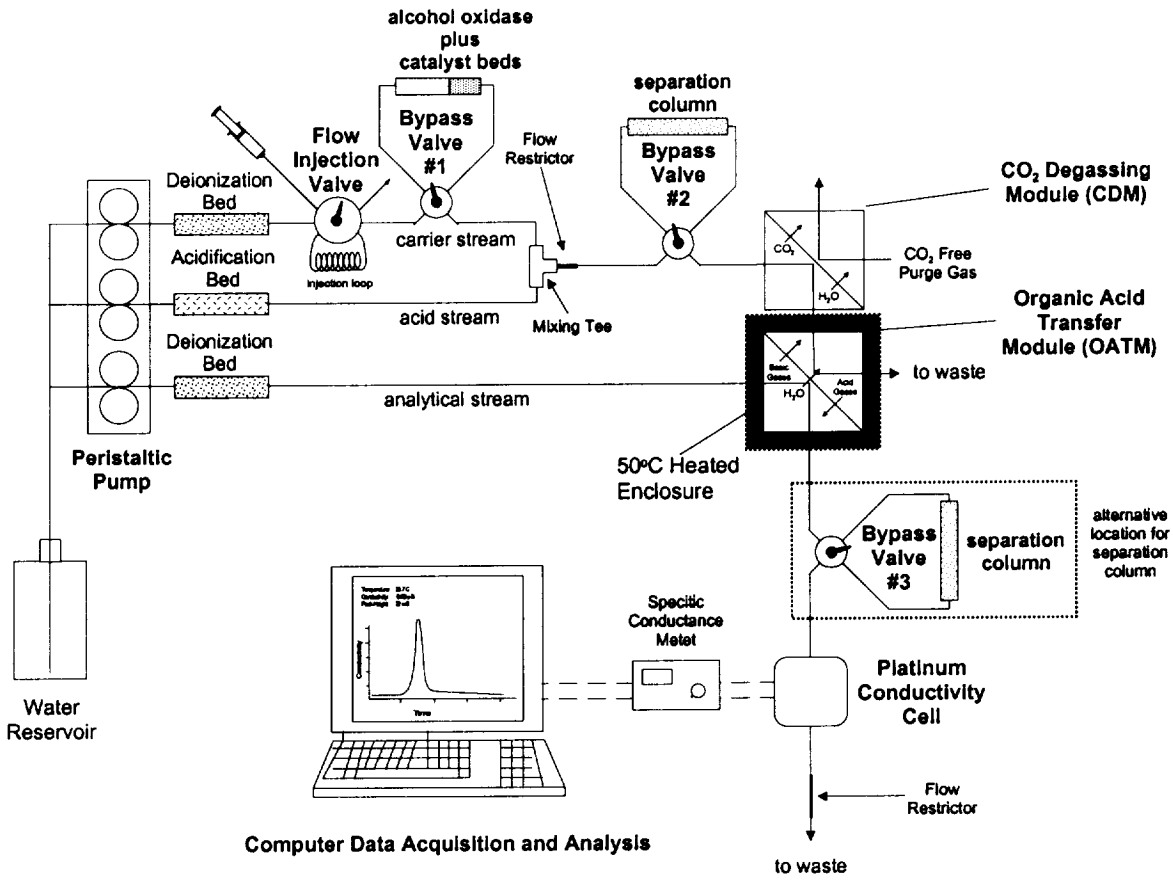

Figure 2. Organic Acid and Alcohol Monitor (OAAM) Schematic.

reagents, eliminates reagent preparation and replacement, and reduces the expenditure of valuable astronaut time to performance of the immediate analysis only. Water is withdrawn from a selected sample port within the WRS either manually or by an automated sampling device. The 1 mL injection loop of the OAAM is then filled with sample, the flow injection valve is actuated, and a plug of sample enters the carrier stream. This plug is carried into the mixing Tee where it is acidified with an equal volume from the acid stream. The acid stream was created by flowing water through a Solid Phase Acidification Module (SPAM). The SPAM contains a bed of $CaSO_4$ particles followed by a bed of strong acid ion exchange (IX) resin in the hydrogen ion form. The dissolution of $CaSO_4$ produces Ca^{2+} and $SO_4^{=}$ ions. When this solution passes through the IX bed, each Ca^{2+} ion is exchanged for two H^+ ions and a dilute sulfuric acid solution is generated with a pH of 1.60 to 1.75.[12-14] Mixing of the acid and carrier streams lowers the pH and protonates acid gas species causing them to volatilize. In the sample, these acid gases include the chief interferant, CO_2, and organic acids. As the acidified sample plug passes through the CO_2 Degassing Module

(CDM), CO_2 is selectively removed by a flow of CO_2 free N_2 gas. The degassed sample plug then passes into the Organic Acid Transfer Module (OATM). In the OATM, volatile organic acids diffuse across the OATM membrane into the deionized analytical stream. Due to the pH gradient between the analytical and carrier streams, the analytical stream acts as an organic acid sink. In the analytical stream, organic acids dissociate and cause the conductivity to increase. This solution then passes through the conductivity detector which determines the solution's specific conductance. The quadratic relationship between organic acid concentration and the specfic conductance corresponds to the equilibrium speciation of organic acids as a function of pH.

To determine the concentration of each organic acid in a mixture, they must be chromatically separated prior to detection. Two choices exist for the position of the separation column. In the first, the carrier stream is directed at bypass valve #2 into a separation column immediatedly after the mixing Tee. In this position, organic acids are chromatically separated using the acidified solution as the eluent. Alternatively, the separation column is placed in the analytical stream immediately downstream of the OATM. In this position, organic acids are chrmatically separated using water as the eluent.

For alcohols, the sample plug is initially directed through bypass valve #1 to flow through an immobilized alcohol oxidase bed. This enzyme converts alcohols to the corresponding aldehyde. Immediately downstream from the enzyme bed, a catalyst bed converts any aldehyde to the corresponding organic acid.[15-17] After the conversion of an alcohol to an organic acid has been completed, the sample plug flow path is identical to that of an organic acid analysis and the specific conductance response is utilized to quantitate the alcohol concentration.

During the first year of the program, the first OAAM was assembled and tested. Both CDM and OATM were optimized to improve transfer of carbon dioxide and organic acids, respectively. A new SPAM was developed capable of a lower achievable pH between 1.60 and 1.75, allowing better transfer of organic acids. Detection limits of 0.125 mg/L for formic acid and 1.0 mg/L for acetic acid were demonstrated with a predictable conductiometric response over a wide concentration range up to 40 mg/L for both contaminants. This early version of the OAAM utilized a flow injection configuration with a response time of 10 minutes.

During the second year, a stopped flow variation of the OAAM was constructed utilizing the optimized CDM and OATM that were developed during the first year. Using

these components the OAAM was capable of determining formic, acetic, and propionic acids at concentrations between 0.005 and 40 mg/L (i.e., 5 ppb to 40 ppm) in less than 20 minutes. The limits of detection were between 0.001 to 0.003 mg/L (i.e., 1 to 3 ppb). Chromatographic separation of individual organic acids in mixtures at much higher concentrations was demonstrated. Alcohol oxidase immobilized on diatomaceous earth successfully oxidized methanol, ethanol, and n-propanol to the corresponding aldehyde. Subsequent oxidation of aldehydes to organic acids over platinum catalysts supported on zirconia and alumina was demonstrated; however, adsorption of organic acids by the catalyst support degraded sensitivity and time response. Software was also developed to digitize and store conductivity data, allowing analyte concentrations to be determined from the stopped flow peak height. These results were disseminated at the AEMC PI meeting, the 4th *Life Support and Biosphere Scence Conference*, the *Bioastronautics Investigators' Workshop*, and on our Web site at http://www.umpqua-research.com/oam.htm.

During the third year, a FIA configuration for the OAAM was developed which allowed rapid and consistent data aquisition. In particular, the time required to reduce background conductivity in the new OAAM configuration was reduced and simplified by continuously flowing both carrier and analytical streams, and eliminating switching valves. The sensitive quatitation of alcohols was accomplished with the development of platinum catalysts supported on mesoporous silica. The open mesoporous structure of these catalysts results in a high surface area and oxidation activity as well as a surface charge that precludes strong adsorption of organic acids at intermediate pH values. These catalysts quantitatively converted aldehydes to organic acids without significant adsorption or memory effects. The determination of individual organic acids within a matrix using conductiometric detection was a significant challenge, which centered around the ability to chromatographically separate these species on a packed column using water as the eluent. Separation of formic, acetic, and propionic acids was accomplished using a HPLC column at concentrations above 200 μg/L; however, as the concentration decreased further, the peaks associated with each acid tended to coalesce. This version of the FIA OAAM was capable of quantifying formic, acetic, and propionic acid concentrations individually between 5 μg/L and 10 μg/L (ppb), and methanol, ethanol, and isopropanol concentrations between 20 μg/L (ppb) and 100 μg/L (ppb). The time for each analysis depends on concentration, with the lowest concentrations requiring ~30 minutes.

The prototype OAAM is configured as an analyzer capable of evaluating WRS sub-system performance and diagnosing potential problems. The attributes of this technology for ISS operation include: 1) the capability to quantitate contaminants that characterize operational performance of major WRS sub-systems; 2) the elimination of hazardous reagents through the use of solid phase acidification; 3) minimization of reagent preparation time through the use of solid phase reagents and catalytic processes; 4) low dection limits and wide dynamic range; 5) rapid time response, and; 6) a high potential for expanding the list of analytes using many of the basic components.[18,19]

2.0 MATERIALS AND EQUIPMENT

2.1 Chemicals.

Formic acid, acetic acid, propionic acid, drierite, alginic acid, proprionaldehyde, hydrogen hexachloroplatinate(IV) ($H_2PtCl_6 \cdot xH_2O$), alcohol oxidase, cyanogen bromide activated Sepharose 4B, tungsten trioxide,and molybdenum trioxide were purchased from Sigma-Aldrich (Milwaukee, WI). Ethanol, methanol, and 1-propanol were purchased from VWR Scientific Products (Seattle, WA).

2.2 Materials.

Celgard X10 400 microporous polypropylene hollow fibers were obtained from Hoechst Celanese (Charlotte, NC). KPF 360A-12 and 190M microporous polypropylene hollow fibers were obtained from Mitsubishi Rayon (New York, NY). Silastic tubing was purchased from VWR (Seattle, WA). Polyether Ether Ketone (PEEK) fittings, ferrules, tubing, bypass valves, and flow injection valves were purchased from Upchurch Scientific (Oak Harbor, WA). The Chromalox 2110 temperature controller was obtained from Valin Inc. (Bellevue, WA). Thermocouples were acquired from Omega Engineering Inc. (Stamford, CT). A 35.3 W, silicone coated, adhesive backed, circular heating element was purchased from McMaster-Carr (Los Angeles, CA) The Masterflex Console Drive peristaltic pump, 06485-13 peristatic pump tubing, gas flowmeter (No. 23-19), and Model 1054 conductivity bridge were purchased from Cole Parmer (Vernon Hills, IL). A Model 515 conductivity cell was purchased from Amber Science (Eugene, OR). PTFE (Teflon®) tubing was purchased from Jensen Inert Products (Miami FL). Strong acid, IRN-77, and mixed ion exchange IRN-150 resins were purchased from Rohm and Haas.(Philadelphia, PA). High surface area ZrO_2 (XZ 16075 and XZ 16052 at 51 and 90 m^2/g respectively), TiO_2 (XT 25384 and XT 25376 at 37 and 150 m^2/g, respectively), and SiO_2 (XS 16080 at 144 m^2/g) catalyst supports were purchased from Norton Chemical Process Products Corporation (Akron, OH). Celite 560 diatomaceous earth was obtained from Manville Specialty Products Group (Denver, CO). High surface area Al_2O_3 supports, spherical samples KA 275 and K 210, were donated by Condea Chemie (Houston, TX). CARiACT Q-6 silica gel was obtained from Fuji Silysia Chemical Ltd. (Portland, OR). PEEK end fittings 7.5 mm PEEK columns (100 and 150 mm) and 4.6 mm PEEK lined stainless steel columns were purchased from Alltech (Deerfield, IL). Silicone filled silicone epoxy (RTV630A) was purchased from GE Silicone (Wterford, NY). Activated carbon 580-26

was purchased from Barnebey Sutcliffe Corporation (Columbus, OH). Platinum tubing was obtained fom Goodfellow (Berwyn, PA). Teflon® and nylon unions and ferrules were purchased from Eugene Valve and Fitting (Eugene, OR). The fast fruit juice HPLC column (Part Number 10639) was obtained from Waters Chromatography Division (Milford, MA).

2.3 Analytical Equipment.

Aqueous concentrations of methanol, ethanol, propanol, formaldehyde, acetaldehyde, and propionaldehyde were detemined using an HP Model 5710A Gas Chromatograph with an FID detector and an SP1000 column The platinic acid concentration in solution was monitored using an HP 8452A diode array spectrophotometer. TOC determinations were made using an OI Analytical Model 1010 Wet Oxidation Total Organic Carbon (TOC) Analyzer.

2.4 Computer Hardware and Software.

LabVIEW™ software was purchased from National Instruments (Austin, TX). Analogue to digital I/O boards were obtained from Access I/O Products Inc. (San Diego, CA).

3.0 EXPERIMENTAL SECTION

3.1 Solid Phase Acidification Module (SPAM).

Reproducible acidification of organic acid containing samples is a fundamental process in the sequence of steps that separates interfering acid gases such as carbon dioxide from the sample, and then transfers the organic acids to a low conductivity analytical stream to eliminate background conductivity and matrix effects. The attributes of in-line beds containing solid phase media include simplicity, ease of use, and the elimination of corrosive liquid reagents. The first solid phase media investigated was molybdenum trioxide, MoO_3, which dissolves according to (1), forming a weak diprotic acid which releases hydrogen ions via a two step dissociation.

$$MoO_3 + H_2O \rightarrow H_2MoO_4 \qquad (1)$$

In deionized water, an equilibrium pH of 2.5 is attained; however, in flow-through beds pH values between 3 and 3.2 are achieved. As indicated by the dissociation equilibria and pK_a values shown in (2) through (5) for formic acid, acetic acid, propionic, and carbonic acids, respectively, at this pH, most of the common volatile organic acids will exist predominately in the volatile undissociated form at a pH obetween 3 and 3.2, allowing transfer across the microporous membrane in the organic acid transfer module

$$HCO_2^- + H^+ \xleftrightarrow{K_1} HCO_2H(g)\uparrow \qquad pK_1 = 3.75 \qquad (2)$$

$$CH_3CO_2^- + H^+ \xleftrightarrow{K_2} CH_3CO_2H(g)\uparrow \qquad pK_2 = 4.75 \qquad (3)$$

$$CH_3CH_2CO_2^- + H^+ \xleftrightarrow{K_3} CH_3CH_2CO_2H(g)\uparrow \qquad pK_3 = 4.87 \qquad (4)$$

$$H^+ + HCO_3^- \xleftrightarrow{K_4} CO_2(g)\uparrow + H_2O \qquad pK_4 = 6.37 \qquad (5)$$

(OATM). However since the pH due to solid phase media such as MoO_3 is unbuffered, the transfer efficiency across the OATM for all organic acids over a range of concentrations would benefit from a lower initial pH value. By lowering the initial pH, the pH is less affected by the loss of protons due to recombination with the organic acid anion and subsequent volatilization of the organic acid.

Several possible avenues to achieve a lower pH in SPAM effluents were investigated, including: improving the MoO_3 media, utilizing other solid phase media, and using a combination of solid phase media and ion exchange (IX) resins. Although

increased contact times would minimize the pH from the MoO_3 media, very long contact times were required to reach equilibrium pH values in practice. As an alternative, non-stoichiometric MoO_{3-x} was prepared to increase the dissolution rate and lower the effluent pH for shorter contact times. Second, higher surface area MoO_3, WO_3, and HBO_2 particles were encapsulated in alginate beads providing alternative acidification media and improving dissolution rates. Finally, sequential beds of a soluble divalent salt and a strong acid cation exchange resin were incorporated into a composite SPAM which utilized the higher solubility of the soluble divalent cation to exchange for hydrogen ions in the IX bed and produce a lower pH.

These attempts to improve SPAM performance were unsuccessful with one major exception. A variety of non-stoichiometric MoO_{3-x} samples were produced with x depending on thermal treatment and oxygen partial pressure. In more strongly reduced samples, solubility decreased, while in less reduced samples, solubility increased. In general, the pH values produced by these materials were equal to or higher than those of stoichiometric MoO_3. Encapsulation of MoO_3 in alginate beads was a minor success since it allowed the use of very fine MoO_3 powder within the SPAM without producing excessive backpressure. The powder was first mixed with alginic acid and then droplets of this supension were extruded through a syringe needle and allowed to fall into a solution containing divalent cations such as Ca^{2+}, Sr^{2+}, and Ba^{2+}. The droplets gelled into spherical beads as a polymeric structure formed between alginate monomers. Of the divalent cations, only beads formed with Ba^{2+} remained dimensionally stable as cations leached from the beads. Beds of this material produced higher pH values than the crystalline MoO_3 containing SPAM, most probably due to poor exchange of MoO_3 with interstitial water. The final novel SPAM media consisted of sequential beds containing a soluble divalent salt and a strong acid cation exchange resin.

This approach produced much lower pH than previous SPAM beds, since the pH depended on the solubility of the first bed which could be adjusted by selection of the appropriate salt. In the most successful modification, the first bed contained $CaSO_4$ (i.e., hydrated Drierite®) which dissolves according to (6). The solubility product for $CaSO_4$ at 25°C is also given in (6). Dissolution of this salt releases Ca^{2+} which then

$$CaSO_4 \xleftrightarrow{K_{sp}} Ca^{2+} + SO_4^{=} \qquad K_{sp} = \left[Ca^{2+}\right]\left[SO_4^{=}\right] = 2.45x10^{-5} \qquad (6)$$

enters into the strong acid cation exchange resin bed which is in the hydrogen ion form. The Ca^{2+} quantitatively displaces two H^+ ions, creating a strong acid whose concentration is dependent on the solubility of the salt. Based upon the solubility product of anydrous $CaSO_4$ at 25°C, a pH of 2.0 should be produced; however, based upon the solubility of $CaSO_4 \bullet 2H_2O$ (i.e., gypsum) a pH of 1.55 should be produced. A composite SPAM with the first bed filled with $CaSO_4$ particles between 300 to 990 μm in diameter and the second bed filled with hydrogen form strong acid cation exchange resin produced an effluent pH of 1.74. This is a significant improvement over the pH attainable using MoO_3 crystalline particles, and was adopted as the preferred SPAM for the OAAM.

3.2 CO_2 Degassing Membrane (CDM).

Following acidification, CO_2 must be removed from the sample. This is required because CO_2, as an acid gas, mimics the behavior of organic acids in the OAAM, including the formation of ionic species when dissolved in water. This potential interferant is removed using a CO_2 Degassing Module (CDM). To be successful, the CDM must remove CO_2 without affecting the concentration of organic acids in the carrier stream.

To optimize the CDM, four membranes were investigated for CO_2 clearance from a stream containing a sodium bicarbonate solution with a total inorganic carbon (TIC) concentration of 10 mg/L. The membranes included polyimide, polyester, poly-tetrafluoroethylene (PTFE), and polydimethylsiloxane (PDMS). In each case, a thin walled tube-in-shell CDM design was utilized as shown in Figure 3. Of these membranes, very low CO_2 permeation rates were found for polyester and polyimide based CDMs. The PTFE based CDM consisted of a 5 m tube with a 1067 μm inner diameter, an average membrane thickness of 52 μm, an interior volume of 4.47 mL, and a maximum diffusion distance of 500 μm. The surface area to volume ratio for this CDM was 37.5 cm^2/cm^3, which corresponds to the permeable area per unit volume of liquid within the exchange module. The PDMS based CDM utilized 3 m of polydimethylsiloxane (PDMS) membrane with a 305 μm inner diameter, an average membrane thickness of 165 μm, an inner volume of 0.22 mL, and a maximum diffusion distance of 150 μm. The shell side was constructed of FEP tubing with an inner diameter of 1588 μm and an outer diameter of 3175 μm. The end fittings used were PEEK Tees (Upchurch part number P-712) with the bores drilled out to 1,588 μm. The PDMS tubing extended through the Tee and was mechanically captured on the outside

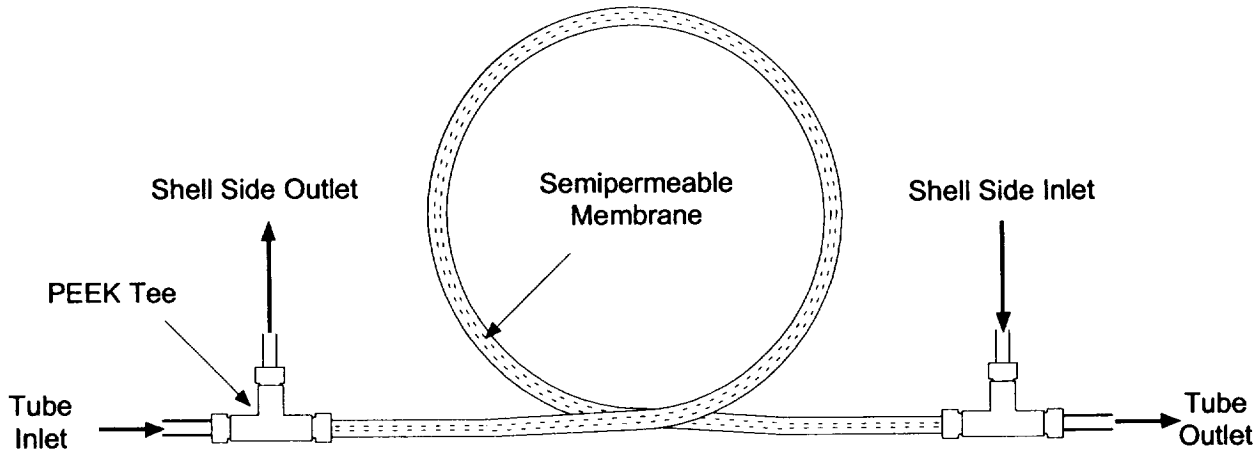

Figure 3. Tube-in-Shell Counter-Current Gas Transfer Module.

junction of the Tee with a compression fitting around the 1588 μm PTFE tubing connection. The PDMS tubing was encased in a single section of PTFE tubing that better matched the inner diameter of the PTFE tubing. A semi-rigid section of polyimide tubing 394 μm in diameter was placed within the PDMS tubing to support the PDMS elastomer when compressed. This CDM design allowed rapid assembly and effective sealing. The surface area to volume ratio in this CDM was 131.1 cm^2/cm^3.

3.3 Organic Acid Transfer Module (OATM).

The Organic Acid Transfer Module (OATM) utilizes a tube-in-shell counter-current design similar to that of the CDM. In the OATM, the analytical stream is contained within a central microporous polypropylene hollow fiber membrane, while the degassed sample flows between the microporous hollow fiber and the stainless steel shell. The 2.0 m OATM consists of a central hollow fiber membrane with outer diameter of 355 μm and an inner diameter of 300 μm. This surface porosity of this membrane varies between 45 and 50%, and the average pore size is 0.05 μm, which corresponds to a bubble point (i.e., the pressure required to force water through the membrane) of 12.1 atm (1.23 MPa). The end fittings on the OATM consist of PEEK Tees similar to those used in the CDM, except that the bores were drilled out to 1016 μ m. The microporous hollow fiber extends through the Tee and into a short section of PEEK tubing 1575 μm in diameter. This hollow fiber was potted inside this outer

section of tubing using silicone epoxy (RTV630A). The shell side is constructed of PEEK tubing with an inner diameter of 762 μm and an outer diameter of 1588 μm. The surface area to volume ratio for the OATM is 133.3 cm^2/cm^3 with an internal volume of 141 μL.

3.4 Modified Conductivity Detector.

The Model 515 flow through micro-conductivity cell was modified to reduce the background conductivity at low flows. The 1/16 inch (i.e., 1.59 mm) outside diameter stainless steel inlet and outlet tubing to the flow through cell were replaced with 2 mm outside diameter platinum tubing. The inside diameters for the stainless steel and platinum tubing were 1.1 and 1.6 mm, respectively. This modification significantly reduced the background due to stainless steel corrosion. The cell constant for the new cell was 5.19 compared to 5.73 for the stainless steel cell. This cell is shown in Figure 4. The active volume of this cell is 7 μL.

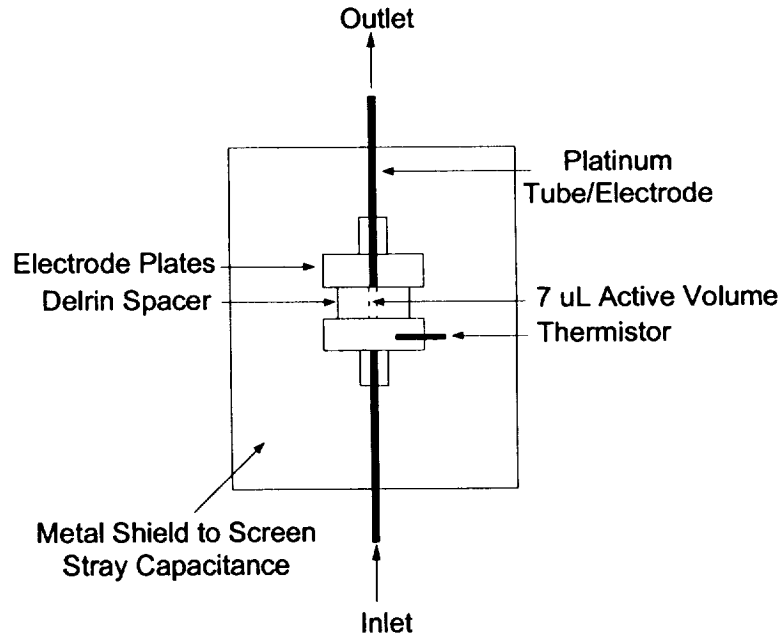

Figure 4. Modified Flow Through Model 515 Micro-Conductivity Cell.

3.5 Immobilization of Alcohol Oxidase.

The quantitation of primary alcohols such as methanol, ethanol, or 1-propanol using the OAAM requires that the alcohol must first be converted to an organic acid. This may be accomplished at ambient temperature using a two step oxidation process.

The first step utilizes an enzyme, alcohol oxidase (AO), that has been immobilized on a solid support. This enzyme catalyzes the reaction between dissolved oxygen and primary alcohols to form the corresponding aldehyde and hydrogen peroxide. In the second step, aldehydes are oxidized to the corresponding organic acid over a heterogeneous catalyst using dissolved oxygen as the oxidant. For these two processes to be successfully applied in the OAAM, the oxidation reactions must occur rapidly at ambient temperature, and the reaction by-products must be rapidly released to the carrier stream. Slow reactions or retention of the aldehyde or organic acid by-products by the immobilized enzyme or the supported catalyst will lead to peak broadening, poor sensitivity, and slow response times.

AO was immobilized onto two supports, diatomaceous earth and agarose. Diatomaceous earth is a structured natural product of diatoms which consists primarily of SiO_2 with minor amounts of clay consisting of Na, K, Mg, and Al containing silicates. Agarose is another natural product consisting of chemically modified, crosslinked polysaccharrides derived from seaweed. Different immobilization procedures were used for these two supports. For diatomaceous earth, the titanium activation procedure was used, while for agarose, a cyanogen bromide activation process was employed. In addition to oxidation rates, enzyme life and release of aldehyde and/or organic acid reaction byproducts were two issues of concern during the development of immobilized enzyme beds. The diatomaceous earth support was impregnated with platinum catalytic sites to decompose the hydrogen peroxide formed by action of the oxidase enzyme on primary alcohols.[15,17] This was intended to extend the AO enzyme life by preventing denaturing reactions with the hydrogen peroxide.

The reaction scheme for immobilization of AO on diatomaceous earth using the titanium activation procedure is shown in Figure 5.[15,17] In this procedure, surface hydroxyls are first linked to titanium chloride. To achieve this linkage, diatomaceous earth is immersed in a 15 % titanium oxychloride solution (in 10% HCl) which is then evaporated to dryness over several hours at 45°C. The titanium linked support is then washed with methanol and dried. Next, the titanium bound chlorines are reacted with ethylenediamine to create a surface coating with terminal primary amine functional groups. This is accomplished by immersion of the titanium activated diatomaceous earth in a 5 % ethylenediamine solution in carbon tetrachloride at 45°C for two hours. The diatomaceous earth is then washed with methanol and dried. The terminal amine groups provide sites for the Schiff base addition of a dialdehyde. This addition is accomplished by rolling the diatomaceous earth in a 5% glutaraldehyde solution in a pH

7.5 phosphate buffer overnight. The diatomaceous earth is then rinsed with distilled water. At this point, terminal aldehyde groups are available for a second Schiff base addition to terminal amino groups on alcohol oxidase. In the final step, 1000 EU of alcohol oxidase per gram of diatomaceous earth is dissolved in a pH 7.5 phosphate buffer, and the mixture is rolled overnight at ambient temperature.

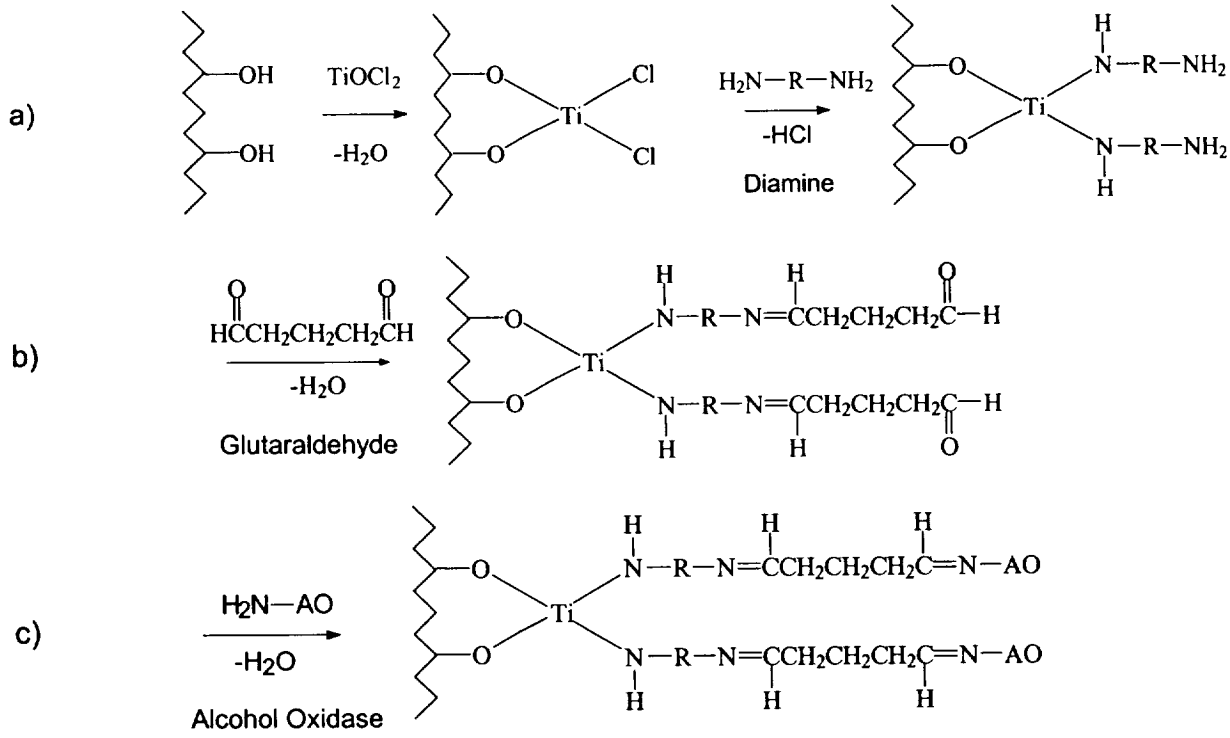

Figure 5. Titanium Activation Method for Immobilization of Alcohol Oxidase.

Alcohol oxidase was also immobilized on agarose using cyanogen bromide activation. The general procedure is shown in Figure 6. To simplify the immobilization, cyanogen bromide activated agarose beads were purchased. The cyanogen bromide activated beads were first hydrated in 10 mM HCl for 15 min at ambient temperature. They were then washed with distilled water and bicarbonate buffer (pH 8.3). One gram of the swollen beads was added to 1000 EU of alcohol oxidase in the pH 8.3 bicarbonate buffer. This mixture was placed in a test tube and rotated at 4 °C overnight. The preferred immobilization structure from Figure 6 is the substituted imidocarbonate, due to stability and the absence of residual charge; however, an isourea derivative may also form. The substituted imidocarbonate structure is promoted by the selection of reaction conditions. After rinsing the resin with buffer,

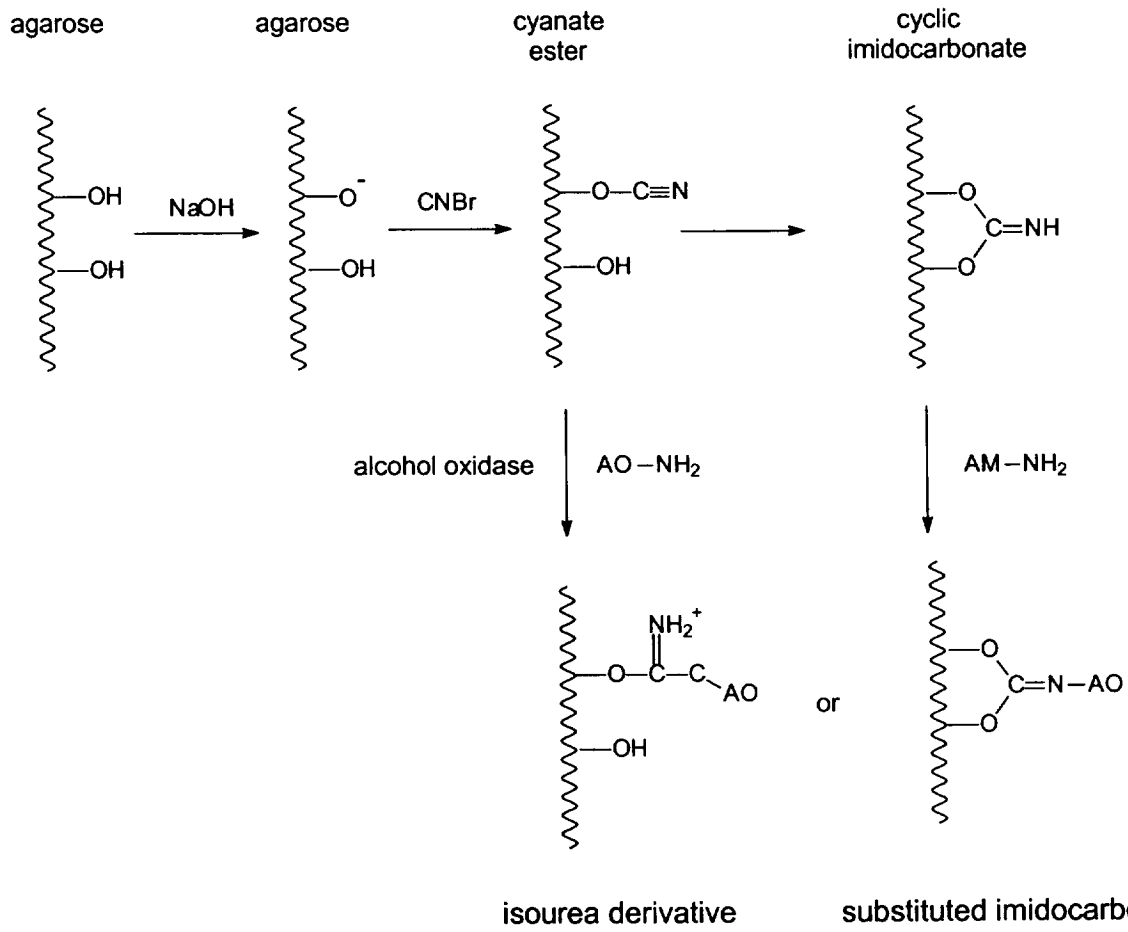

Figure 6. Immobilization of Alcohol Oxidase on Cyanogen Bromide Activated Agarose.

unreacted surface groups were blocked by adding a high concentration of ethanolamine. The mixture was agitated in a tube rotator at ambient temperature for 2 hours. This reduces multiple bonds to terminal amino groups on the enzyme. Four rinse cycles with pH 8.3 borate buffer and pH 4 acetate buffer were used to remove excess reagents.

3.6 Preparation of Improved Oxidation Catalyst Supports.

The preliminary investigation of the conductiometric response for organic acids produced from alcohol oxidation using sequential beds of alcohol oxidase immobilized on diatomaceous earth and platinum catalysts impregnated on various supports produced flow injection peaks that were broadened, and at low concentrations, spread out to the point where they were undetectable. This was attributed to organic acid

adsorption on the materials used to support the noble metal catalyst. Significantly, adsorption was traced to hydrogen bonding between the organic acid anions and the positively charged, protonated surface of the support. A brief description of the relationship between surface charge and oxide surfaces will clarify this conclusion.

3.6.1 Surface Charge and Organic Acid Adsorption.

When a solid contacts water, an electric potential difference develops at the interface due to a number of mechanisms, including the affinity of ions and electrons for the two phases, the ionization of surface groups, and the physical entrapment of non-mobile charge.[20] Associated with this electric potential difference is the development of a double layer in which surface charge is compensated by a distribution of counter ions in solution.[21-23] The electric potential that develops between charges firmly bound to the surface and ions that are free to move in solution is called the zeta potential. The zeta potential is a measureable quantity that reflects the charge that develops on a surface immersed in a solution. For oxides in aqueous solutions, the zeta potential varies strongly with pH due to protonation and deprotonation reactions with the surface. For each oxide, the zeta potential may be reduced to zero by adjustment of pH. The pH at which a zero surface charge is reached is called the isoelectric point (IEP). At a pH above the IEP, the zeta potential is negative and the surface is negatively charged. At a pH below the IEP, the zeta potential is positive and the surface is positively charged. IEP values for common oxide surfaces are shown in Table 1.[24]

A positive zeta potential will attract organic acid anions, and if the positive surface charge is due to hydrogen ions, hydrogen bonding can occur. Accordingly, a catalyst support should preferably exhibit a negative zeta potential or at the very least a neutral zeta potential at the pH of the alcohol oxidase bed effluent. Of the oxides listed in Table 1, SiO_2 will naturally repell, while Al_2O_3 will naturally attract organic acid anions at the nominal 5.8 pH downstream of the alcohol oxidase bed. The properties of oxides such as ZrO_2 or TiO_2 are less clear. Consequently, SiO_2 was the focal point of the search for a more effective catalyst support without a strong affinity for organic acids. Other properties of the ideal silica support include high surface area, porosity characterized by low pore diffusion resistance, and means to homogeneously impregnate the support surface with small, highly active noble metal catalyst nuclei.

Table 1. Isoelectric Points for Common Oxides.

Material	Isoelectric Point (IEP) pH
MgO	12.4
NiO	10-11
La_2O_3	10.4
CuO	9.5
ZnO	9
α-Al_2O_3	8-9
Cr_2O_3	7.0
CeO_2	6.7
Fe_3O_4	6.5
$3Al_2O_3 \bullet 2SiO_2$	6-8
$BaTiO_3$	5-6
TiO_2	4-6
ZrO_2	4-6
MnO_2	4.0-4.5
SiO_2 (amorphous)	2-3

3.6.2 Silica Mesocellular Foams (MCFs).

Silica Mesocellular Foams (MCFs) are a new class of sol-gel prepared materials that exhibit many of the properties expected for an ideal silica support. These include high surface area, three dimensional interconnected mesoporosity of uniform size between 20 and 30 nanometers, and high fractional porosity. Monolithic pieces of MCFs which would be suitable as a catalyst support were prepared using an adaptation of previously developed methods for the synthesis of MCF particles.[25-27] The basic approach utilized an acidic hydrolysis of tetraethyl orthosilicate (TEOS) in the presence of a surfactant and swelling agent to self-assemble into a three dimensional interconnected structure. The three dimensional surfactant - swelling agent structure serves as template for the sol-gel formation of the silica network that forms the MCF. The non-ionic surfactant is an amphiphilic block copolymer (i.e., P123 or EO_{20}-PO_{70}-EO_{20} where EO = ethylene oxide and PO = propylene oxide) that contains hydrophilic (i.e., poly(ethylene oxide) blocks) and hydrophobic regions (i.e., poly(propylene oxide) blocks). The swelling agent, 1,3,5-trimethyl benzene (TMB), is attracted to the poly(propylene oxide) regions of the surfactant, initially forming an oil-in-water microemulsion and effectively increasing the size of the hydrophobic region. When mixed together at the appropriate temperature, TMB, P123, and acidified water will self-

assemble into a three dimensional interconnected structure.[28,29] Water surrounds these cores and fills the interconnected channels with the phase assembly representing the thermodynamically most favorable structure for each composition and temperature.

The preparation of an MCF begins with the dissolution of P123 in an HCl solution at room temperature. TMB is then added under vigorous magnetic stirring until a homogeneous, opalescent microemulsion is formed. The solution is heated to 37 - 40 ° C and stirred for an additional 30 minutes. TEOS is added to the microemulsion with continuous stirring at temperatures between 35° and 60°C. This begins the TEOS hydrolysis process shown in (7). First a sol is formed, and as the silica network grows,

$$nSi(OCH_2CH_3)_4 + 2nH_2O \rightarrow nSiO_2 + 4nCH_3CH_2OH \qquad (7).$$

eventually the viscosity increases and a gel is formed. The newly formed colloidal sols are amorphous and protonated under acidic conditions.[30-33] Due to the amphiphilic surfactant, the positively charged silica sol preferentially associates with the hydrophilic EO outward facing component of the microemulsion.[28-31] A continuous network of silicon oxygen bonds begins to cover the three dimensional surfactant - swelling agent structure. The silica network continues to expand and intergrow, forming a three dimensional structure surrounding the surfactant - swelling agent structure. This surfactant structure will eventually form the pores and interconnected channels in the MCF. After 20 hours at the lower temperatue, the mixture is heated to 80°-120°C and aged for an additional 20 hours in an autoclave. The silica network is incompletely formed at the lower temperature, and by raising the temperature additional interconnections are made and the network matures. At the same time, the size of the hydrophobic surfactant - swelling agent cores increase due to interfacial tension.[30] The combination of silica network maturation and swelling cores leads to larger pores. The overall process results in well formed MCF with large pores. By a combination of network expansion and intergrowth, larger MCF aggregates form.

In the synthesis procedure described in the literature for the preparation of MCF particles, 4.4 g of TEOS was added to the structured mixture of P123, TMB, and acidified water which was then stirred for 20 hours at 37 - 40°C. Under these conditions, MCF particles and aggregated particles are formed; however, these are limited in size due to the availability of reactants and the concentration of surfactant and swelling agent (i.e., TMB). To prepare a continuous monolithic intergrown MCF structure, the concentration of the three major components, P123, TMB, and TEOS

must be sufficient to allow continuous intergrowth of MCF islands. In the standard monolithic MCF formulation, 6 g of P123 and 6 g of TMB were added to 75 mL of 1.6 M HCl. As in the formation of individual MCF particles, this solution was heated to 37 - 40 °C for 30 minutes and then 13.2 g of TEOS was added. This solution was mixed for 5 to 60 minutes and then allow to sit undisturbed, which promotes the formation of a continuous gel. This gel was then autoclaved at temperatures between 115 and 120°C for an additional 20 hours to mature the MCF. The green MCF contains entrained P123 and TMB. Some of this is removed by washing with deionized water. The green MCF is dried at 50°C. Some shrinkage occurs during drying, resulting in the formation of cracks within the monolith. This is minimized by slow drying and lower temperatures. These pieces were then heated in air to temperatures between 450 and 700°C to remove P123 and TMB, and consolidate the silica network. Temperatures in excess of 500°C resulted in white, char free monolithic SiO_2 pieces. These pieces exhibited very low density and were almost translucent in appearance.

A range of compositions and initial synthesis temperatures were evaluated following the same general preparation scheme. The compositional variables included the P123 to TMB ratio, the concentration of P123 and TMB, the relative amount of TEOS, and the presence of ammonium fluoride, NH_4F. The use of ammonium fluoride is designed to promote maturation of the silica network, since it increases silica solubility. The use of ammonium fluoride generally produced more readily gelled and mechanically strong MCFs. Two compositions were selected for catalyst preparation. The first preparation utilized 6 g of P123, 6 g of TMB, and 13.2 g of TEOS processed at 37°-40°C for 20 hours, and then at 115°C for 20 hours. The second preparation utilized 12 g of P123, 12 g of TMB, 26.4 g of TEOS, and 0.023 g of NH_4F processed at 37°-40° C for 20 hours, and then at 115°C for 20 hours.

3.7 Preparation of Oxidation Catalysts on MCF Supports.

Selected MCFs were impregnated with platinum salts in solutions designed to utilize the MCF surface charge to promote homogeneous adsorption of the noble metal species. Initial investigations utilized 2.0% platinum by weight of the support. The surface charge of silica as a function of pH is shown in Figure 7. These data show that below a pH of ~2.4 the surface of silica becomes positively charged due to protonated surface sites. Above this pH, the surface becomes progressively more negatively charged until all surface sites become deprotonated. At a pH of 2.4, the isoelectric point, the surface becomes uncharged. The surface charge strongly influences

adsorption of the platinum ionic species, $PtCl_6^{-2}$. Since it is a weak acid, a platinic acid solution will have a pH close to the isoelectric point for amorphous silica, and platinum will not strongly adsorb. One can acidify this solution; however, changes in the ionic strength resulting from the introduction of chloride, sulfate, or nitrate counter-ions will change the isoelectric point, and hence, will affect the adsorption of the hexachloroplatinate anion.

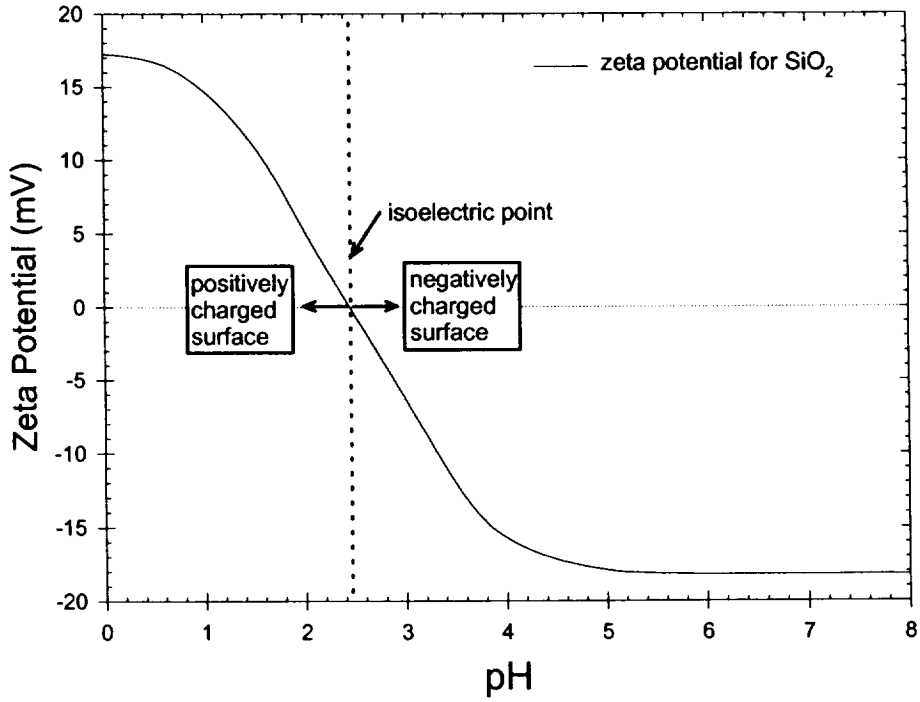

Figure 7. Zeta Potential for Amorphous Silica.

A successful approach to improve surface adsorption involved the addition of hydrogen hexachloroplatinate ($H_2PtCl_6 \cdot xH_2O$) to a 0.1 M ethylenediamine solution. Ethylenediamine, $H_2N(CH_2)_2NH_2$, is a strongly alkaline diamine which in an aqueous solution will form a monoprotonated, $H_2N(CH_2)_2NH_3^+$, or diprotonated amine, $^+H_3N(CH_2)_2NH_3^+$, depending on concentration. The pK_{a1} and pK_{a2} for ethylenediamine are 10.71 and 7.56, respectively, meaning that at a pH of 10.71 an equal concentration of unprotenated and monoprotenated ethylenediamine species exist, while at a pH of 7.56, an equal concentration of diprotonated and monoprotonated ethylenediamine species exist as shown in (8) and (9).

$$H_2N(CH_2)_2NH_3^+ \leftrightarrow H_2N(CH_2)_2NH_2 + H^+ \qquad K_{a1} = \frac{[H_2N(CH_2)_2NH_2][H^+]}{[H_2N(CH_2)_2NH_3^+]} = 10^{-10.71} \qquad (8)$$

$$^+H_3N(CH_2)_2NH_3^+ \leftrightarrow H_2N(CH_2)_2NH_3^+ + H^+ \qquad K_{a2} = \frac{[H_2N(CH_2)_2NH_3^+][H^+]}{[^+H_3N(CH_2)_2NH_3^+]} = 10^{-7.56} \qquad (9)$$

Since the pH of a 0.1 M ethylenediamine solution is 11, these equilibria are significant, with respect to the adsorption of platinum from this solution, in two ways. In the first place, the highly alkaline pH insures that the surface charge of amorphous silica will be strongly negative. Secondly, most of the amine will be unprotonated. Ethylenediamine (ED) is known to complex Pt(IV), forming $Pt(ED)_2Cl_2^{2+}$,[34] and since the complex is positively charged, it will be strongly sorbed by amorphous silica at this pH. MCF silicas were immersed in this solution and heated to temperatures between 50° and 110°C. These solutions quickly discolored (i.e., yellow to clear) as shown by the UV-VIS spectrum in Figure 8, indicating rapid incorporation of the platinum complex. When these amorphous silicas were fired under reducing conditions, homogeneity was retained as evidenced by uniform coloration.

3.8 Evaluation of Oxidation Catalysts Performance.

Oxidation catalysts consisting of 2 % platinum on an MCF support were evaluated using the test stand shown in Figure 9. In this arrangement, a plug flow reactor containing the catalyst bed was challenged with an aqueous stream containing propionaldehye at ambient temperature. Under controlled flow conditions, the effluent concentration of the contaminant was determined as a function of contact time by gas chromatography using an SP 1000 column, a FID detector, and a column temperature of 60°C. These data were then reported as fractional conversions.

Global oxidation rates were determined using pseudo first order plug flow kinetics. This model provided a practical approach for gathering and comparing catalysts without detailed knowledge of the reaction mechanism. Since the oxidation of propionaldehyde involves dissolved oxygen and propionaldehyde, the presence of a large oxygen excess eliminates the O_2(aq) concentration term from the rate expression given by,

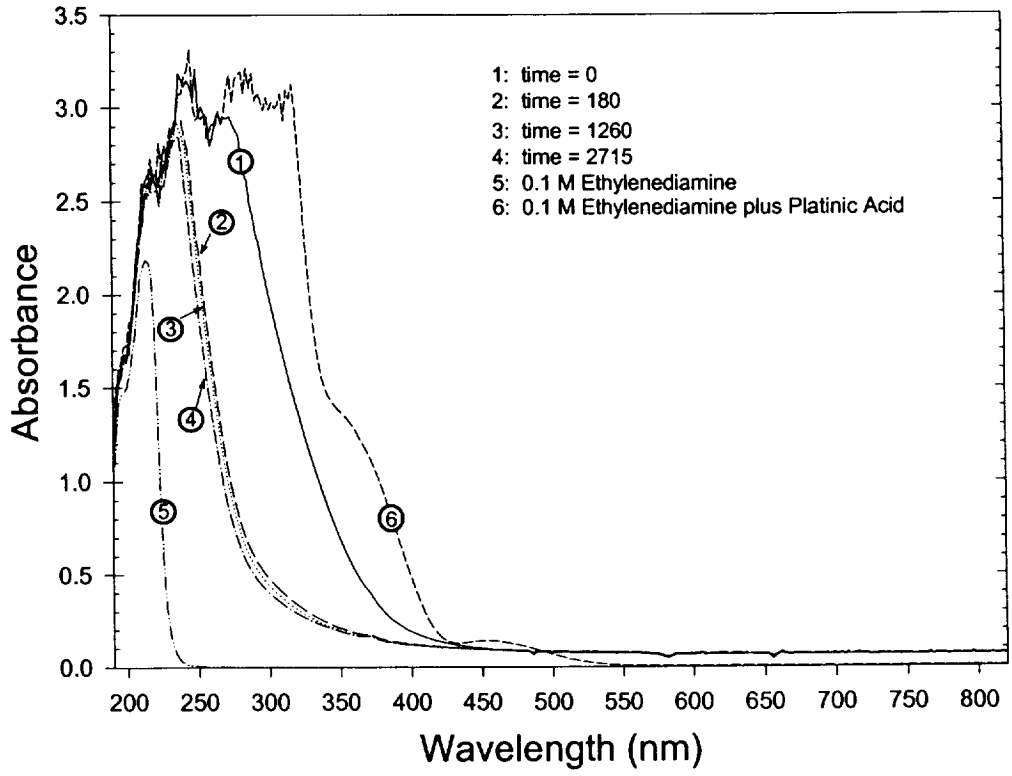

Figure 8. UV-VIS Spectra from Ethylenediamine Solution Containing Platinic Acid.

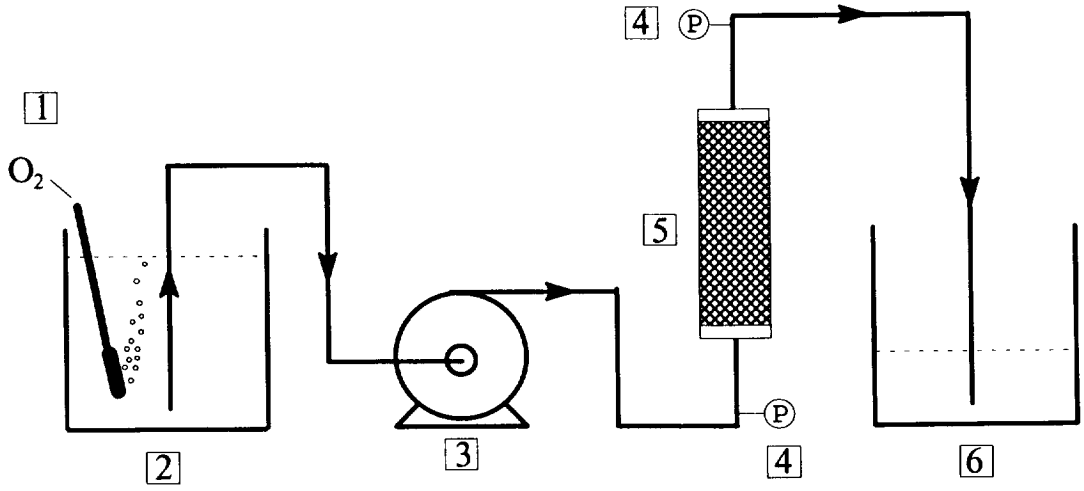

Figure 9. Flow Test Apparatus: 1- Oxygen Sparger, 2- Influent Reservoir, 3- Pump, 4- Pressure Transducers, 5- Plug Flow Catalyst Bed, and 6- Effluent Reservoir.

$$\frac{dC}{dt} = kC_{O_2}C_A \qquad (10).$$

Since the O_2(aq) concentration term is constant, it is incorporated into the rate constant and following integration the pseudo first order dependency shown in (11) results,

$$C = C_o e^{-kt} \qquad (11),$$

where C is the outlet organic contaminant concentration, C_o is the inlet organic contaminant concentration, k is the pseudo first order reaction rate constant in s^{-1}, and t is the residence time within the reactor (i.e., reactor space time). The value of t depends on the void volume, V_r,, within the catalyst bed, and the flow rate, Q. The reactor space-time, t, is determined according to (12),

$$t = \frac{V_r \phi}{Q} \qquad (12),$$

where ϕ is the fractional void volume of the packed catalyst bed and V_r is the reactor volume. When the fractional void volume is not known, the empty bed volume is used in place of the fractional void volume and ϕ becomes 1. Plug flow conditions were validated based on flow rates, reactor length, and catalyst particle size. Rate constants (k) for the first order plug flow rate law were derived from the resulting (C, t) ordered pairs using the Levenberg-Marquardt method.[35] Correlation coefficients (r^2) for the derived rate constants were calculated using a linear regression of experimentally observed concentrations versus those calculated from (11).

3.9 Separation of Organic Acids.

The ability to separate organic acids in the analytical stream is a prerequisite for the quantitation of individual organic acids in mixtures. Preliminary work toward this end yielded positive results. A 200 mg/L mixture of formic, acetic, and propionic acids in unbuffered deionized water was fed to a column containing strong acid cation exchange resin in the hydrogen ion form. The absorbance of the effluent at 204 nm was then monitored versus time in a 1 cm path length cell. The resulting chromatogram shown in Figure 10 indicates that the three primary organic acids are separable in a low ionic strength aqueous solution using water as the mobile phase. Adjustment of the ionic strength and pH of the mobile phase by the addition of 0.1, 0.05, and 0.001 % phosporic acid had little affect on the chromotograms for individual organic acids. The mobilities roughly correlate with the relative fraction of each species that is ionized in water. Although these preliminary experiments utilized high concentrations of organic

acids due to low absorbance sensitivity, this approach indicates one method that can be utilized in future work to discriminate between organic acids in mixtures.

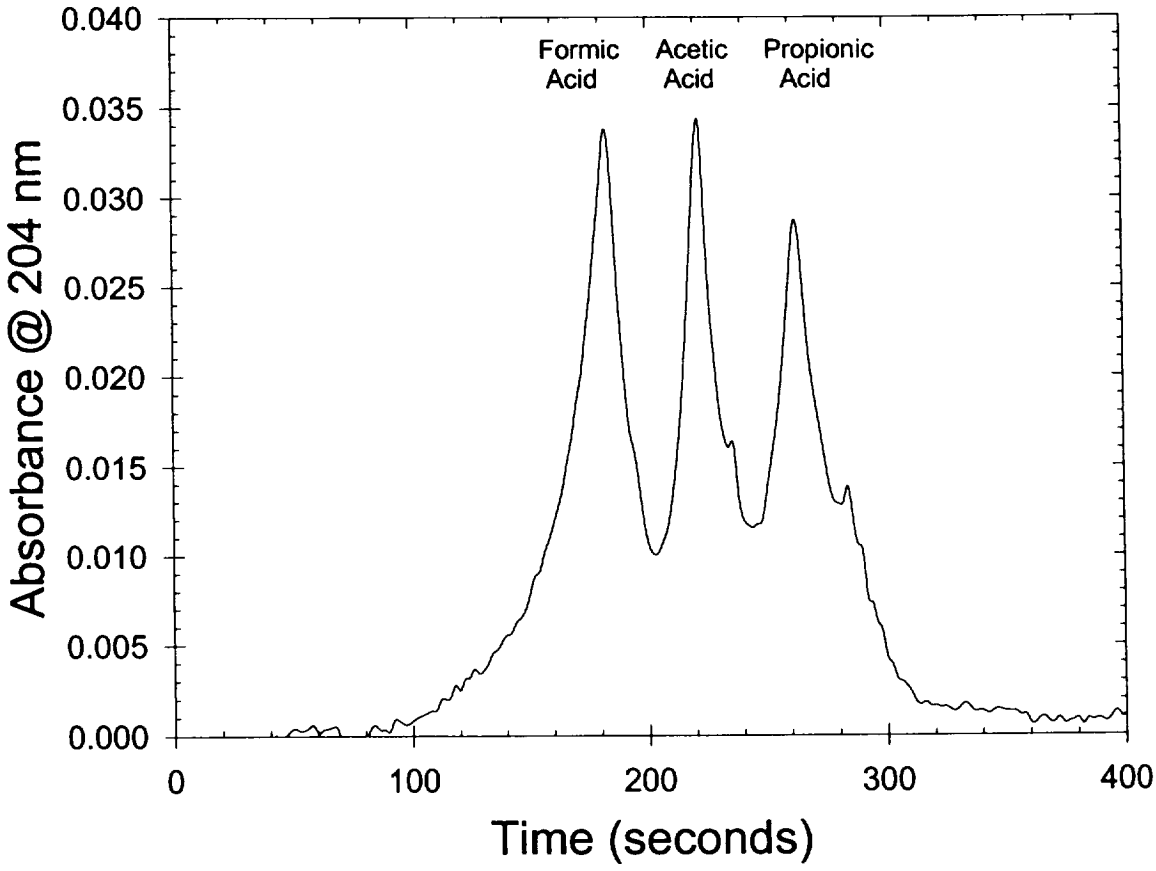

Figure 10. Separation of Organic Acids on Ion Exchange Column with Water as the Mobile Phase.

4.0 DEVELOPMENT OF OAAM COMPONENTS AND OAAM PROTOTYPE .

4.1 Solid Phase Acidification Module (SPAM) Performance.

Control of the pH in the carrier stream of the OAAM controls two vital functions, the removal of the CO_2, an acid gas which mimics the behavior of organic acids, and consequently, will interfere with their quantitation, and the segregation of organic acids away from other ionic constituents in the sample by transfer to the analytical stream. To provide similar levels of transfer for different organic acids, the pH must be sufficiently low that the various organic acids are in the volatile non-dissociated forms. Initially, the utilization of MoO_3 media in the SPAM produced pH values between 3 and 3.2. This was somewhat less acidic than the expected value of 2.5 for equilibrium dissolution of MoO_3; however since dissolution kinetics were involved, it was explainable. To improve the rate of MoO_3 dissolution, several approaches were evaluated. First, substoichiometric MoO_3 was prepared to increase solubility and dissolution rate; however, slightly reduced MoO_3 produced similar pHs to those of fully oxidized MoO_3. Next, fine MoO_3 particles were captured within alginate beads in an attempt to increase solubility and dissolution rate through increased surface area. However, pH values remained in the 3.0 to 3.2 range. A comparison of the attainable pH values with MoO_3 with the dissociation constants for formic, acetic, and propionic anions indicated that unequal protonation would occur and significant differences in membrane transport would apply. Consequently, an alternative solid phase acidification approach was investigated.

An innovative usage of a sparingly soluble salt in combination with a strong acid cation exchange resin in the hydrogen form proved capable of significantly lowering the achievable pH using solid phase media. Sequential beds of $CaSO_4$ and a strong acid ion exchange resin lowered the effluent pH to 1.74 using a pure water feed. The dissolution of $CaSO_4$ releases Ca^{2+} which then displace hydrogen ions from the strong acid cation exchange resin. Since each Ca^{2+} ion quantitatively displaces two H^+ ions, the achievable SPAM pH depends only on the salt solubility and $CaSO_4$ dissolution kinetics. At this pH, the transfer of different organic acids across the OATM proceeded much more equally than when using the previous SPAMs.

4.2 CDM Performance.

The CDM membranes that were tested included polyimide, polyester, polytetrafluoroethylene (PTFE), and polydimethylsiloxane (PDMS). The thinnest membranes were polyimide and polyester with thicknesses of 6.4 and 19 μm,

respectively. These membranes displayed very poor CO_2 permeation even at temperatures as high as 96 °C in the case of polyimide tubing. Only PTFE and PDMS tubing exhibited significant CO_2 permeability in these tests.

To quantify the performance of the PTFE and PDMS CDMs, a challenge solution containing 20 mg/L of Total Inorganic Carbon (TIC) as sodium bicarbonate was fed to each CDM and the TIC clearance following acidification was determined. In these tests, a nitrogen purge gas flow of 26 cm^3/min was utilized. The TIC in the effluent was monitored as a function of flow rate through the CDM. The results are shown in Figure 11. The PTFE based CDM removed 90% of the influent CO_2 at the lowest flow rate of 0.2 mL/min, corresponding to a contact time of 22.4 seconds, while the PDMS based CDM removed all CO_2 at flow rates up to 0.6 mL/min, corresponding to a contact time of 22 seconds. Clearly the PDMS based CDM provided superior performance for CO_2 clearance.

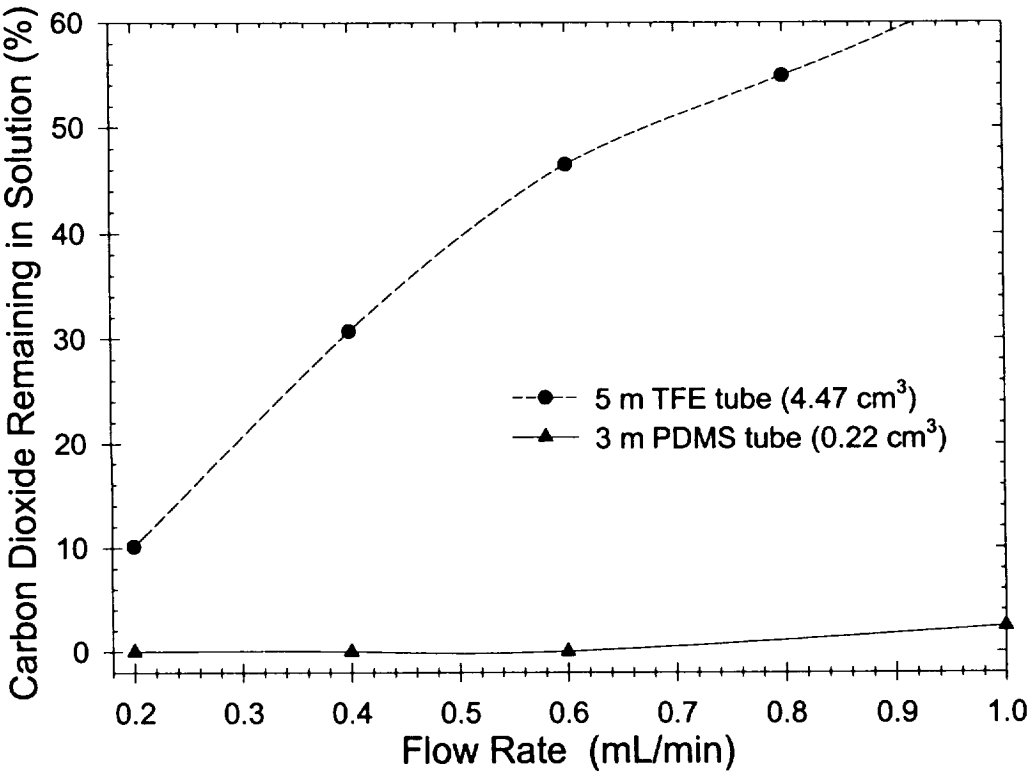

Figure 11. CO_2 Degassing Performance for PTFE and PDMS Membranes.

Since the goal of the CDM in the OAAM is to remove CO_2 while retaining organic acids, the retention of organic acids by the CDM was examined. To simultaneously evaluate the effectiveness of the PDMS CDM at CO_2 clearance and organic acid

retention, inlet and outlet TIC and Total Organic Carbon (TOC) levels were determined separately for challenge solutions of formic, acetic, and propionic acids. In addition to the organic acid, each solution contained 10 mg/L of TIC. For a contact time of 22 seconds, CO_2 clearance was uniformly high in all cases. The relative TOC retentions of formic, acetic, and propionic acids were 94.8, 97.8, and 95.2%, respectively. These important results clearly demonstrates that the PDMS based CDM effectively clears CO_2, while retaining simple organic acids. The PDMS based CDM was selected for incorporation into the OAAM.

4.3 OATM Performance.

Initial operation of a breadboard OAAM as a FIA with the PDMS CDM and the 2.0 m OATM, resulted in an organic acid detection limit of ~50 μg/L. With this level of uncertainty in organic acid concentration, the TOC uncertainty would range between ± 13 and ±24 μg/L, depending on the specific organic acid being detected. Since the effluent TOC from the WRS must be less than 500 μg/L, of which 300 μg/L must be identified, significant improvements in the OAAM sensitivity was required to enable effective diagnostic analysis of process water.

4.3.1 Temperature Effects.

The most obvious area for improvement in OAAM sensitivity was the OATM and its transfer efficiency for organic acids. Such improvements could take the form of better membranes or improved membrane performance. In the latter area, a straightforward approach was to increase diffusivity of the volatile organic acid vapors by raising temperature. The OATM transfer efficiency for formic acid as a function of temperature was determined using a continuous flow of both carrier and analytical streams. In this configuration, the carrier stream was formed by combining formic and dilute sulfuric acid solutions in a mixing Tee. The formic acid concentration in the combined carrier stream was 19.1 mg/L. Downstream from the mixing Tee, the carrier stream flowed through the 3 m PDMS CDM and a special 0.24 m OATM at 0.6 mL/min. The analytical stream flowed through the OATM at 0.1 mL/min. The contact time for the analytical stream within the OATM was 10 seconds. The transfer efficiency was then determined based on comparison of the specific conductances between the carrier and analytical streams. The data for temperatures between 20°C to 50°C are shown in Figure 12. The relatively low fraction transferred in this test arrangement was primarily due to the small dimensions of the OATM and the short contact time. These data indicated a threefold improvement in transfer efficiency when the temperature was

raised from 20° to 50°C. As a result of this information, 50°C was selected as the operation temperature for the OATM.

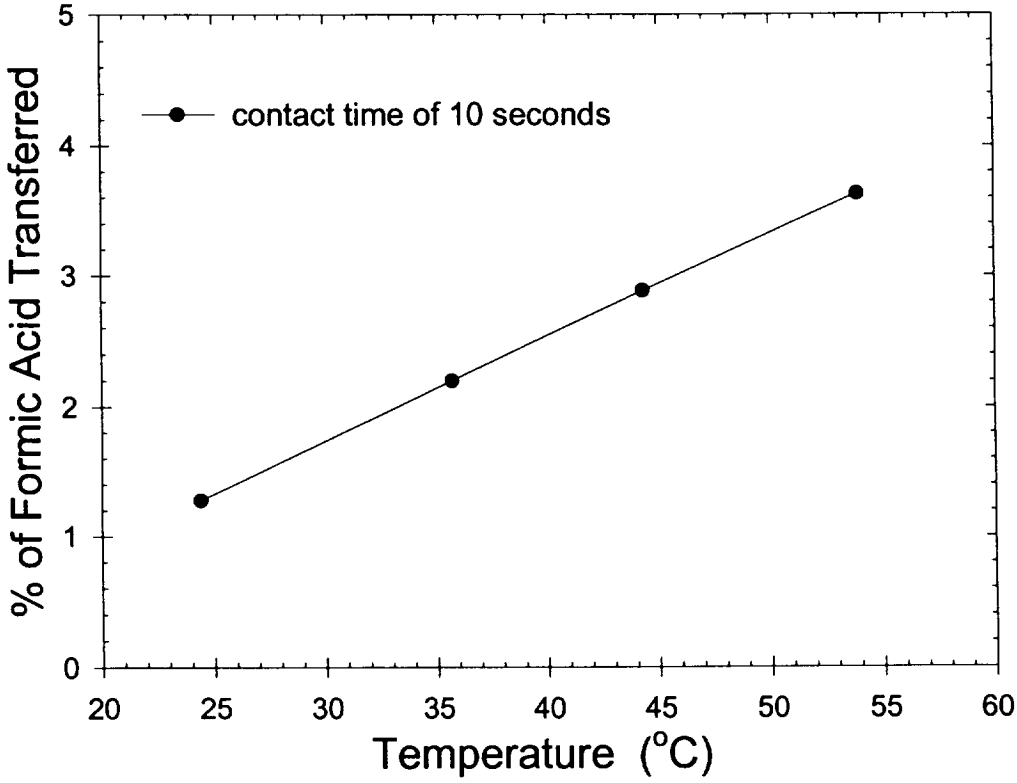

Figure 12. Effect of Temperature on OATM Transfer Efficiency for Formic Acid.

4.4 Performance Testing of Stopped Flow OAAM Configuration.

The next improvement that was investigated was modification of the time during which organic acids from the carrier are pumped down the concentration gradient into the analytical stream. Increasing the transfer time between the carrier and analytical streams will increase the transfer of organic acids. The OAAM was operated as a stopped flow analyzer. The sample stream was continuously pumped through the OATM at 0.6 mL/min, while the analytical stream was stopped for a specified time. At the end of the stopped flow time, the analytical stream was then pumped through the conductivity detector at 0.4 mL/min. To reduce background conductivity levels a continuous flow was maintained through the conductivity detector. This was accomplished using two solenoid valves which bypassed the stopped flow plug in the OATM during the stopped flow time. At the end of this time, flow was resumed through the conductivity detector. Using this arrangement, spurious contributions to the conductivity signal from the dissolution of metal in the conductivity cell and the in-

diffusion of ion forming species such as CO_2 was prevented. On the shell side of the OATM, the continuous passage of the acidified carrier creates a concentration gradient across the membrane. On the carrier side, organic acids are present in the protonated and volatile form, while on the analytical stream side, organic acids are present in the ionized and non-volatile form. Consequently, organic acids are driven from the carrier into the analytical stream. By increasing the stopped flow time, the concentration of organic acids in the analytical stream increases. This is demonstrated in Figure 13 where the specific conductance of the analytical stream is given as a function of the stopped flow time for formic, acetic, and propionic acids. A stopped flow time of 10 minutes was selected as the best compromise between response time and sensitivity based on these results. A detection limit of ~20 µg/L for formic acid was obtained operating the OAAM at 50°C with a 10 minute stopped flow time. The stopped flow specific conductance peak remained unchanged below this concentration.

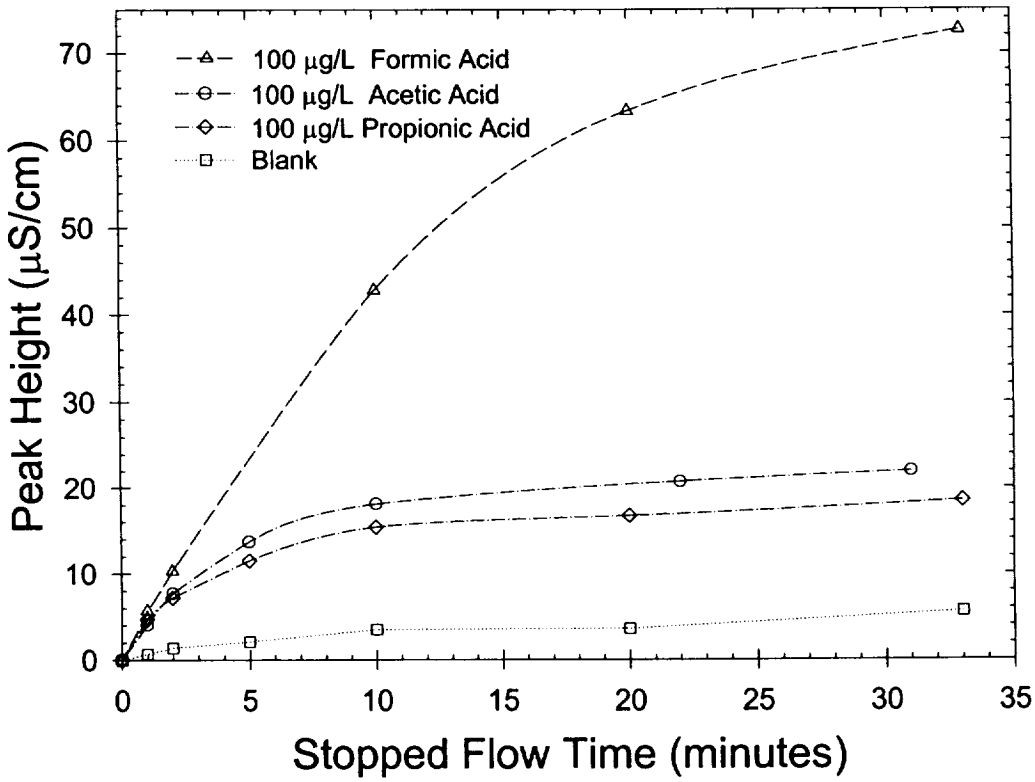

Figure 13. Stopped Flow Time Conductiometric Response for Various Organic Acids.

Further investigation of the response fall off at low concentration indicated that adsorption of organic acids by the thin protective oxide layer (i.e., Cr_2O_3) on the stainless steel surface of the OATM shell limited organic acid detectability. The

detection limits were significantly improved when a new OATM was fabricated in which the stainless steel outer tube was replaced with a PEEK (poly ether ether ketone) tube. The new OATM consisted of a 2 m PEEK shell with an inner diameter of 762 μm and a coaxial microporous polypropylene tube with a 355 μm outer diameter, a 300 μm inner diameter, 0.05 μm pores, and 45% open porosity.

The OAAM performance was evaluated with the new OATM operated at 50°C, with a 10 minute stopped flow time. The specific conductance responses for standard solutions of formic, acetic, and propionic acids were determined. The results for concentrations between 0.1 and 40 mg/L are shown in Figure 14, while the results for lower concentrations between 5 μg/L and 1000 μg/L are given in Figure 15. Each curve was fit to a third order polynomial, resulting in correlation coefficients of better than 0.9993. Sensitivity was dramatically improved over previous OAAM configurations with detection limits for all organic acids on the order of 1-5 μg/L. The theoretical conductiometric response for acetic acid concentrations between 1 and 2000 μg/L is shown in Figure 16. A comparison of the measured and theoretical values demonstrates that the exchange of acetic acid during the 10 minute stopped flow time

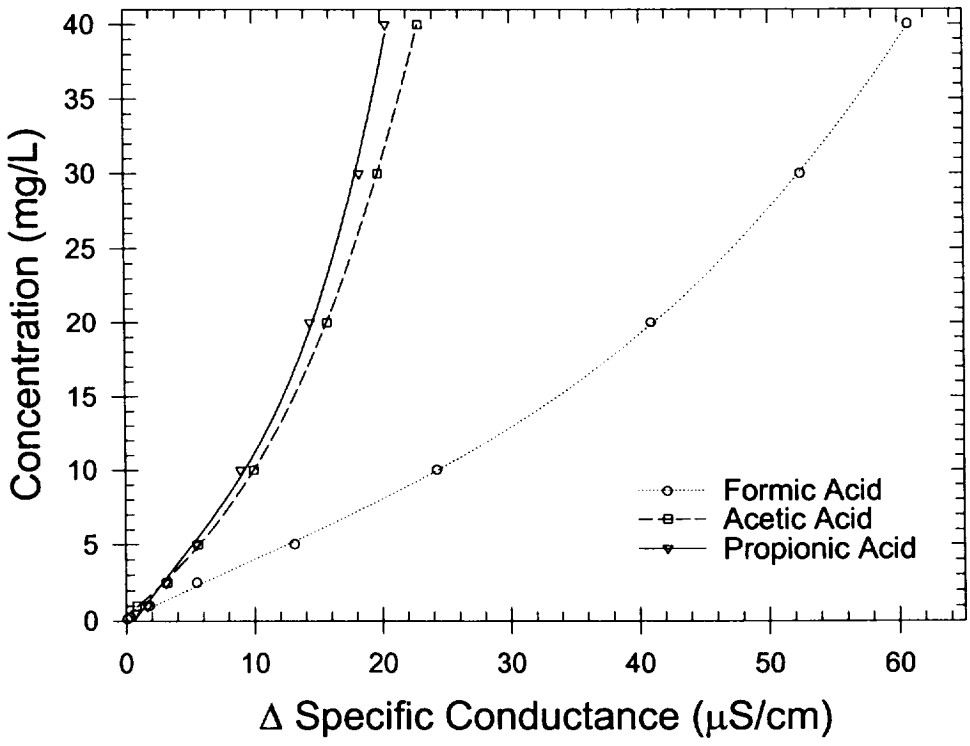

Figure 14. High Level Organic Acid Response Curves.

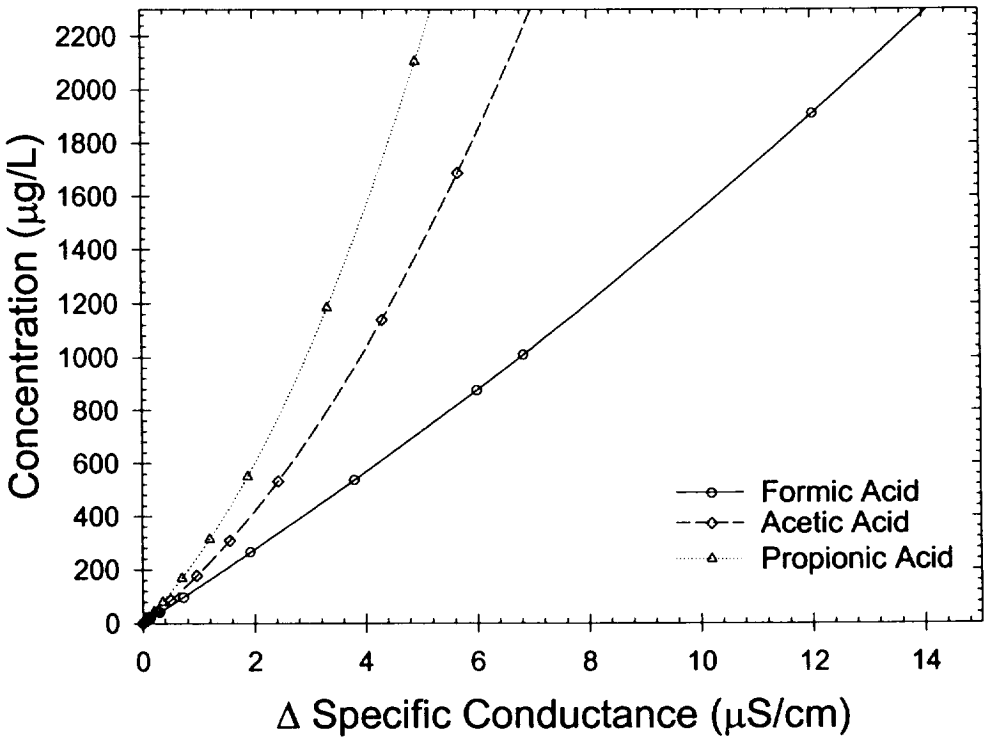

Figure 15. Low Level Organic Acid Response Curves.

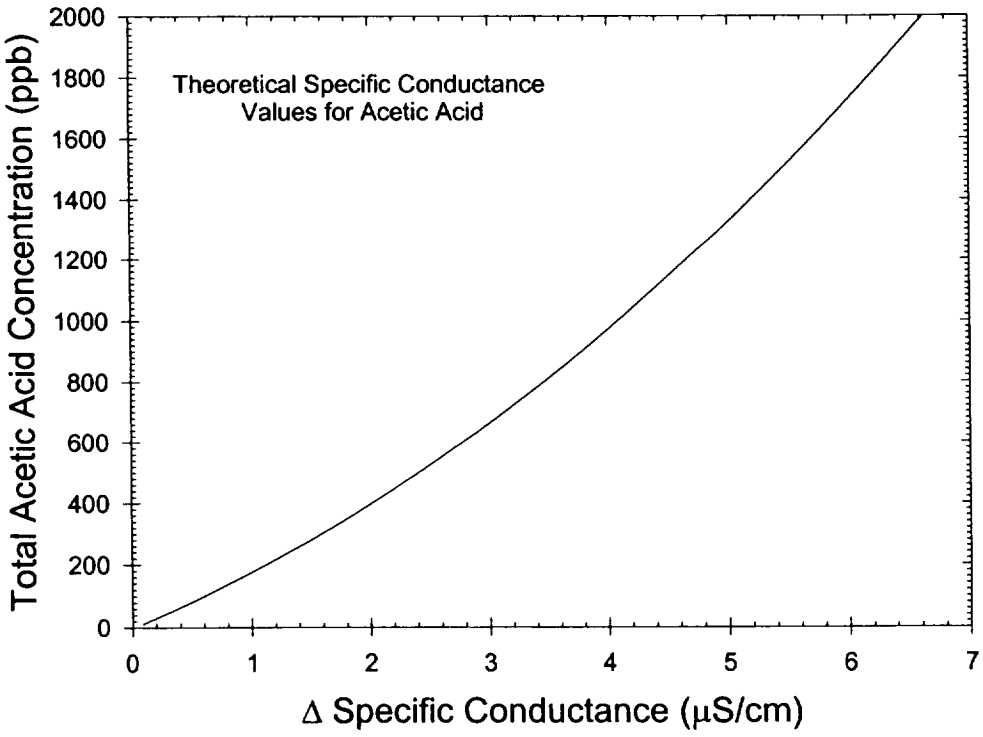

Figure 16. Theoretical Equilibrium Conductiometric Response for Acetic Acid.

very nearly achieved equilibrium values (i.e., 6.4 versus 6.6 μS/cm at 2000 μg/L). This confirms that the pH derived concentration gradient rapidly pumps acetic acid from the carrier to the analytical stream. Due to this efficient transfer, low detection limits were achieved without improvements in the conductivity detector sensitivity (i.e., 0.001 μ S/cm). This OAAM configuration, consisting of a PDMS CDM and a heated, microporous polypropylene OATM, provided a reasonable time response with sufficient sensitivity to determine organic acids in the WRS for diagnostic purposes. However, the utilization of a continuously flowing carrier stream with this configuration had several drawbacks including system complexity with multiple switching solenoids and associated tubing runs, and sample withdrawal required hard plumped connections. Due to the improvements in sensitivity achieved by the elimination of stainless steel components and operation of the OATM at higher temperatures, a second look at the more versatile FIA configuration was initiated.

4.5 Performance Testing of Flow Injection Analyzer(FIA) OAAM Configuration.

The FIA version of the OAAM utilized the configuration shown previously in Figure 2. In this OAAM, the CDM was 2 m long using a coaxial tube-in-shell design. The outer shell had an inside diameter of 1.59 mm and the inner tube had an inside diameter of 305 μm inner diameter. The CO_2 selective membrane thickness was 165 μ m and the volume within the inner tube was 141 μL. The surface to volume ratio was 131.1 cm^2/cm^3 for the CDM. The shell side of the OATM was constructed of 1.5 m of PEEK tubing with an inside diameter of 762 μm. The transfer membrane inside diameter was 400 μm and the membrane thickness averaged 30 μm. The surface to volume ratio was 100 cm^2/cm^3 for the OATM. The injection volume was 1 mL.

Response curves were determined for high and low acetic acid concentration ranges. These results are shown in Figures 17 and 18. These curves were fit to a second order polynomial. The correlation coefficients for were 0.9990 and 0.9973 for the higher and lower ranges, respectively. The detection limits were on the order of 10 μg/L and depended on the flow rates and injection volume used. The absolute value of the conductiometric response was significantly lower than in the stopped flow case at equivalent concentrations. This was expected since the concentration gradient across the membrane changes more rapidly in the FIA case, as compared to the stopped flow case, due to the limited quantity of organic acids in the injection plug. The curve shape also differed from the stopped flow case yielding an increasing conductivity response with concentration (i.e., the curves bend down rather than up). This counters the

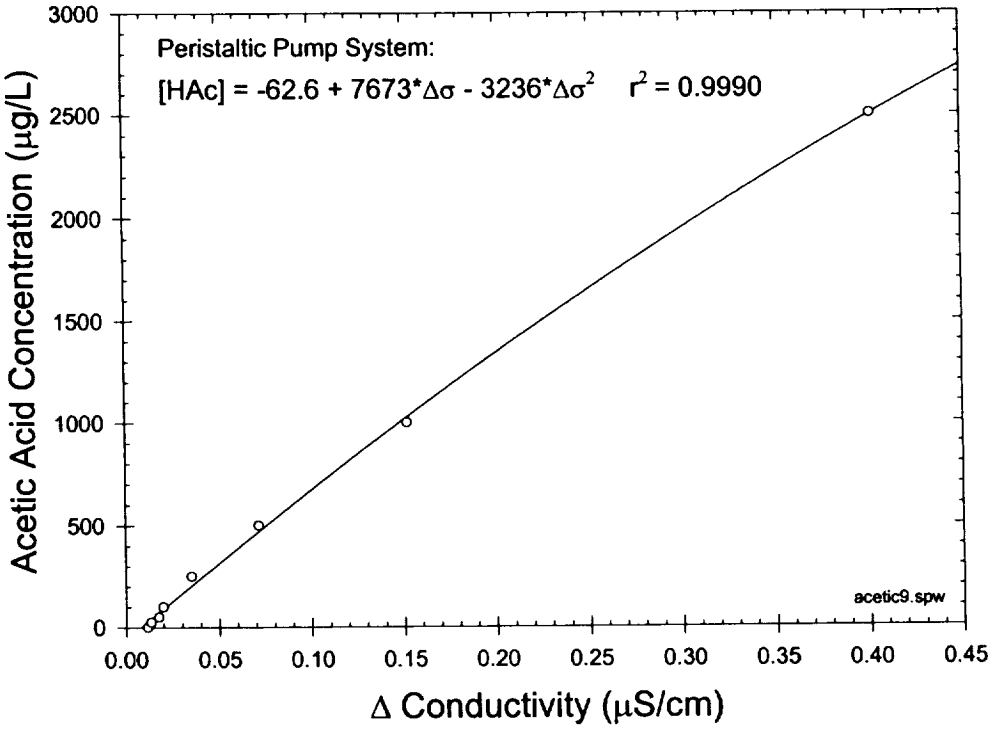

Figure 17. Acetic Acid High Range Response Curve for FIA Version of the OAAM.

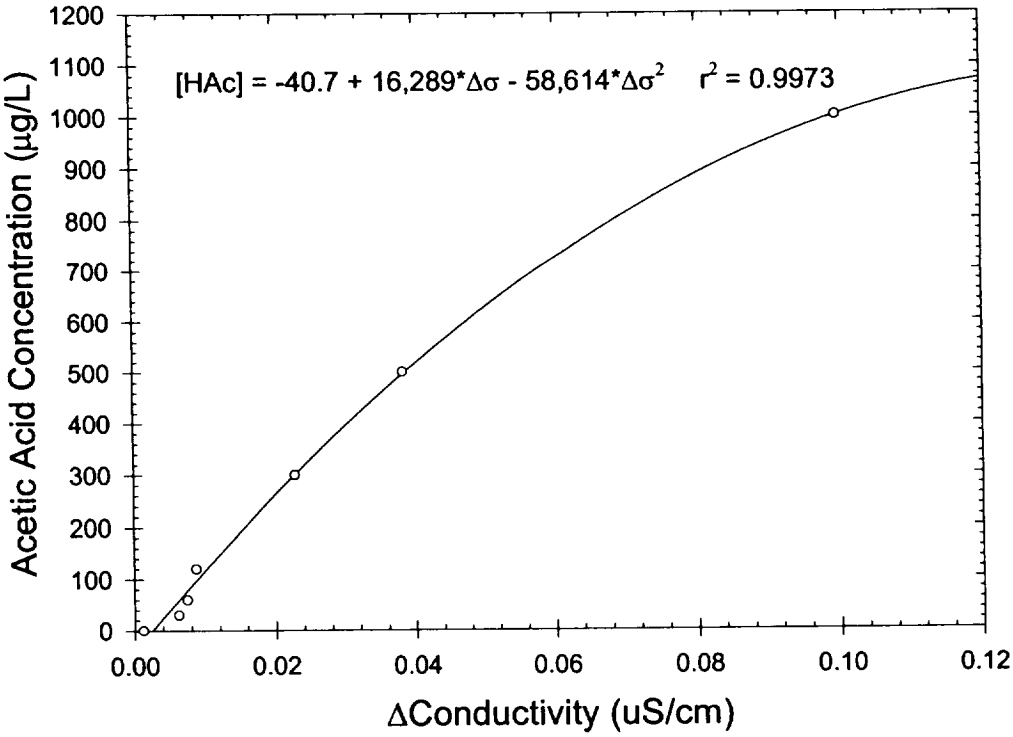

Figure 18. Acetic Acid Low Range Response Curve for FIA Version of the OAAM.

equilibrium case seen with the stopped flow analysis where conductivity changes reflect changing equilibria and a decreasing degree of ionization with concentration. The relative increase in analytical stream conductivity with concentration was also due to the limited quantity of organic acids in the injection plug. As the concentration increases, the concentration gradient is maintained at a higher level for a longer time, and a proportionately lower fraction of organic acids are lost due to non-transfer mechanisms.

4.6 Performance Testing of Immobilized Alcohol Oxidase.

The oxidation of methanol and ethanol catalyzed by immobilized alcohol oxidase (AO) on diatomaceous earth is shown in Figure 19. These data showed that rapid oxidation of methanol and ethanol to formaldehyde and acetaldehyde is possible at ambient temperature. However, initial attempts to determine alcohols using the OAAM with the addition of an immobilized AO bed in combination with a heterogeneous catalyst bed did not produce the expected response except at relatively high alcohol concentrations. These data indicated that either the aldehyde or the organic acids produced by the two oxidation steps were being adsorbed in one of the two beds.

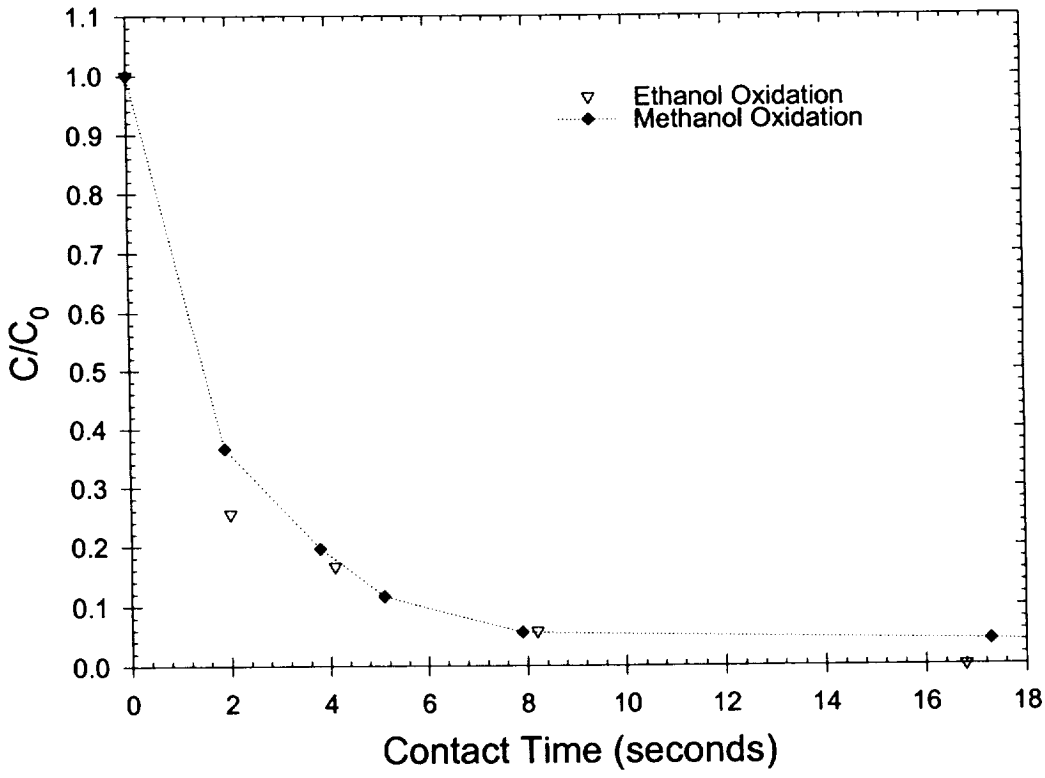

Figure 19. Oxidation of 7.9 mg/L Methanol and Ethanol Over Immobilized Alcohol Oxidase on Diatomaceous Earth at Ambient Temperature.

4.7 Performance Testing of Oxidation Catalysts.

A new experiment was devised to determine whether adsorption of aldehydes or organic acids was the cause of disproportionately low conductiometric responses for the conversions of alcohols to organic acids. In this experiment, alcohol oxidase immobilize on agarose beads was challenged with 1-propanol. The agarose support was used for these experiments to eliminate propionaldehyde oxidation by the platinum catalyst co-immobilized on the diatomaceous earth with alcohol oxidase since sorption by the diatomaceous earth support would then be an issue. The complete oxidation of 1-propanol to propionaldehyde using alcohol oxidase was verified using gas chromatography. When this AO bed was combined with a 1 % platinum on zirconia catalyst and coupled to the OAAM, however, a disproportionately low response was seen, as with the bed containing alcohol oxidase immobilized on diatomaceous earth. This is shown in Figure 20 where the actual conductiometric response is compared to the theoretical response for 1-propanol that has been completely converted to propionic acid. These data strongly suggest that a significant fraction of the organic acids produced by the two step oxidation was adsorbed by the catalyst bed. It became

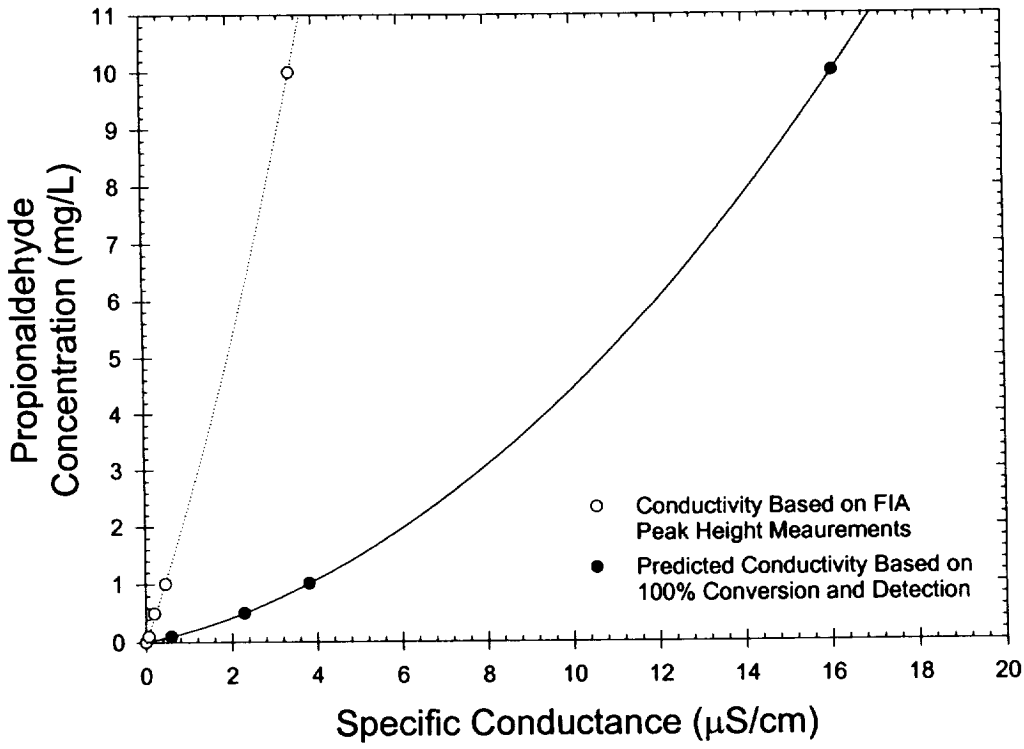

Figure 20. Comparison of Theoretical and Measured Conductiometric Response of Oxidized 1-Propanol.

evident that another heterogeneous catalyst was needed to oxidize aldehydes to organic acids without undo adsorption. This becomes particularly important as the alcohol concentration is lowered. These efforts focused on silica MCF supports because catalysts using activated carbon, alumina (Al_2O_3), and titania (TiO_2) as supports produced similar results to those for the zirconia (ZrO_2) support.

A MCF was prepared using 6 g of P123, 6 g of TMB, and 13.2 g of TEOS under the standard preparation conditions. The material was calcined at 600°C for 2 hours and then sized to -16 +50 mesh. This support was impregnated with 2.0% platinum and fired under reducing conditions at 600°C for 2 hours. A catalyst bed was prepared containing 33 mg (i.e., 0.51 cm^3) of this catalyst. The catalyst was then challenged with 10 mg/liter of propionaldehyde. The influent was saturated with air, resulting in 8 mg/liter of dissolved oxygen, corresponding to 2.9 times the stoichiometric requirement to oxidize propionaldehyde to propionic acid. The oxidation results at ambient temperature are shown in Figure 21. The influent and effluent propionaldehyde concentrations were determined as a function of flow rate. These data were fit to a pseudo first order kinetics model, yielding an r^2 of 0.9972. The reaction rate constant,

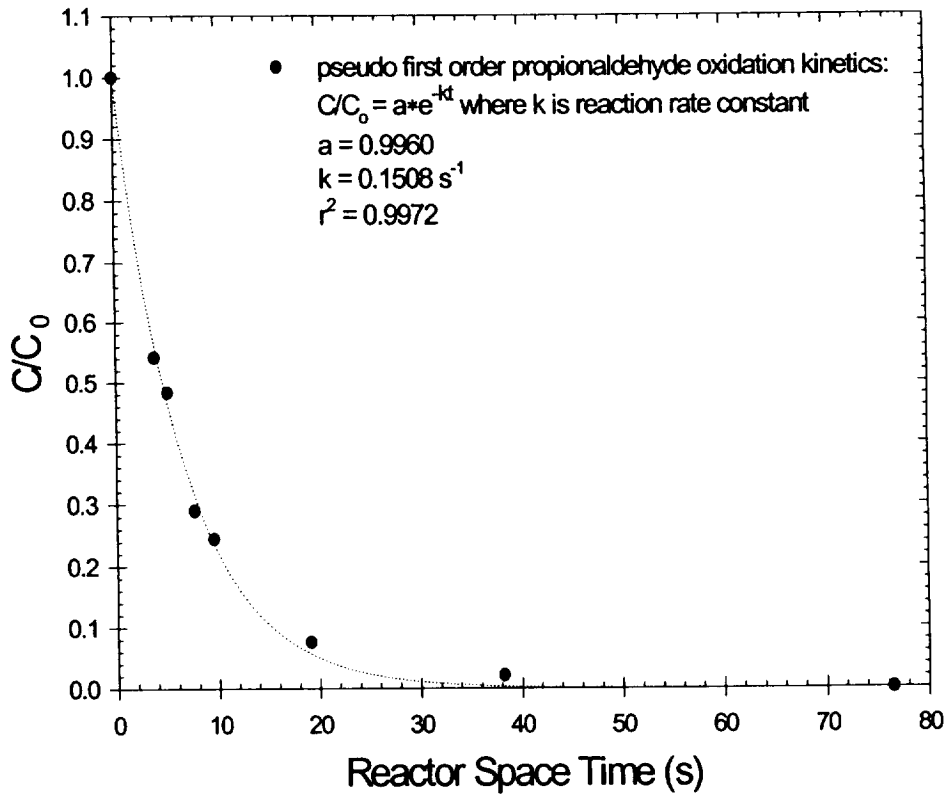

Figure 21. Propionaldehyde Oxidation Kinetics Curve for MCF #1: 2.0% Pt Catalyst.

k, was 0.151 s^{-1} which indicated that propionaldehyde oxidized rapidly over this catalyst. Since the oxidation activity was high, other catalysts were not investigated. This oxidation catalyst was combined with an alcohol oxidase bed to determine whether sorption of organic acids was a problem.

4.8 Determination of Alcohols Using Improved Oxidation Catalysts.

The OAAM was assembled with an alcohol oxidase bed followed by the MCF supported platinum catalyst as an FIA. The alcohol oxidase was immobilized on cyanogen bromide activated Sepaharose A. This support was used to insure that none of the aldehyde or organic acid product would be retained by the alcohol oxidase support. A series of ethanol injections were performed covering concentrations between 25 and 2500 μg/L. The results are presented in Figure 22. These data show good conversion, and since each 1.0 μg/L of ethanol corresponds to 1.3 μg/L of acetic acid, this FIA configuration provided equivalent or better response than that determined for acetic acid in Figure 18. Unfortunately, the alcohol oxidase bed was short-lived, failing after 72 hour of continuous flow. The most likely cause of failure was contamination by bacteria which disrupt the enzyme.

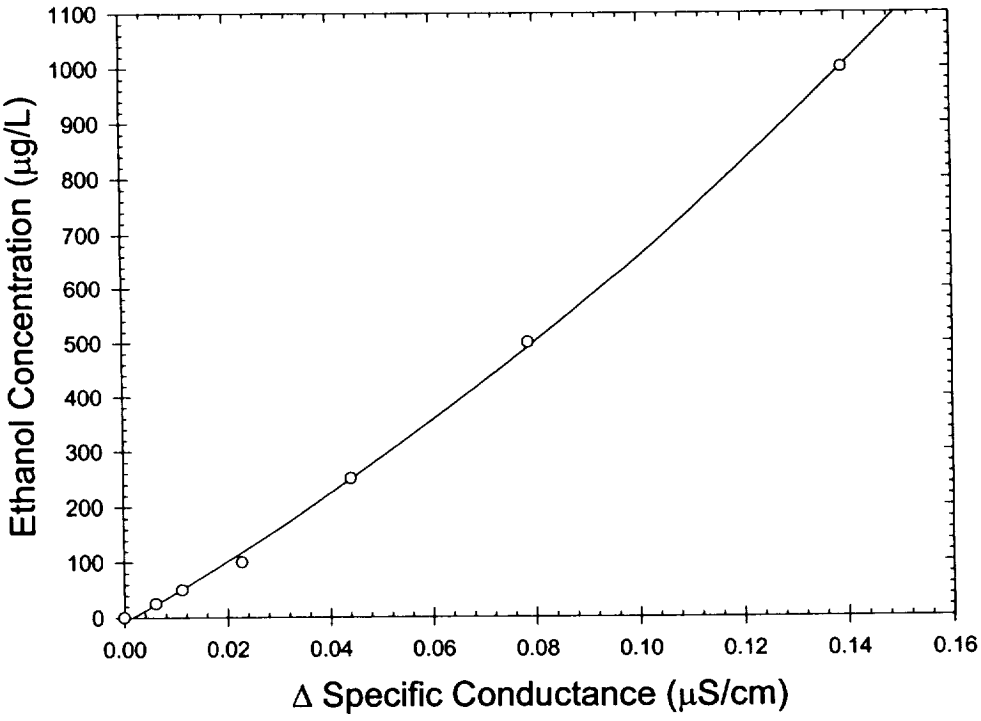

Figure 22. Ethanol Response Curve using Alcohol Oxidase plus MCF: 2.0% Pt Catalyst Sequential Oxidation Beds.

5.0 CHARACTERIZATION OF PROTOTYPE OAAM PERFORMANCE.

Based on the preliminary testing of OAAM stopped flow and flow injection configurations, the computer controlled OAAM was configured as a flow injection analyzer (FIA). A schematic of this configuration was shown earlier in Figure 2. A more complete description including the control programs is given in the Operation Manual. A brief description of the FIA OAAM follows. Three aqueous streams flow into the OAAM. These include analytical and carrier streams, and an acidified stream. These streams are fed by a three channel peristaltic pump with flow rates between 0.15 and 0.17 mL/min. After passing through ion exchange beds, the deionized carrier stream passes into the flow injection valve where a sample plug may be introduced via a 1 mL injection loop. Following the flow injection valve, the carrier passes through or bypasses two sequential beds containing alcohol oxidase and catalyst that convert alcohols to organic acids. In either case, the carrier is then mixed with the acidified stream, lowering its pH to ~2. Downstream from the mixing Tee, the acidified carrier passes through the CO_2 Degassing Module (CDM) where CO_2 is removed across 2 m of PDMS membrane in a tube-in-shell arrangement to a counter-current, CO_2 free purge gas flowing at 35 mL/min. From the CDM outlet, the carrier passes into a 1.5 m microporous polypropylene membrane in the tube-in-shell OATM. The CO_2 free carrier stream flows through the shell side, while the analytical stream, which has been deionized by passage through the ion exchange bed, flows through the central tube. The OATM is operated at 50°C. After passage through the OATM, the carrier stream flows to waste and the analytical stream flows to the conductivity detector, or through a chromatographic separation column and then to the conductivity detector.

The operation of the OAAM control program requires several operator inputs. These include the pump speed, file name for the sample, the file name for the matrix blank that will be used to correct conductivity data, the file name for the calibration curve that will be used to calculate the concentration, and the run time. When the program is initiated and a sample injected, the conductivity signal is continuously read, displayed on the CRT screen, and stored to a file. After the conductivity returns to the baseline value, the control program will determine the matrix corrected flow injection peak height and area, and assign a concentration dependent on the selected calibration file. For either organic acids or alcohols, between 15 and 30 minutes are required for the flow injection peaks to clear the conductivity detector. At concentrations in excess of 1000 μg/L, the return to baseline requires a longer time period due to sample

retention within the carrier and analytical stream flow paths. This is especially evident for alcohols, due to retention in the alcohol oxidase and catalyst beds.

5.1 Organic Acids - OAAM Analytical Performance.

After the OAAM was assembled, it was tested against formic, acetic, and propionic acid standard solutions. The analytical and carrier stream flow rates were set at approximately 0.175 and 3.45 mL/min, respectively. The most critical task prior to sample injection was to reach a low and stable background specific conductance in the analytical stream. For the organic acid detection configuration of the instrument, specific conductance readings generally were less than 0.09 μS/cm, which closely approaches that for pure water (i.e., 0.056 μS/cm). At this point, a matrix blank consisting of the distilled water from which the standard solutions were made was first injected, followed by organic acid standards over the concentration range of 20 μg/L to 10,000 μg/L. The matrix contained a detectable volatile acid gas component. The source of this contaminant was unclear, but most probably originated from either the packaging or via airborne contamination. Response curves were determined for concentration as a function of baseline corrected peak heights. Figure 23 presents flow injection peaks for 60, 150, and 300 μg/L standards of formic, acetic and propionic

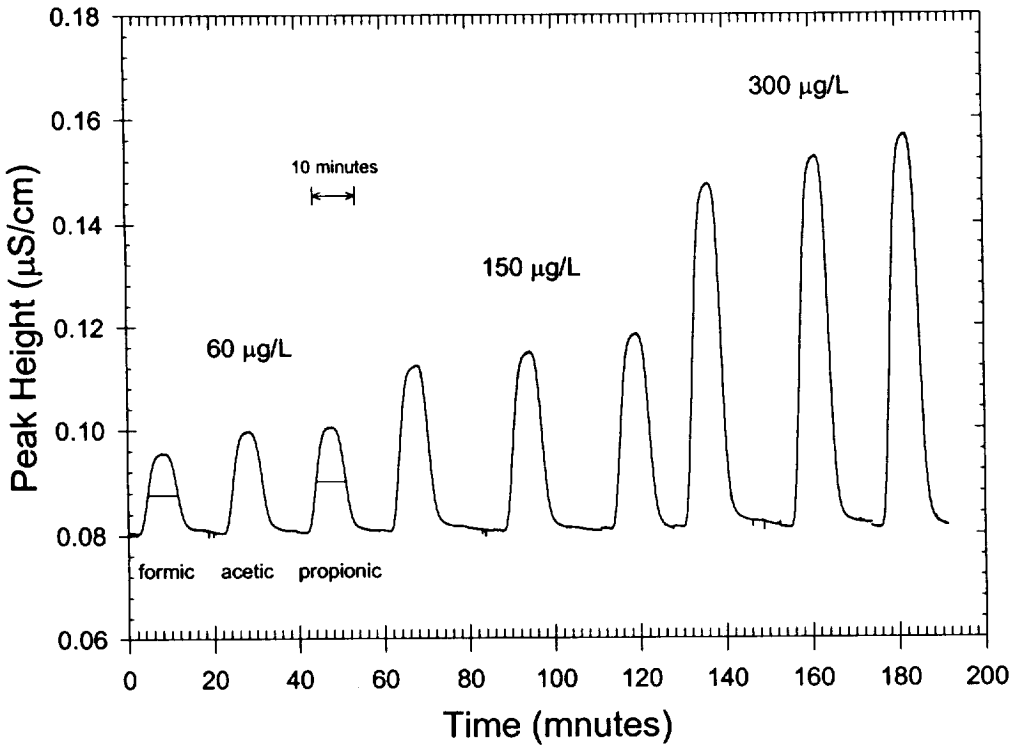

Figure 23. Flow Injection Peaks for Formic, Acetic and Propionic Acid Standards.

acids. The response from different organic acids was similar at similar concentrations, with slight increases in peak height going from formic to acetic to propionic acids. The peaks were characterized by a peak width at half maximum of ~7 minutes. In general, between 20 and 25 minutes were required between each injection.

The OAAM response to formic acid was evaluated first. The formic acid response curve for concentrations between 10 μg/L to 10,000 μg/L is shown in Figure 24. These data were plotted as concentration versus baseline corrected peak height. The concentration data were fit to a second order polynomial expression for baseline corrected peak heights. The choice of a quadratic fit originated from the concentration dependent ionization and consequent specific conductances for organic acids shown in Figures 25 and 26, respectively. Quadratic least squares fits of these theoretical values gave r^2 values of six nines or better. Over the concentration range between 10 μg/L to 10,000 μg/L, the fit was excellent with an r^2 of 0.9995. A similar response curve was determined for the concentration range between 10 μg/L to 1,000 μg/L and is shown in Figure 27. The r^2 value for a polynomial fit for this curve was 0.9991. Overall these

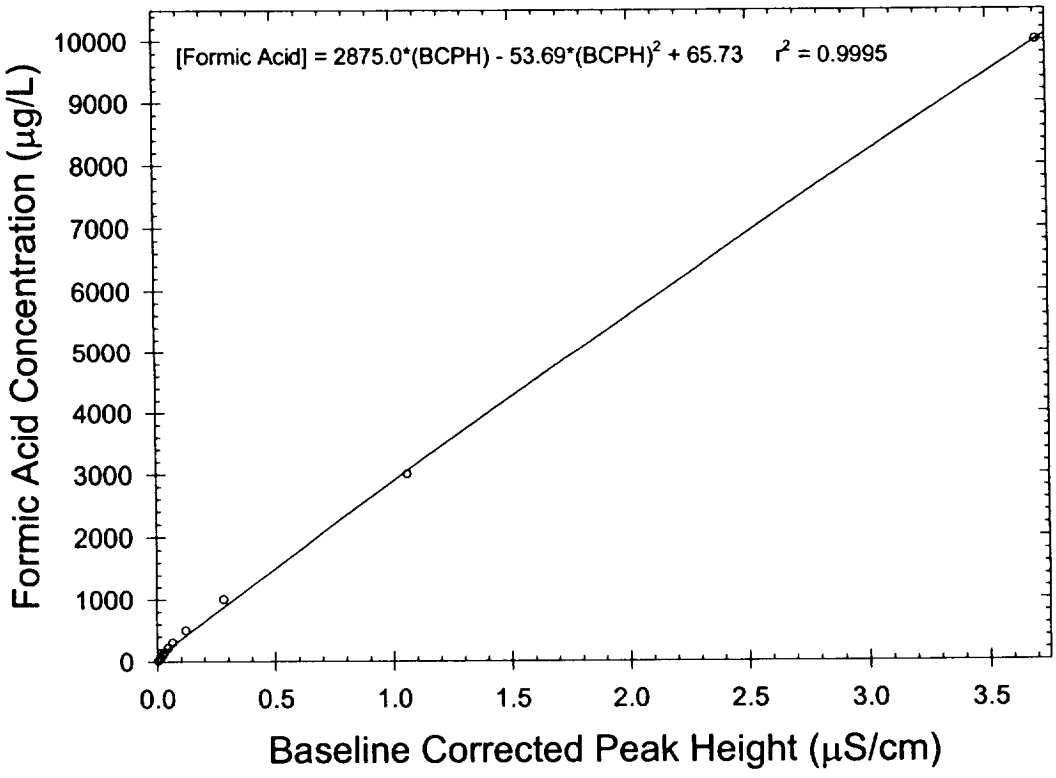

Figure 24. High Range Formic Acid Response Curve.

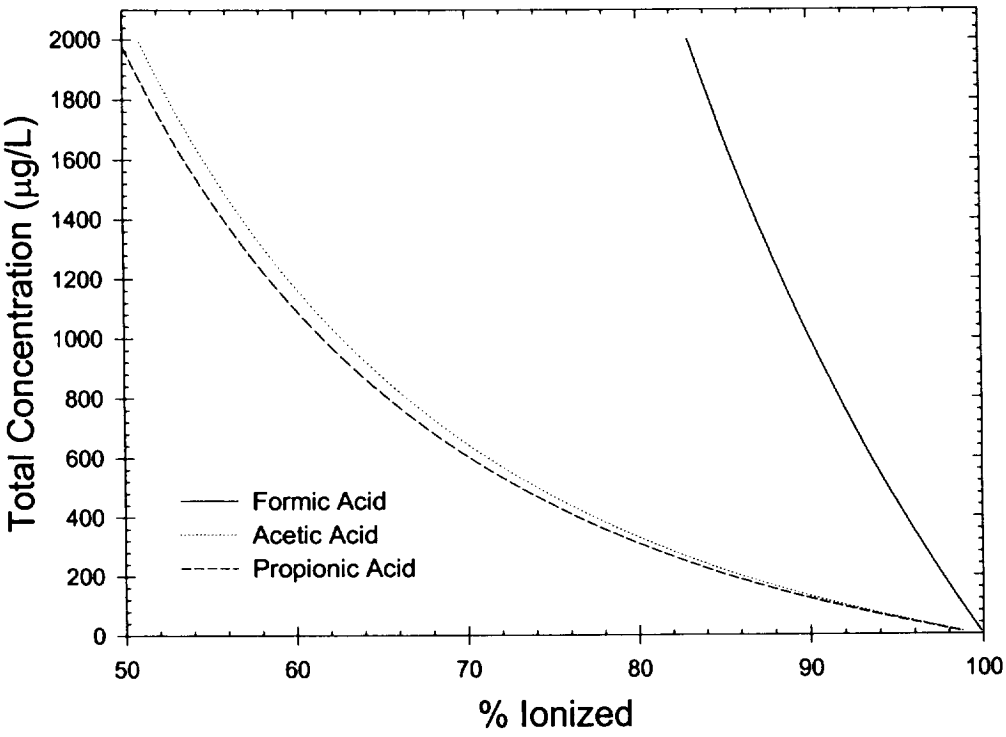

Figure 25. Ionization of Organic Acids versus Concentration.

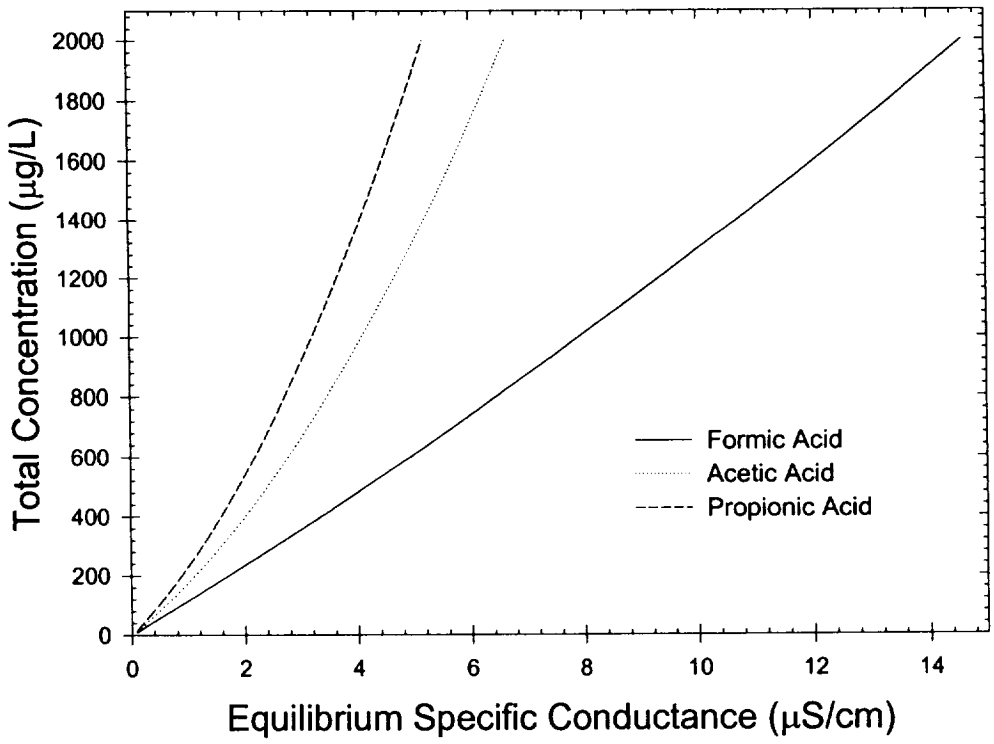

Figure 26. Equilibrium Specific Conductance for Organic Acids versus Concentration.

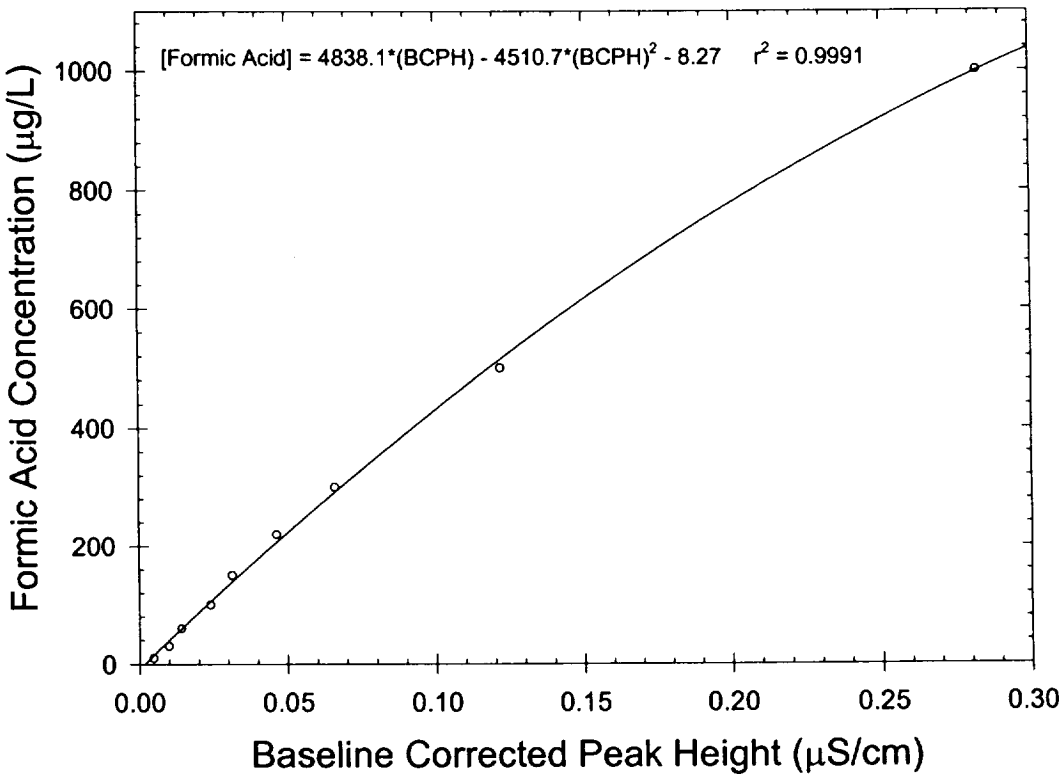

Figure 27. Low Range Formic Acid Response Curve.

was 0.9991. Overall these data demonstrate very good sensitivity and a wide dynamic concentration range of the OAAM for formic acid.

A comparison of the theoretical and experimental results show two distinct differences. First, the theoretical conductiometric response is much larger than the experimental specific conductance. Secondly, the concentration dependencies have different curvatures, with the theoretical specific conductances curving upward with concentration, while the OAAM specific conductances curve downward with concentration. These differences are understandable in terms of the transfer efficiency for formic acid in the OAAM. As was shown in the experimental section, the transfer efficiency for formic acid is low, and consequently, the concentration of formic acid in the analytical stream will be lower than that in the sample. As the formic acid concentration in the sample increases, the analytical stream concentration also increases. Evidently, the increase in formic acid concentration in the analytical stream overrides the relative decrease in ionization with concentration that would normally be observed for formic acid resulting in an increasing conductiometric response with concentration (i.e., downward curvature). The analytical results for formic acid

indicated a detection limit between 5 and 10 μg/L. This may be improved by increasing the injection loop size, slowing the analytical stream flow rate, or both.

The OAAM response to acetic acid was then evaluated. The acetic acid response curve for concentrations between 10 μg/L to 10,000 μg/L is shown in Figure 28. The fit for the polynomial equation given by [HAc] = 4625.3(peak height) + 320.6(peak height)^2 -23.3 was excellent with an r^2 of 0.9999. Interestingly, the curve displayed an upward concentration dependency. As with formic acid, the cause of this dependency lies in the interaction between the concentration dependence for ionization and the transfer efficiency. Another interesting feature is the lower specific conductance response at the higher acetic acid concentrations when compared to those for formic acid. This is expected, based on the lower fractional ionization for acetic acid, as was shown in Figure 25. The low level acetic acid response curve for concentrations between 10 and 1,000 μg/L is shown in Figure 29. The fit for this curve was also very good at 0.9994. Based on the low level response curve, the detection limits for acetic acid is between 5 and 10 μg/L.

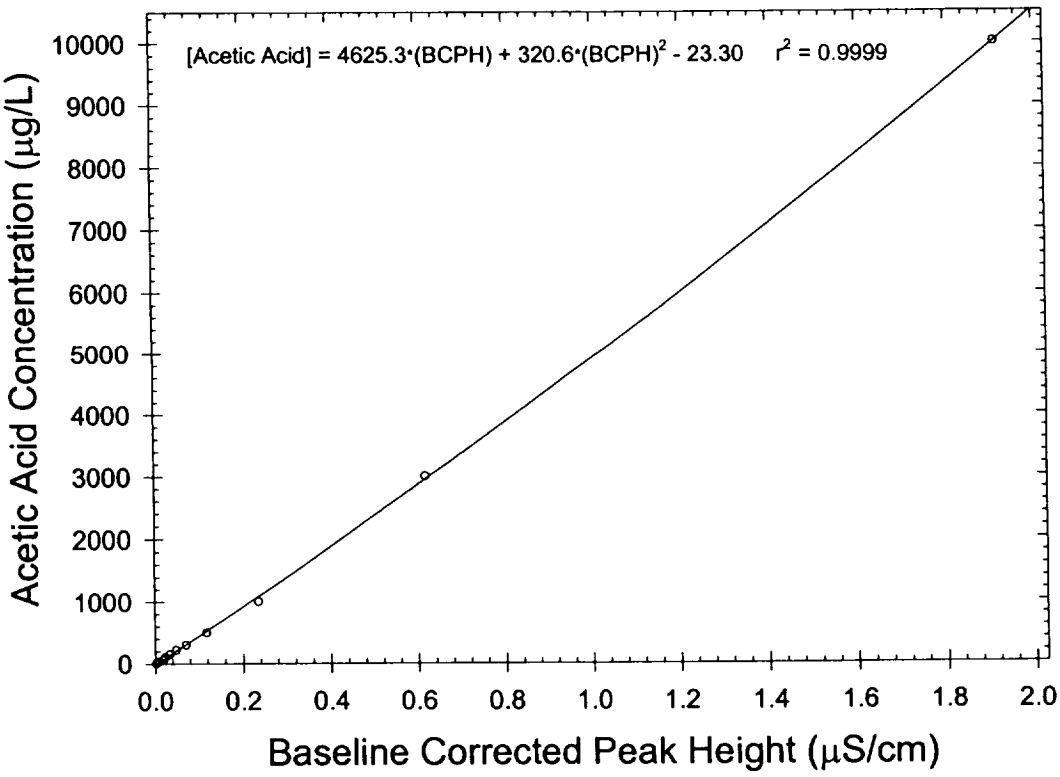

Figure 28. High Range Acetic Acid Response Curve.

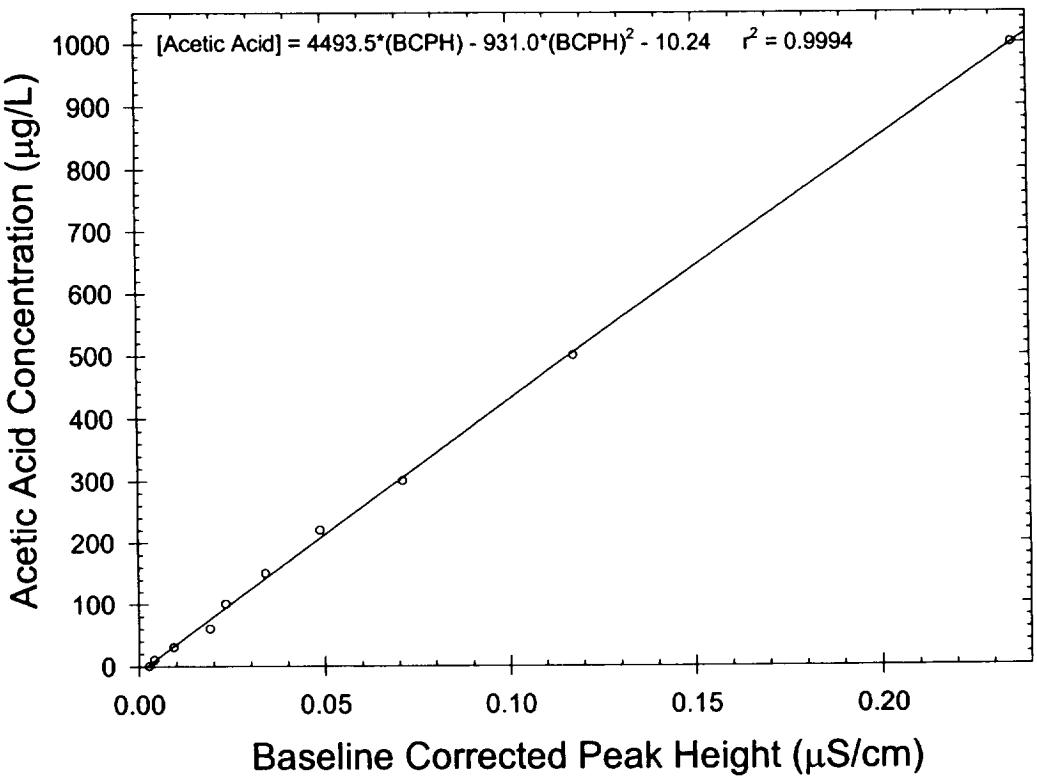

Figure 29. Low Range Acetic Acid Response Curve.

The final organic acid that was examined was propionic acid. Response curves were determined for propionic acid concentrations between 10 and 10,000 µg/L. The higher range curve is shown in Figure 30. The conductiometric response for propionic acid was similar to those for formic and acetic acids at low concentration, and as with acetic acid, the response fell off at high concentrations when compared to formic acid. This fall off was attributed to the relative fraction of the propionic acid molecules that are dissociated at these concentrations. The polynomial fit at high concentration was excellent with an r^2 of 0.9998. The upward curvature of this plot indicated the strong concentration dependence for the degree of ionization. The low level response curve for propionic acid concentrations between 10 and 1,000 µg/L is shown in Figure 31. The nearly linear curve resulted in an excellent least squares fit with an r^2 value of 0.9998. Based on this curve, the detection limit for propionic acid is similar to that of formic and acetic acids, between 5 and 10 µg/L.

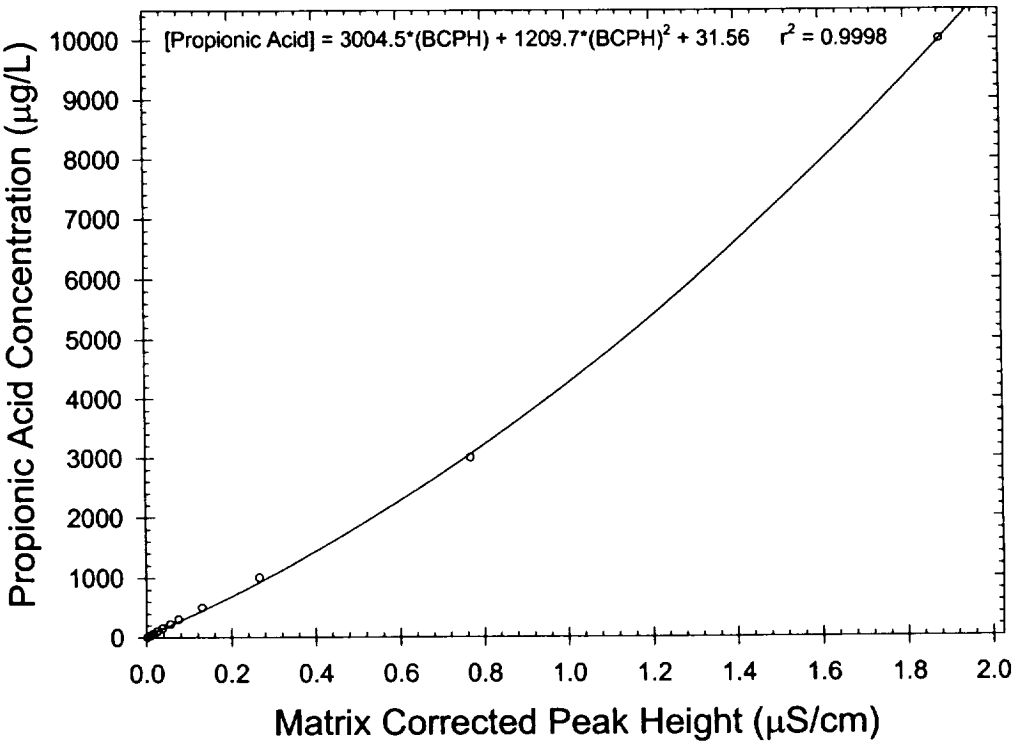

Figure 30. High Range Propionic Acid Response Curve.

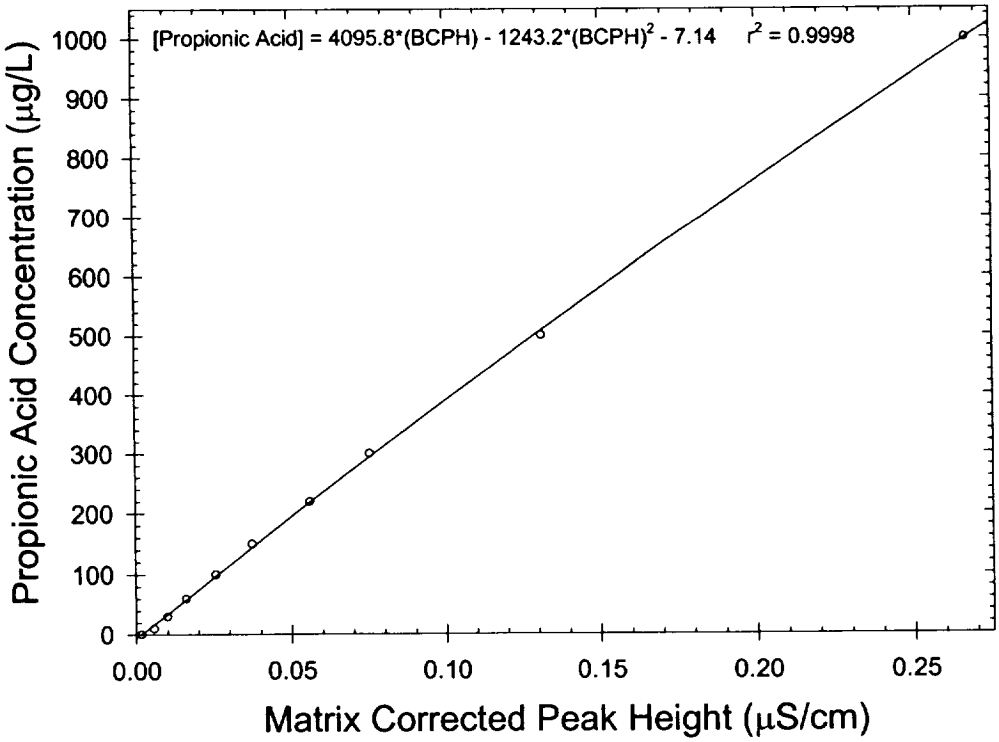

Figure 31. Low Range Propionic Acid Response Curve.

5.2 Separation of Organic Acids on OAAM Prototype.

A chromatography column for the separation of organic acids was inserted into the analytical stream flow path of the OAAM downstream of the OATM. This HPLC column was designed to separate organic acids present in fruit juices using a 0.1 % phosphoric acid solution as the eluent. When operated in this manner, formic, acetic, and propionic acids are well separated with retention times increasing with increasing carbon number. Figure 32 through 34 show flow injection peaks for 500 μg/L samples of formic, acetic, and propionic acids for carrier and analytical stream flow rates of 0.484 and 0.233 mL/min, respectively. The retention times were 13.7, 15.5, and 16.8 minutes, respectively, using water as the eluent. The longer retention times for the less ionic organic acids reflect ion exclusion by the strongly sulfonated styrene divinylbenzene resin contained within this column. Due to the highly ionic nature of this resin, highly ionic organic acids are excluded from the sulfonated resin and the associated hydration sphere, while protonated organic acids are retained by the resin, since they are not ionized. In addition, the affinity of the protonated form of the organic acid for the resin increases with carbon number. The retention times for propionic, acetic, and formic acids reflect their progressively increasing affinities for the resin. The peak at 29.5 minutes is an unknown contaminant present in the blank water sample.

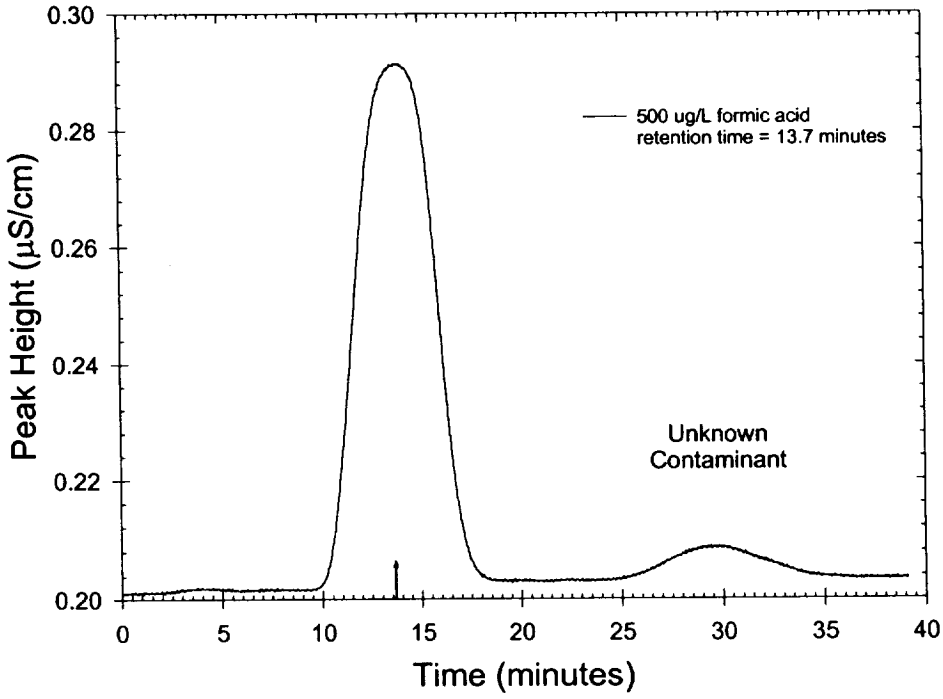

Figure 32. 500 μg/L Formic Acid Injection with Analytical Stream Separation Column.

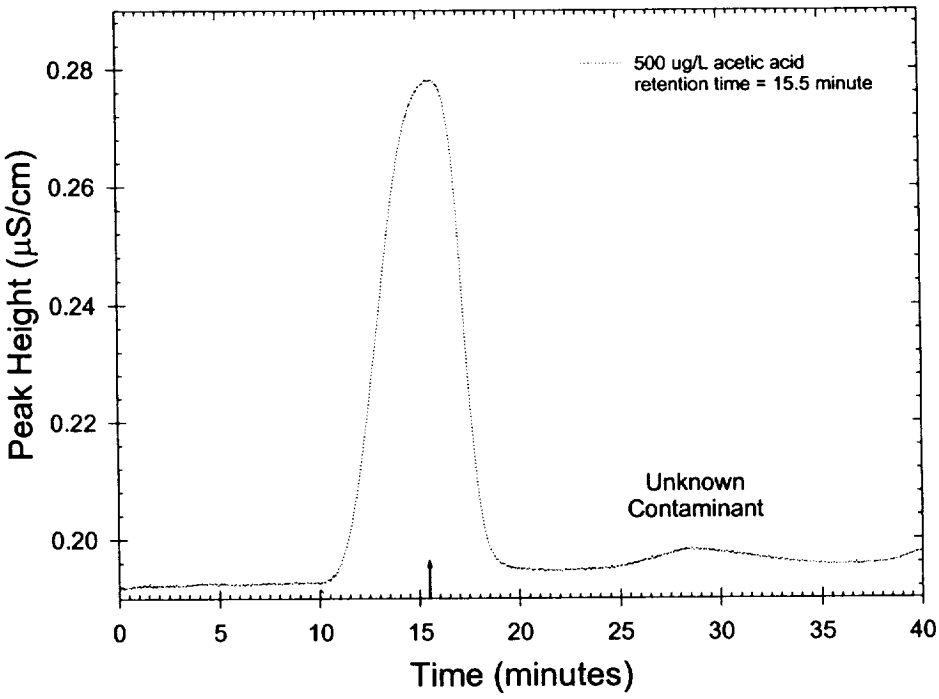

Figure 33. 500 µg/L Acetic Acid Injection with Analytical Stream Separation Column.

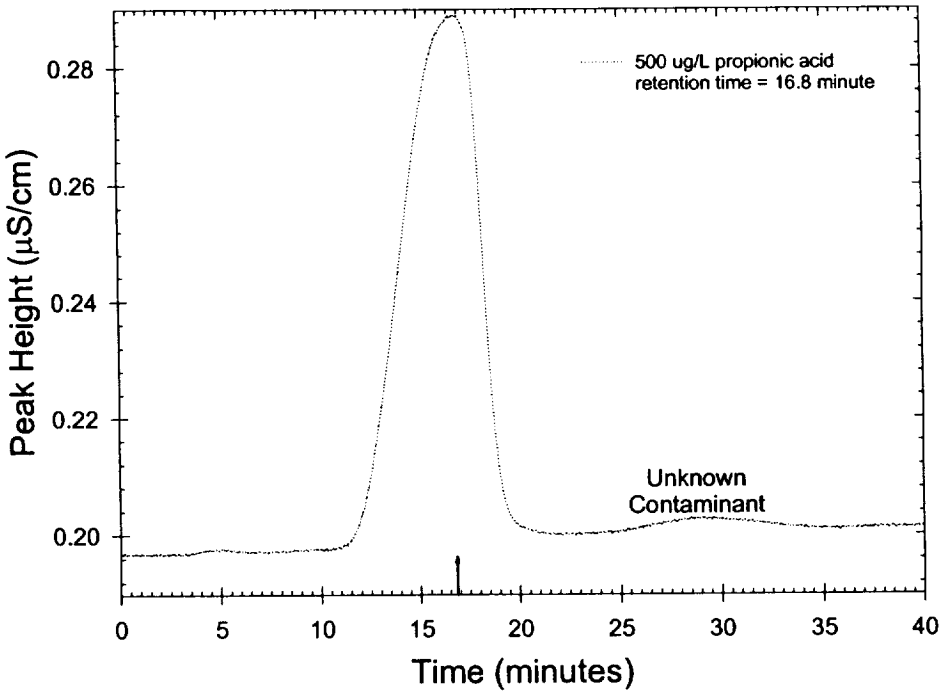

Figure 34. 500 µg/L Propionic Acid Injection with Analytical Stream Separation Column.

This is seen in Figure 35. This contaminant has been seen for all injections of sample blanks and is responsible for the matrix contribution for distilled water. analytical stream. As an example, Figure 41 shows the chromatogram for 10 mg/L each of formic, acetic,

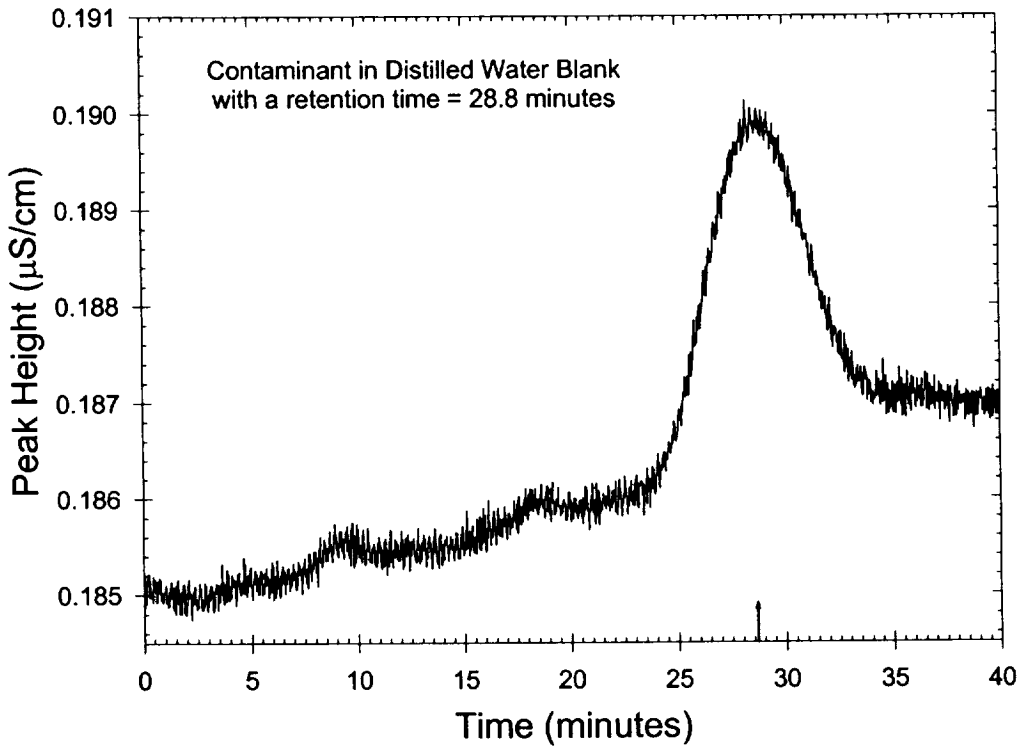

Figure 35. Blank Injection with Analytical Stream Separation Column.

Mixtures containing different concentrations of formic, acetic, and propionic acids were then injected into the OAAM. The results are shown in Figure 36 for 10,000, 500, and 100 μg/L of each acid. At the highest concentration, separation of the three organic acids is evident, although the retention times do not correspond to those for injections of a single organic acid. The peaks correspond at progressively longer retention times for formic, acetic, and propionic acids based on the ion exclusion mechanism. As the concentration of the organic acid mixture decreases; however, separation between organic acids disappears and the retention time for the peak centroid shifts to shorter times. The loss of peak separation as well as the retention time shift is due to the decrease in hydrogen ion concentration. In pure water, the analyte concentration influences the degree of ionization for each organic acid due to the changing pH. Thus, efforts to quantitate organic acids in mixtures using a

separation column in the analytical stream would be extremely difficult due to the changing nature of the peaks as their concentration and the pH is changed.

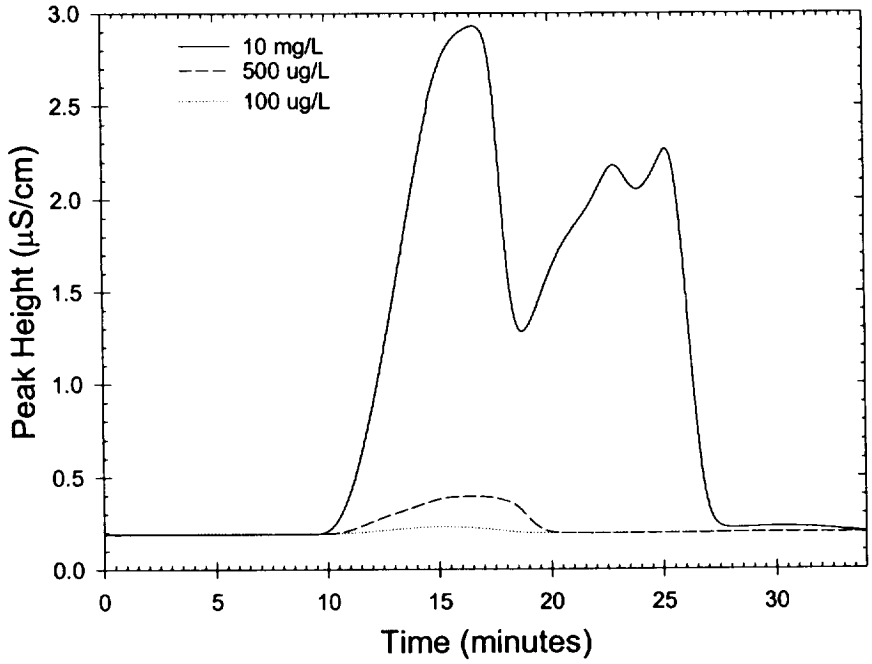

Figure 36. Separation of Organic Acid Mixtures with Analytical Stream Column.

Due to the problems intrinsic to an analytical stream separation column, a second set of experiments was initiated with the separation column in the carrier stream immediately upstream of the CDM. In this arrangement, the sample plug is first acidified and then flows through the separation column. The carrier and analytical stream flow rates were 0.167 and 0.213 mL/min, respectively. In this arrangement, pH is controlled by the SPAM (or its equivalent) and any influence of the organic acid concentration on the pH will be minor. Using the new configuration, 500 µg/L samples of formic, acetic, and propionic acids were injected into the carrier stream. The chromatograms for individual organic acids are shown in Figures 37 through 39. The retention times for formic, acetic, and propionic acids were 21.0, 27.1, and 32.0 minutes, respectively. A mixture containing 500 µg/L each of formic, acetic, and propionic acids was then injected into the carrier stream. The resulting chromatogram is shown in Figure 40. At this concentration, the peaks are not well separated, but there is a clear correspondence for peaks associated with each organic acid. Next, a series of samples containing 200 µg/L, 2 mg/L, and 10 mg/L each of formic, acetic, and

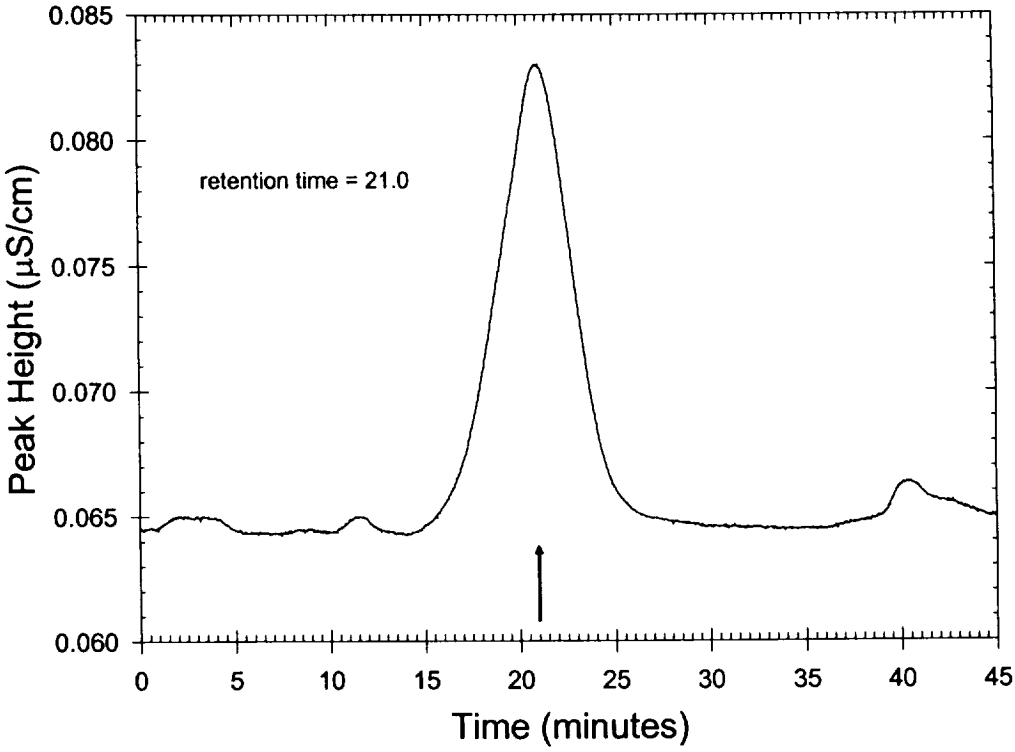

Figure 37. 500 µg/L Formic Acid Injection with Carrier Stream Separation Column.

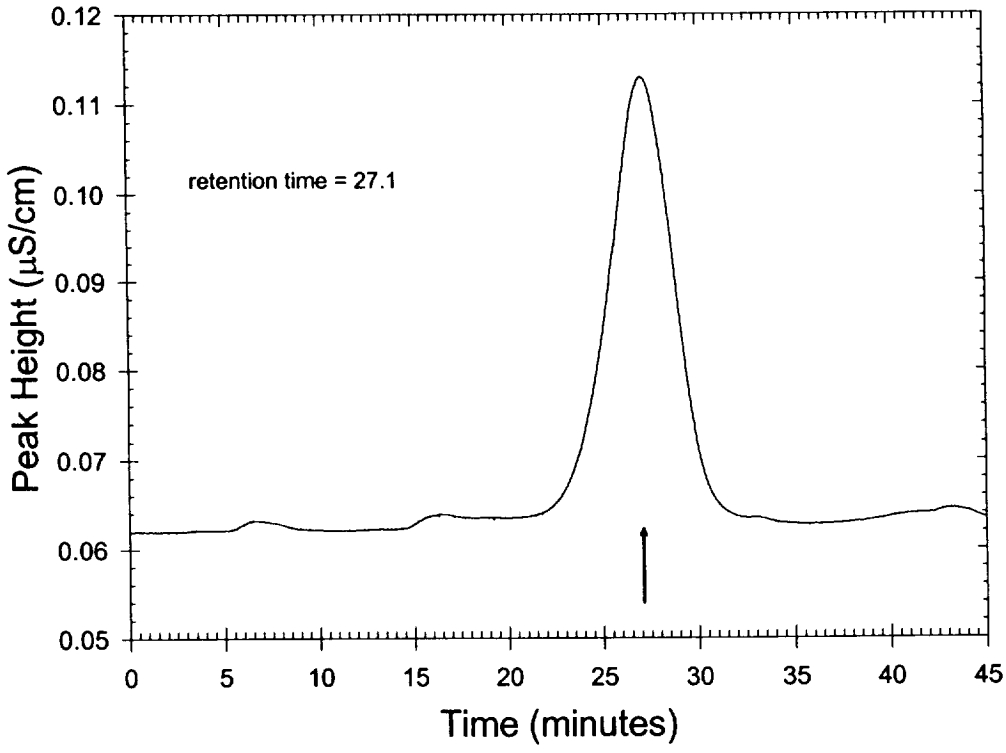

Figure 38. 500 µg/L Acetic Acid Injection with Carrier Stream Separation Column.

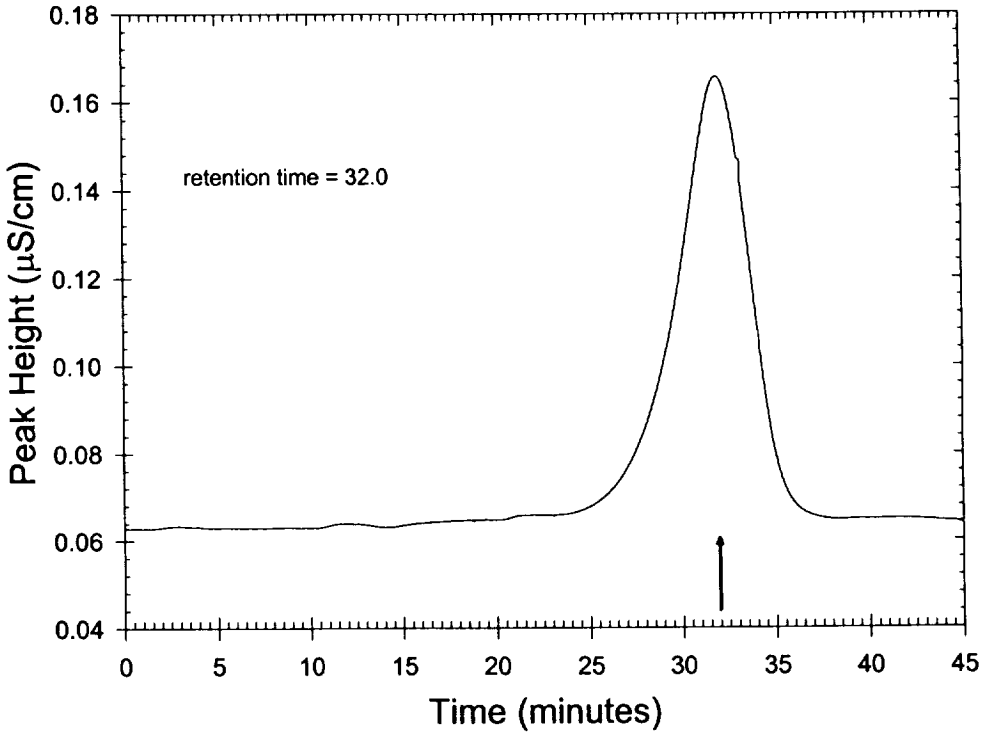

Figure 39. 500 µg/L Propionic Acid Injection with Carrier Stream Separation Column.

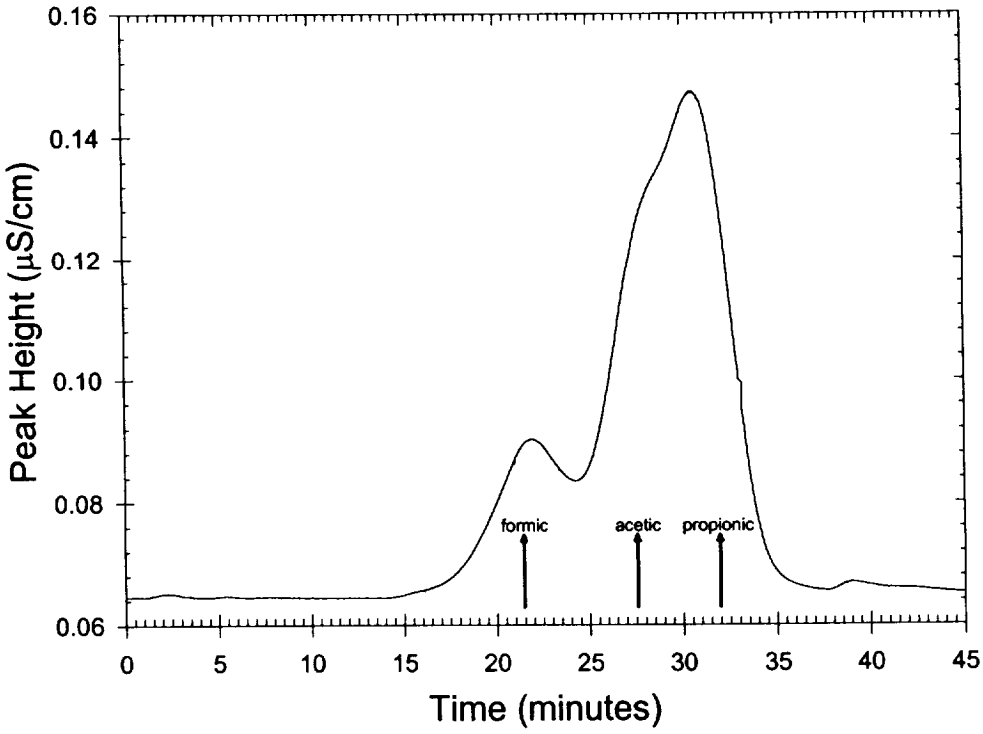

Figure 40. Chromatogram for 500 µg/L Each of Formic, Acetic, and Propionic Acids with Corresponding Single Acid Retention Times.

propionic acids were injected into the carrier stream. These chromatograms displayed the same shifts in retention times that were observed with the separation column in the analytical stream. As an example, Figure 41 shows the chromatogram for 10 mg/L each of formic, acetic, and propionic acids. There is better separation for the individual organic acid peaks which correspond well to the retention times for a 10 mg/L injection of a single organic acid. The retention times for formic, acetic, and propionic acids were 27.4, 34.3, and 39.3 minutes, respectively. After changing the organic acid concentration by a factor of twenty the retention times increased 6.4, 6.2, and 7.3 minutes for formic, acetic, and propionic acid, respectively. The reason for these concentration dependent retention times under the controlled pH conditions is unknown.

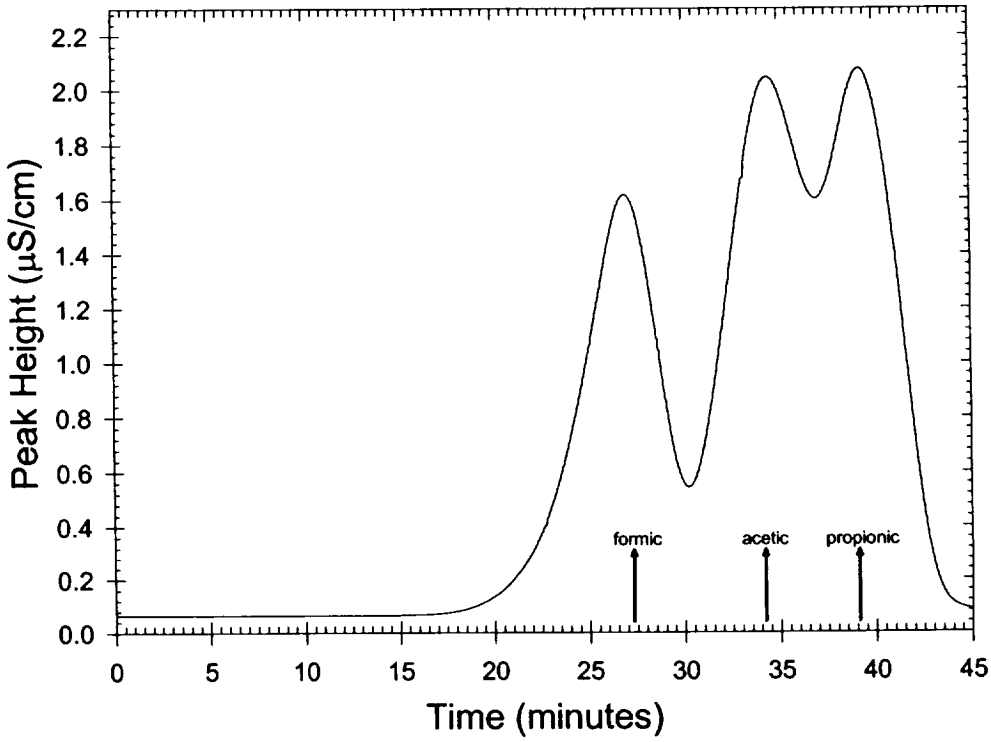

Figure 41. Chromatogram for 10 mg/L Each of Formic, Acetic, and Propionic Acids with Corresponding Single Acid Retention Times.

These data show that separation can be accomplished using either water or an acid solution as an eluent. Although this separation column showed potential for the determination of individual organic acids in a mixture, the effort would involve a complex transformation and accuracy would be low. Other separation media should be investigated for organic acid separation and quantitation. In particular, the FIA

configuration allows the use of a dilute acid solution to elute organic acids from such a column without the need to utilize special reagents. This provides added flexibility in the selection of the most appropriate chromatography media.

5.3 Alcohols - OAAM Prototype Analytical Performance.

Following the determination of the simple organic acids, the OAAM response to low molecular weight primary alcohols was characterized. This was accomplished by first processing the sample through sequential layers of immobilized alcohol oxidase and catalyst in the alcohol conversion loop. The alcohol oxidase and catalyst layer volumes were 0.44 and 0.19 cm^3, respectively. Flow injection peaks for concentrations between 50 and 400 µg/L are shown in Figure 42. The specific conductiometric responses for alcohols were lower than those for the corresponding organic acids on a per mole basis (with a molar conversion for methanol, ethanol, and propanol of 0.69, 0.77, and 0.81, respectively). This was expected, due to peak broadening during passage through the alcohol conversion loop. The peak widths at half maximum were also larger than for the equivalent organic acid and increased from 7.8 minutes for methanol to 9.2 minutes for propanol. Taken together, the analytical response for alcohols indicated a somewhat lower sensitivity than for the equivalent organic acid.

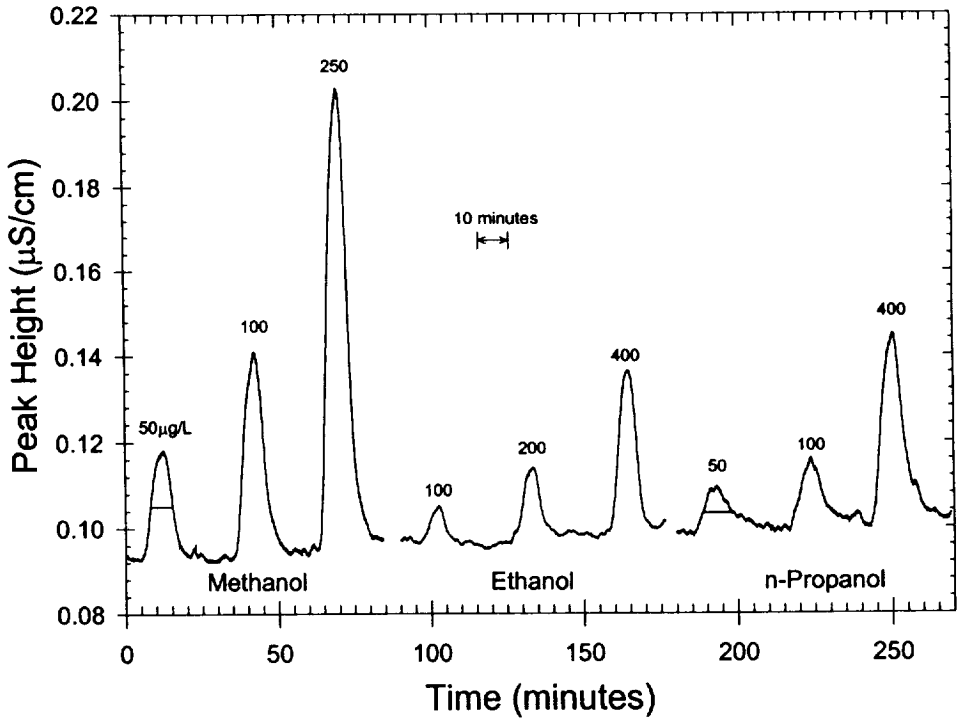

Figure 42. Flow Injection Peaks for Methanol, Ethanol and n-Propanol.

The analytical response of the OAAM to methanol was evaluated for concentrations between 25 and 10,000 μg/L. The baseline corrected conductiometric response varied between 0.011 and 2.75 μS/cm over this concentration range. This compares to a range of 0.0096 to 4.318 for formic acid, indicating significantly lower peak heights for equivalent sample concentrations. The response curve over this range for methanol is shown in Figure 43. The data were fit to a second order polynomial with an r^2 value of 0.9993, indicating an good fit. A comparison of the polynomial coefficients for formic acid and methanol reinforces the nearly equivalent but lower analytical response of methanol. The polynomial fit at lower concentrations between 25 and 1,000 μg/L is shown in Figure 44. These data fit the polynomial expression even better, with an r^2 value of 0.9999. Comparison of the two curves indicates a transition in conversion efficiency with a decided upward curvature at higher methanol concentrations. This may well have been due to a falling conversion efficiency as the methanol concentration increased. This explanation is plausible since the equilibrium specific conductance for formic acid (see Figure 26), the methanol oxidation product giving the specific conductance response, exhibited the least upward curvature with concentration of all the organic acids because it dissociates more readily than the other

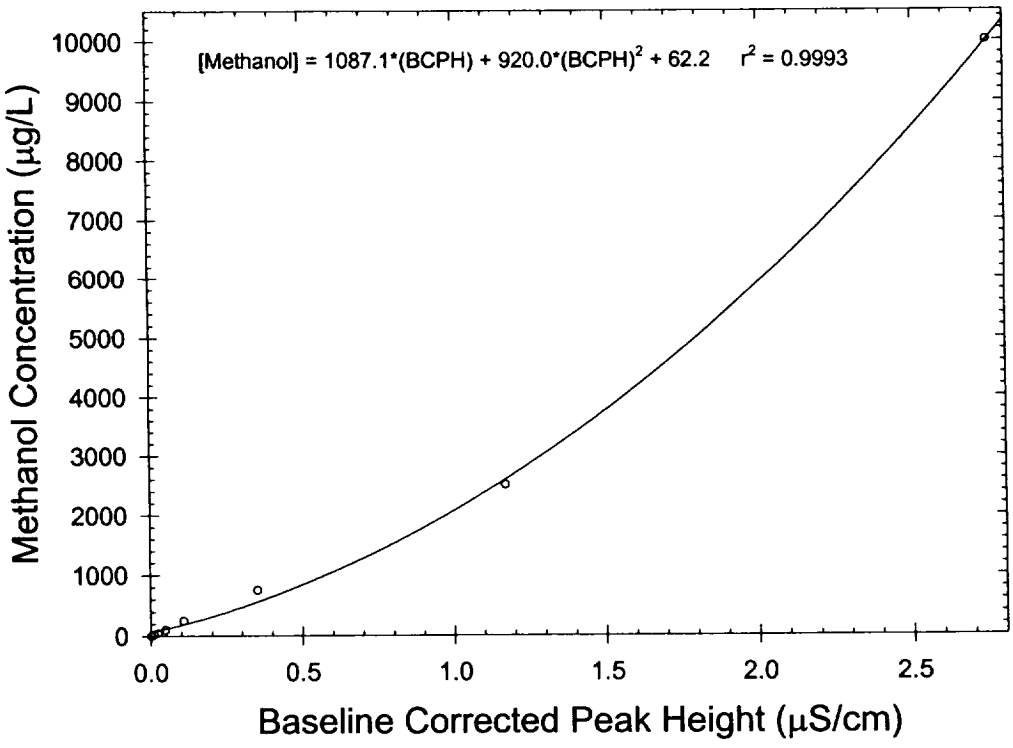

Figure 43. Methanol Response Curve.

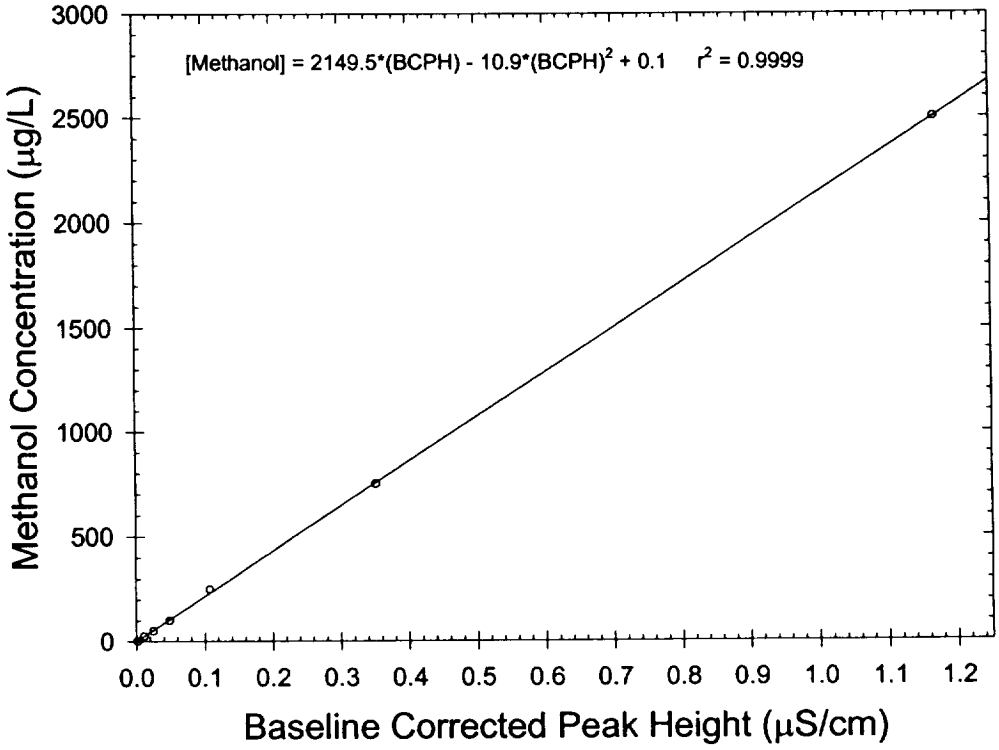

Figure 44. Methanol Low Level Response Curve.

organic acids. Based on these results, the detection limits for methanol are between 20 and 40 µg/L.

The analytical response of the OAAM to ethanol over the concentration range of 100 to 10,000 µg/L was determined next. The experimental results are shown in Figure 45. The baseline corrected specific conductance over this concentration range varied between 0.008 and 0.399 µS/cm, as compared to 0.033 and 2.394 for acetic acid. As with methanol, the values for ethanol are significantly lower than for equivalent concentrations of acetic acid, especially at higher concentrations. There are several factors that influence this response including slow conversion in the alcohol oxidase bed, and retention of the acetic acid product. The response curve made an excellent fit to a second order polynomial expression with an r^2 value of 0.9999. Figure 46 shows the analytical data for concentrations between 100 and 1,000 µg/L. Although the fit to a second order polynomial is quite good with an r^2 of 0.9995, the curve exhibits poor resolution at concentrations below 100 µg/L. The poor conversion of ethanol to acetic acid in combination with peak broadening and the high background limits the minimum

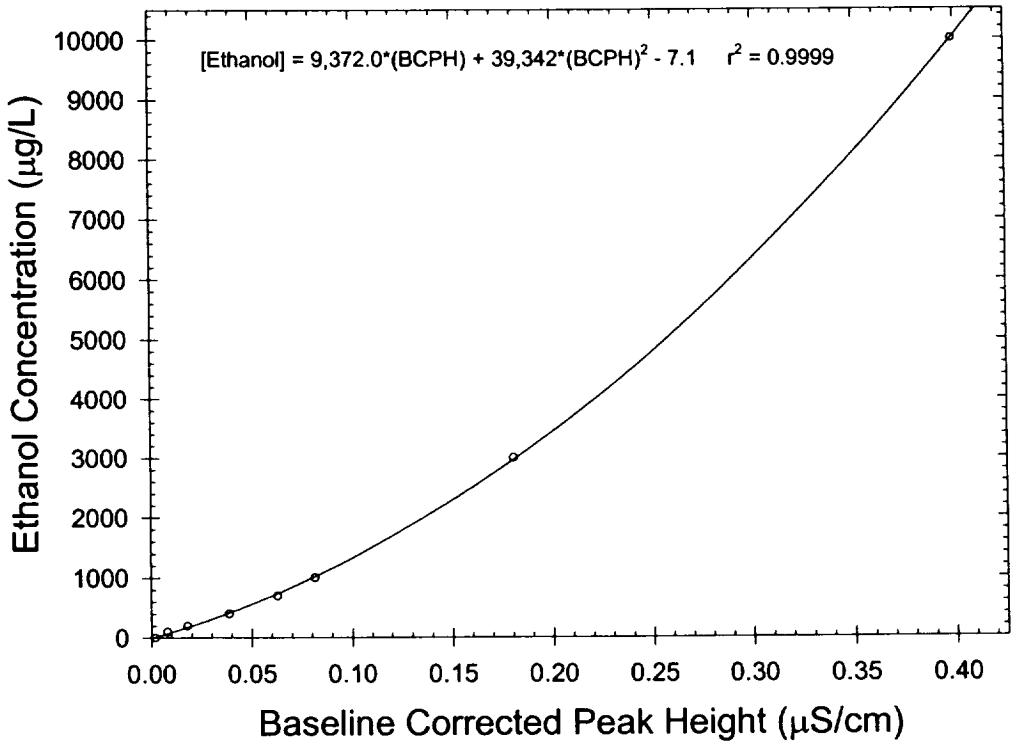

Figure 45. Ethanol Response Curve.

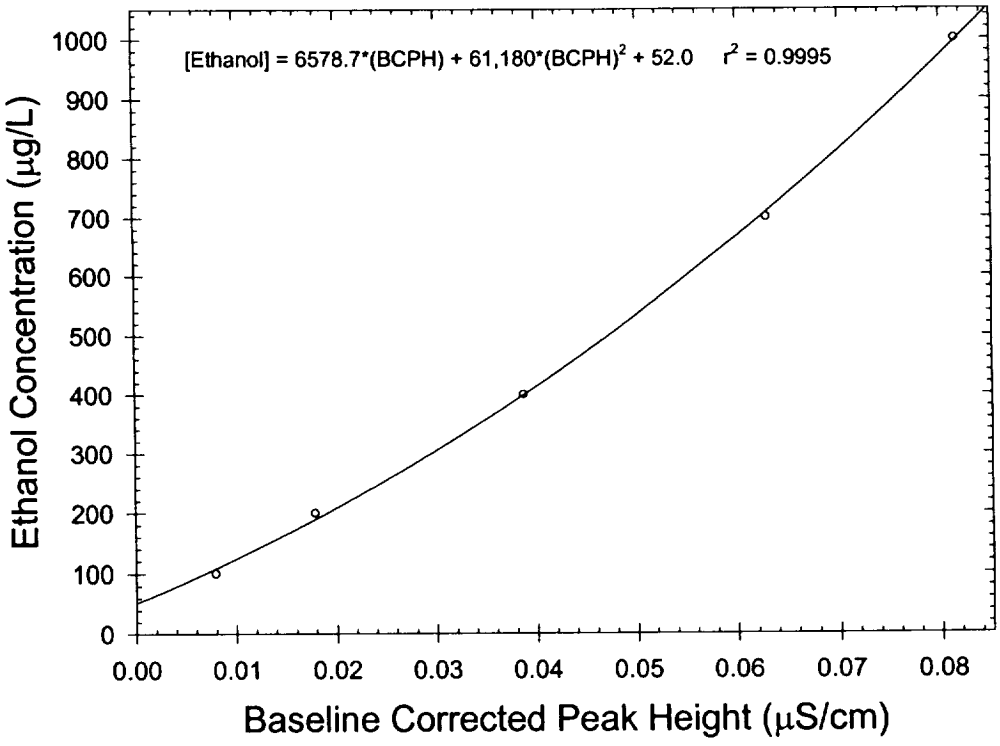

Figure 46. Ethanol Low Level Response Curve.

detectble levels for ethanol to approximately 100 μg/L. The relatively high detection limit for ethanol may well have been due to the fact that the alcohol oxidase bed had been installed within the OAAM for nearly 10 days, in which time it had processed over 5,000 mL of water. As a consequence of this extended use, the bed's performance may well have degraded.

The OAAM analytical response to n-propanol was also evaluated. The high level response curve for propanol concentrations between 25 and 10,000 μg/L is shown in Figure 47. The conductiometric response varied between 0.0065 and 0.389 μS/cm over that range, as compared to 0.0057 and 4.98 μS/cm for equivalent concentrations of propionic acid. As with ethanol, the data at high concentrations indicate some loss mechanism, either due to incomplete conversion or retention in the conversion loop. The least squares fit to a second order polynomial resulted in a good r^2 value of 0.9993. As with acetic acid, the plot curves upward, most likely for the same reasons. The low level response curve for concentrations between 25 and 1,000 μg/L is shown in Figure 48. The least squares fit for this curve provided a better r^2 value of 0.9998 than did the fit for the higher concentrations, yet at very low levels, insensitivity becomes evident. The detection limit was estimated at 25 to 50 μg/L.

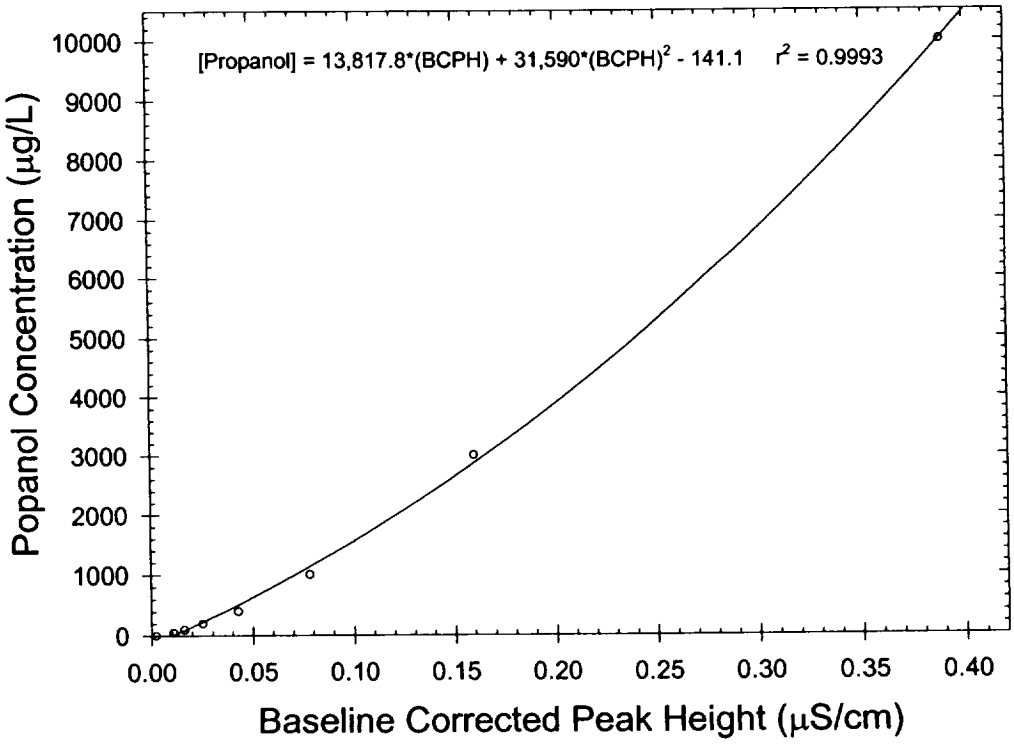

Figure 47. n-Propanol Response Curve.

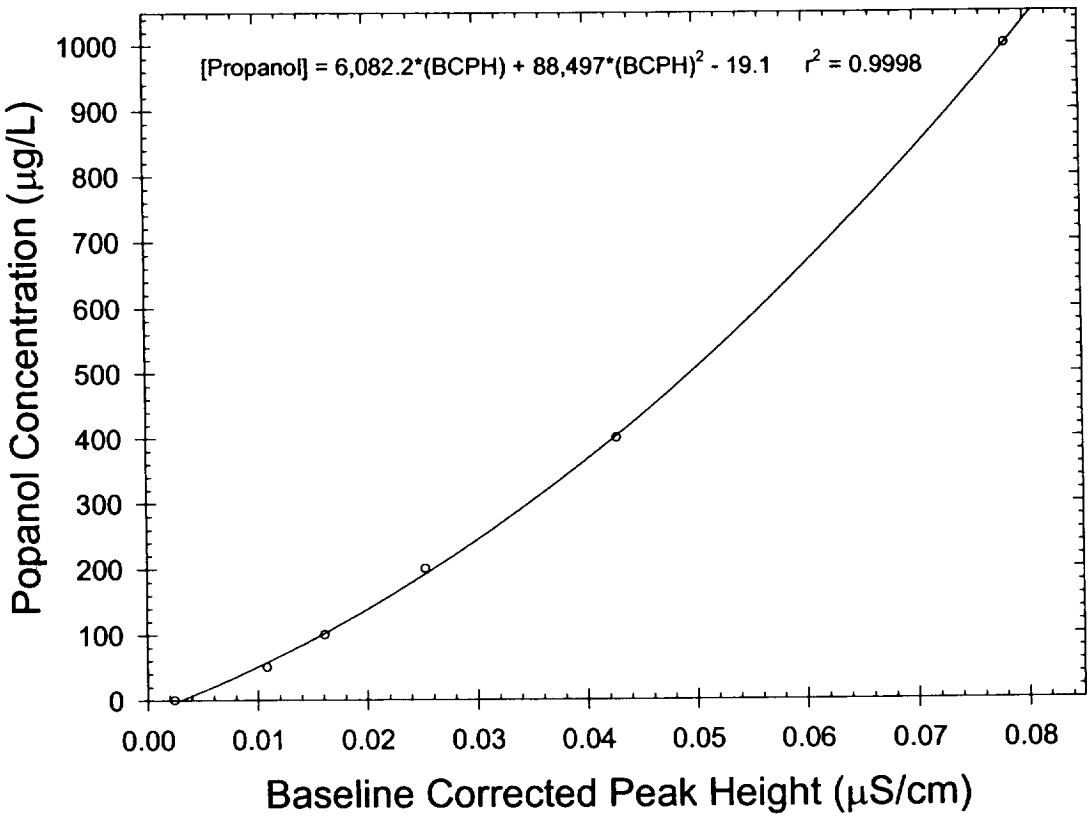

Figure 48. n-Propanol Low Level Response Curve.

6.0 CONCLUSIONS.

The Organic Acid and Alcohol Monitor (OAAM) development program has resulted in a computer controlled prototype analyzer capable of accurately quantitating organic acids and primary alcohols in water over a large dynamic range with high sensitivity and without the use of pre-formulated reagents, eluents, or other potentially hazardous chemicals. The OAAM operates as a Flow Injection Analyzer (FIA) utilizing membrane separation of organic acids from interfering ions followed by conductiometric quantitation. Formic, acetic, and propionic acids were accurately quantified at concentrations as low as 5 to 10 μg/L in under 20 minutes, and at concentrations as high as 10 to 20 mg/L in less than 30 minutes. Methanol, ethanol, and propanol were determined at concentrations as low as 20 to 100 μg/L, or as high as 10 mg/L in under 30 minutes following conversion to the corresponding organic acid by a combined biocatalytic and catalytic conversion process. New technologies developed during this program include solid phase acidification media capable of producing a pH of 1.60 to 1.75 in a flow through bed, a selective membrane for the removal of carbon dioxide from an acidified solution of volatile organic acids, a highly efficient membrane system for the transfer of volatile organic acids from an acidified carrier stream to a pure water stream, and an enzyme based process for the quantitative in-line oxidation of primary alcohols to organic acids without retention of intermediate or final oxidation products. These developments were incorporated into a versatile instrument requiring only water, power, and a carbon dioxide free purge gas. The OAAM was designed to allow the early diagnosis of underperforming or failing sub-systems within the Water Recovery System baselined for the International Space Station, while minimizing expendable supplies, hazardous materials, and reagent preparation and handling time. These goals were achieved through the development of several new technologies.

The quantitation of organic acids by specific conductance requires that the organic acids must be separated from other ionic contaminants. This was achieved by acidification of the sample to a pH of ~2, which protonates organic acids in solution converting them to the volatile form. This pH was achieved without the need for an acid solution by using a flow through Solid Phase Acidification Module (SPAM) containing two layers of solid phase media. The first layer consisted of $CaSO_4$ granules, a sparingly soluble salt, while the second layer was composed of strong acid ion exchange (IX) resin beads in the hydrogen ion form. The dissolution of $CaSO_4$ produces Ca^{2+} ions which upon contact with the IX resin is exchanged for two H^+ ions, resulting in a dilute sulfuric acid solution with a pH of 1.60 to 1.75. This pH was much

lower than that obtained by flow through beds of MoO_3 or other acidic oxides. Acidification of the sample volatilizes organic acids as well as other acid gases. Since carbon dioxide is the most common acid gas and also interfers with the determination of organic acids, its removal was necessitated. This was accomplished by a selective membrane process in the CO_2 Degassing Module (CDM). Numerous membranes at different temperatures were investigated. Polydimethylsiloxane (PDMS) membranes proved capable of facilitating CO_2 removal to a flowing CO_2 free gas without a significant loss of the volatile organic acids. The quantitation of organic acids requires their separation from the dilute sulfuric acid solution by a membrane process in which organic acids are transferred into the deionized water of the analytical stream. This is accomplished by a membrane process in the Organic Acid Transfer Module (OATM). In the OATM, due to the pH differences between the analytical and carrier streams, volatile organic acids diffuse down a concentration gradient across the membrane. Of the numerous membranes and transfer conditions evaluated for the OATM, a counter-flow arrangement of carrier and analytical streams separated by a hydrophobic microporous membrane operated at 50°C proved to be the best. Once in the analytical stream, the organic acids dissociate, and the increase in specific conductance is used to quantitate the organic acid concentration.

The quantitation of each organic acid in a mixture utilized a HPLC chromatographic column with the capability to separate organic acids prior to conductiometric detection. An anion exclusion resin proved capable of this task at high organic acid concentrations. This strongly sulfonated styrene divinylbenzene resin separates organic acids based on the affinity of the resin for the protonated and ionized organic acid forms under the separation conditions. The ionized form will have the least affinity due to the repulsion between the sulfonate anion moiety and the organic acid anion. Although protonated organic acids are still polar, they will exhibit affinity for the styrene divinylbenzene polymer resin, the degree of which will depend on the functionality and length of the carbon backbone. The separation of organic acids was evaluated at two locations in the OAAM. The first location was in the analytical stream immediately upstream of the conductivity detector. The second location was in the carrier stream immediately upstream of the CDM. In the analytical stream, separation of organic acids was poor and dependent on the total concentration of organic acids. The latter effect was attributed to the influence of total organic acid concentration on pH which controls the relative fraction of protonated and unprotonated organic acid species. Placement of the separation column in the carrier stream improved separation

conditions, since the pH of ~2 was constant and controlled. At high concentrations, a good correlation was achieved between the retention times of a single organic acid and the same organic acid in a mixture. Using this arrangement, formic, acetic, and propionic acids were sufficiently separated at high concentrations to deconvolute the overlapping peaks and quantitate individual organic acids. At lower concentrations, peak separation suffered and quantitation was less than optimal. These results indicated that, with additional work and optimized separation media, the probability of success for the quantitation of individual organic acids in a mixture is high.

The quantitation of alcohols utilizes the same components developed for the detection of organic acids, following oxidation steps which result in the formation of the corresponding organic acid. The oxidation of alcohols at ambient temperature in a process compatible with the analytical objectives required the development of an improved biocatalyst and an innovative heterogeneous catalyst that did not significantly adsorb the organic acid product. Immobilized alcohol oxidase which utilizes molecular oxygen to rapidly oxidize primary alcohols, forming the corresponding aldehyde and hydrogen peroxide, served as the biocatalyst. Since hydrogen peroxide will rapidly denature the enzyme due to the formation of free radicals, the biocatalyst carrier must contain means to destroy hydrogen peroxide and lengthen the enzyme life. This was accomplished using a novel impregnation method to apply 0.5% by weight of highly distributed platinum onto the diatomaceous earth support. Following the partial oxidation of the alcohol, a heterogeneous catalyst is employed to complete the oxidation to the corresponding organic acid. The major requirements for this catalyst to succeed in this analytical application were rapid oxidation kinetics and low adsorptivity of the organic acid product. Catalyst development resulted in unique mesocellular silica supports homogeneously impregnated with 1% by weight of platinum. This catalyst rapidly oxidized aldehydes, forming organic acids, and more importantly, did not adsorb any of the organic acid product due to the support's surface charge. Consequently, flow injection peaks were sharp and detection limits were low.

The prototype OAAM was computer interfaced using programs which control pump speeds, acquire data, and analyze data. The main sample analysis program requires operator inputs to identify the file name where analytical data is to be stored, the calibration curve that will be used to evaluate the analyte concentration, the matrix blank used to correct for the sample matrix effects, and the pump speeds used during analysis. When the program is initiated and the sample injected, conductivity data are recorded on the screen and written to the sample file. Data acquisition continues until

the program is stopped manually or automatically. Data is acquired until a pre-set time has been reach after sample injection, a pre-set time has been reached after a peak maximum has occurred, or when the operator has decided to truncate the run. When the run is terminated, raw data are recorded permanently in the sample file, the matrix corrected peak height and area are determined, and the analyte concentration is evaluated based upon the calibration file selected. A separate program allows the operator to retrieve preexisting calibration standards and create a calibration file. Based on this calibration file, the sample analysis program will determine the concentration of each peak from its baseline corrected specific conductance in terms of either peak height or peak area using a second order polynomial fit from the calibration file. The sample analysis program provides great flexibility in viewing, storing, and analyzing FIA data for the determination of organic acid and alcohol concentrations in water.

The computer controlled prototype OAAM developed during this program is capable of rapidly determing alcohols and organic acids in water with great sensitivity and a wide dynamic range. This enabling technology requires only power, water, a carbon dioxide purge gas, and solid phase reagent beds to operate. The elimination of reagent preparation, and the storage and handling of acid solutions enhances safety, simplifies operation, and significantly reduces time required by astronauts to perform analyses. These attributes fit well with a potential role as an analytical instrument that will characterize sub-system performance in the Water Recovery System (WRS) that has been baselined for the International Space Station. Full development of this technology will allow a real time evaluation of WRS performance and the diagnosis of incipient and evident sub-system malfunctions. This technology also has the potential for expansion to other analytes of interest including nitrate, nitrite, and ammonia with minor modification of the basic components.

The results from the OAAM development program have been reported in Life Support and Biosphere Science.[36] In addition, a synopsis of the operation principles used by the OAAM as well as some analytical results is presented on the UMPQUA Research Company webpage at http://www.urc.cc/oam.htm.

7.0 REFERENCES.

1. Carter, D.L.; Holder, D.W.; Alexandre, K.; Shaw; R.G.; and Hayase, J.K., Preliminary ECLSS Waste Water Model, SAE Technical Paper Series 951150, presented at the 21st International Conference on Environmental Systems, San Francisco, 1991.
2. Carter, D.L.; Cole, H.; Habercom, M.; Griffith, G.; and Slivon, L., Determination of Organic Carbon and Ionic Accountability of Various Waste and Product Water Derived from ECLSS Water Recovery Tests and Spacelab Humidity Condensate., SAE Technical Paper Series 921313, presented at the 22nd International Conference on Environmental Systems, Seattle, 1992.
3. Atwater, J.E., Thermodynamics of the Oxidation of Dissolved Organic Contaminants in Shuttle Orbiter Humidity Condensates, *J. Environ. Sci. Health*, A30 (4), 817-830, 1995.
4. Sauer, R.L.; Pierre, L.M.; Schultz, J.R.; Sinyak,Y.E.; Skuratov, V.M.; Protasov, N.N.; and Bobe, L.S., Chemical Analysis of Potable Water and Humidity Condensate: Phase One Final Results and Lessons Learned, SAE Technical Paper Series 1999-01-2028, presented at the 29th International Conference on Environmental Systems, Denver, 1999.
5. Carter, D.L.; and Bagdigian, R.M., Phase III Integrated Water Recovery Testing at MSFC: Single Loop Test Results and Lessons Learned, SAE Technical Paper Series 932048, presented at the 22nd International Conference on Environmental Systems, Colorado Springs, 1993.
6. Bagdigian, R.; Parker, D.S.; and O'Connor, E.W., ISS Water Reclamation System Design, SAE Technical Paper Series 1999-01-1950, presented at the 29th International Conference on Environmental Systems, Denver, 1999.
7. Atwater, J.E.; Akse, J.R.; DeHart, J.; and Wheeler, Jr., R.R., Fiber-Optic Chemiluminescent Biosensors for Monitoring Aqueous Alcohols and Other Water Quality Parameters, Final Report, NASA Contract NAS9-19021, 1994.
8. Akse, J.R. and Atwater, J.E., Advanced Catalytic Methods for the Destruction of Environmental Contaminants, Paper No. 95-LS-70, presented at AIAA Life Sciences and Space Medicine Conference '95, Houston, April 3-5, 1995.
9. Akse, J.R. and Jolly, C.D., Catalytic Oxidation for Treatment of ECLSS & PMMS Waste Streams, SAE Technical Paper Series No. 911539, *Regenerative Life Support Systems & Processes*, SP-873, SAE, Warrendale,. PA, 1991.
10. Atwater, J.E.; Akse, J.R.; DeHart, J.;. Wheeler, Jr, R.R; and Verostko, C.E., Fiber-Optic Chemiluminescent Biosensors for Monitoring Aqueous Alcohols and Other Water Quality Parameters, U.S. Patent 5,792, 621, 1998.
11. Thompson, J.O.; Akse, J.R.; Wheeler, Jr., R.R.; Wisely, M.T.; and Atwater, J.E., Microgravity Compatible Reagentless Instrumentation for Detection Of Dissolved Organic Acids in Potable Water, Final Report, NASA Contract NAS9-97095, 1997.
12. Jolly, C.D., Solid Phase Calibration Standards, U.S. Patent 5,559,035, 1996.
13. Jolly, C.D. and DeHart, J., A Reagentless Separator for Removal of Inorganic Carbon from Solution, Final Report Contract NAS8-38460, Marshall Space Flight Center, June 1990.

14. Jolly, C.D., Reagentless Separator for Removal of Acid Gases and their Hydrolysis Products from Solutions, U.S. Patent 5,244,478, September, 1993.
15. Jolly, C.D.; Schussel, L.J.; and Carter, L., Advanced Development of Immobilized Enzyme Reactors, *Regenerative Life Support: Systems & Processes*, Behrend, A.F., MacElroy, R.D., and Reysa, R.P., Eds., Society of Automotive Engineers, Warrendale, PA, 1991.
16. Jolly, C.D. and Schussel, L.J., Enzymatic Catalytic Beds for Oxidation of Alcohols, *NASA Tech Briefs,* May 1993.
17. Schussel, L.J. and Atwater, J.E., A Continuous Alcohol Oxidase Bioreactor for Regenerative Life Support, *Enzyme Microb.Technol.*, 18, 229-235, 1996.
18. Akse, J.R.; Atwater, J.E.; Thompson, J.O.; and Sauer, R. L., Reagentless Flow Injection Determination of Ammonia and Urea Using Membrane Separation and Solid Phase Basification, *Microchem. J.*, 59, 372-382, 1998.
19. Akse, J.R.; Atwater, J.E.; Thompson, J.O.; and Sauer, R. L., Ammonia Monitor, U.S. Patent 5,882,937, 1999.
20. Hunter, R.J., *Zeta Potential in Colloid Science Principles and Applications*, Academic Press, New York, 1981.
21. Adamson, A.W., *Physical Chemistry of Surfaces*, John Wiley and Sons, New York, 1976.
22. Stern, O., *Z. Elektrochem.*, 30, 508, 1924.
23. Laitinen, H., *Chemical Analysis*, McGraw-Hill Book Company, New York, 1960.
24. Lewis, J.A., Colloidal Processing of Ceramics, *J. Am. Cer. Soc.*, 83, 2341-2359, 2000.
25. Yang, P., D. Zhao, B.F. Chmelka, and G.D. Stucky, Triblock-Copolymer-Directed Syntheses of Large Pore Mesoporous Silica Fibers, *Chem. Mater.*, 10, 2033-2036, 1998.
26. Schmidt-Winkel, P., W. Lukens, Jr., P. Yang, D.I. Margolese, J.S. Lettow, J.Y. Ying, and G.D. Stucky, Microemulsion Templating of Siliceous Mesostructured Cellular Foams with Well-Defined Ultralarge Pores, *Chem. Mater.*, 12, 686-696, 2000.
27. Schmidt-Winkel, P., W.W. Lukens, Jr., D. Zhao, P. Yang, B.F. Chmelka, and G.D. Stucky, Mesocellular Siliceous Foams with Uniformly Sized Cells and Windows, *J. Am. Chem. Soc.*, 121, 254-255, 1999.
28. Shefelbine, T.A., M.E. Vigild, M.W. Matsen, D.A. Hajduk, M.A. Hillmyer, E.L. Cussler, and F.S. Bates, Core-Shell Gyroid Morphology in a Poly(isoprene-block-styrene-block-dimethylsiloxane) Triblock Copolymer, *J. Am. Chem. Soc.*, 121, 8457-8465, 1999.
29. Goldacker, T. and V. Abetz, Core-Shell Cylinders and Core-Shell Gyroid Morphologies via Blending of Lamellar ABC Triblock and BC Diblock Copolymers, *Macromolecules*, 32, 5165-5167, 1999.
30. Lettow, J.S., Y.J. Han, P. Schmidt-Winkel, P. Yang,, D. Zhao, G.D. Stucky, and J.Y. Ying, Hexagonal to Mesocellular Foam Phase Transition in Polymer-Templated Mesoporous Silicas, *Langmuir*, 16, 8291-8295, 2000.
31. Schmidt-Winkel, P., C.J. Glinka, and G.D. Stucky, Microemulsion Templates for Mesoporous Silica, *Langmuir*, 16, 356-361, 2000.

32. Zang, P., D. Zhao, D. Margolese, B.F. Chmelka, and G.D. Stucky, Generalized Sytheses of Large-Pore Mesoporous Metal Oxides with Semicrystalline Frameworks, *Nature*, 396, 152-155, 1998.
33. Zhao, D., Q. Huo, J. Feng, B.F. Chmelka, and G.D. Stucky, Nonionic Triblock and Star Diblock Copolymer and Oligomeric Surfactant Syntheses of Highly Ordered, Hydrothermally Stable, Mesoporous Silica Structures, *J. Am. Chem. Soc.*, 120, 6024-6036, 1998.
34. Cotton, F.A. and G. Wilkerson, Advanced Inorganic Chemistry: A Comprehensive Text, 4th Edition, John Wiley & Sons, New York, 1980.
35. Press, W.H., Flannery, B.P., Teukolsky, S.A., and Vetterling, W.T., *Numerical Recipes: The Art of Scientific Computing*, Cambridge, New York, 1986.
36. Akse, J.R., Atwater, J.E., and Holtsnider, J.T., Development of a Microgravity-Compatible Organic Acid and Alcohol Monitor (OOAM), *Life Support & Biosphere Science*, Vol. 8, pp. 55-63, 2001.

APPENDIX

PUBLICATION IN LIFE SUPPORT & BIOSPHERE SCIENCE

ENTITLED

"DEVELOPMENT OF A MICROGRAVITY-COMPATIBLE REAGENTLESS ORGANIC ACID AND ALCOHOL MONITOR (OAAM)"

Life Support & Biosphere Science, Vol. 8 pp. 55–63
Printed in the USA.

1069-9422/01 $20.00 + .00

DEVELOPMENT OF A MICROGRAVITY-COMPATIBLE REAGENTLESS ORGANIC ACID AND ALCOHOL MONITOR (OAAM)

JAMES R. AKSE, JAMES E. ATWATER, and JOHN T. HOLTSNIDER

UMPQUA Research Company, P.O. Box 609, Myrtle Creek, OR 97457

The development of a microgravity-compatible analyzer capable of quantifying organic acids in water is described. The analyzer employs "reagentless" solid phase acidification to convert organic acids to the volatile form followed by membrane separation and specific conductance detection to determine organic acids at concentrations between 0.005 and 40 mg/L. In the future, this technology will be extended to the detection of alcohols, which will be oxidized to form the corresponding organic acid and then determined using the same processes. An immobilized enzyme biocatalyst, alcohol oxidase, oxidizes alcohols to form an aldehyde. Oxidation to the corresponding organic acid is then completed over a heterogeneous catalyst. The combined organic acid and alcohol monitor (OAAM) will be utilized to determine levels of both analyte classes at various points within the water recovery system (WRS) baselined for the International Space Station (ISS). These data will improve water quality through enhanced process control, while allowing early diagnosis of potential problems.

Organic acids Analysis Alcohols Water recovery system

INTRODUCTION

The trace organic content of finished water aboard the International Space Station (ISS) is an important parameter that should be monitored to ensure crew health and to diagnose potential problems with the primary water recovery system (WRS). A significant fraction of the dissolved organic carbon in water produced by current physicochemical water reclamation technology consists of low molecular weight carboxylic acids, including: formic acid, acetic acid, and propionic acid. These low molecular weight organic acids occur in humidity condensate, urine distillate, and composite wastewaters aboard spacecraft (5,9,10,17). They are also produced as by-products from partial oxidation of methanol, ethanol, propanol, and related contaminants in the volatile removal assembly (VRA) catalytic oxidizer, a WRS component baselined for use aboard the ISS. The development of analytical instrumentation that can determine organic acids and alcohols on-line in real time will improve water quality through enhanced WRS process control, allow early diagnosis of potential problems, and thereby ensure crew health. The development of the organic acid component of a combined organic acid and alcohol monitor (OAAM) is presented in this article. Before describing the organic acid monitor development, the current WRS will be summarized, including potential areas of application of the OAAM.

The WRS removes contaminants from wastewater using the three primary physicochemical processes

Address correspondence to James R. Akse, Ph.D., UMPQUA Research Company, P.O. Box 609, Myrtle Creek, OR 97457. Tel: (541) 863-2653; Fax: (541) 863-7770; E-mail: akse@urcmail.net

shown in Figure 1 (8,11). Ionic contaminants such as organic acids and inorganic salts are removed by ion exchange (IX), while the majority of organic species are removed by adsorption on activated carbon. Both of these functions are performed within the multifiltration (MF) subsystem. Highly polar, low molecular weight organic contaminants such as alcohols are not removed by MF and therefore must be catalytically oxidized in the VRA (1,2,6,7). The oxidation of alcohols produces organic acids, which are removed by a posttreatment IX bed.

The current plans for analytical instrumentation for the WRS include an on-line process control water quality monitor (PCWQM) capable of determining pH and specific conductance. Additional off-line analytical capability is embodied in the crew health care system (CHeCS), which includes equipment and instruments to be operated by crew members for determining other water quality parameters, including total organic carbon (TOC). Under current operational strategy, a TOC value that is greater than 500 μg/L would indicate inadequate WRS performance, but would add little diagnostic information to indicate which processes are out of specification and require attention.

This situation can be improved upon significantly by the addition of the capability to detect and quantify dissolved alcohols and organic acids. The concentrations of organic acids and alcohols at the MF, VRA, and posttreatment IX bed outlets indicate the effectiveness of each process at eliminating or chemically modifying the contaminants. With reference to Figure 1, high TOC values in finished water may be due to a variety of circumstances. If the finished water's conductivity and organic acid concentrations are also high, then the MF beds have been exhausted. If conductivity is low, but dissolved alcohols are high, then a problem with VRA performance is suggested. If conductivity and dissolved alcohols are low, but organic acids are high, then exhaustion of the posttreatment IX bed is indicated. The addition of dissolved alcohol and organic acid monitoring capability provides an essential diagnostic tool for rapid remediation of inadequacies in water processor performance to ensure production of potable water capable of sustaining crew health.

A schematic of the organic acid and alcohol monitor (OAAM) is shown in Figure 2 (19). Samples flow through the OAAM by one of two flow paths, depending on whether alcohols or organic acids are being determined. When organic acids are determined, the sample flows directly into the solid phase acidification (SPA) module (14–16). Flow through this module lowers the pH by controlled dissolution of a sparingly soluble salt. pH control by this "reagentless" methodology is characterized by the dissolution kinetics and the lowest attainable pH value. At pH values attainable by flow through the SPA, the equilibrium speciation of weak organic acids and carbon dioxide is shifted to their undissociated volatile forms. Because CO_2 will interfere with the final determination of organic acid concentration, CO_2 is first selectively removed from the

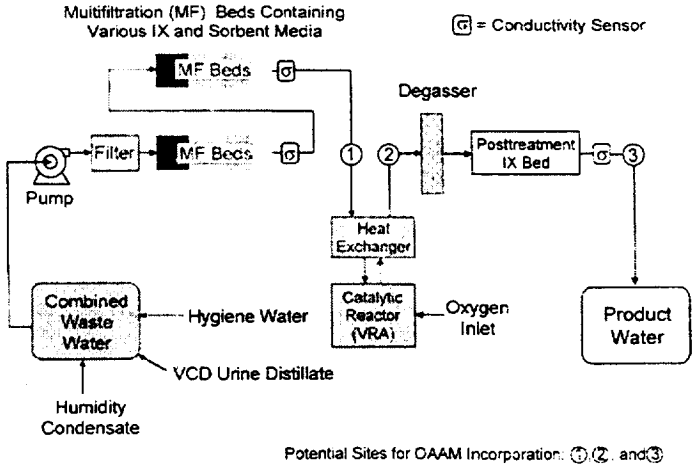

Figure 1. International Space Station water recovery system (WRS) schematic.

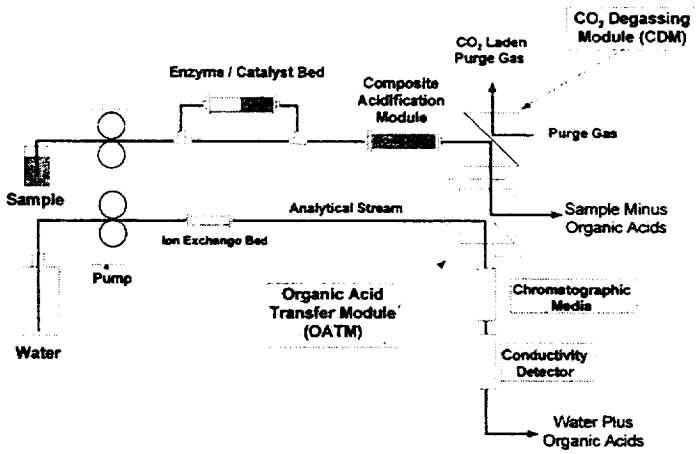

Figure 2. Organic acid and alcohol monitor (OAAM) schematic.

sample by flow through the CO_2 degassing module (CDM). The CDM uses a semipermeable membrane for CO_2 removal. The CO_2-free sample then flows through the organic acid transfer module (OATM). In the OATM, volatile organic acids are transferred to an analytical stream composed of deionized water. The transfer is accomplished using a stopped flow protocol that increases the concentration of organic acids in the analytical stream. The organic acid level is then determined based on the change in specific conductance of the stopped flow peak as it passes through the conductivity detector.

When alcohols are determined, oxidation to the corresponding organic acid must occur by passage through an ambient temperature oxidation reactor prior to entry into the SPA. The reaction scheme is shown in Figure 3. The first oxidation step is accomplished by a bed of immobilized alcohol oxidase, which catalyzes the oxidation of primary alcohols to the corresponding aldehydes in the presence of oxygen (12,13,18). Aldehydes are then oxidized to form the corresponding organic acid over a heterogeneous catalyst. Following completion of the two-step oxidation, alcohol concentrations are determined from the change in specific conductances that arise from transport of the corresponding organic acids into the analytical stream.

To date, a working stopped flow analyzer has been constructed from optimized components that is capable of reproducible quantitation of formic, acetic, and propionic acids at concentrations between 0.005 and 40 mg/L. In the future, this technology will be miniaturized and extended to the quantitation of methanol, ethanol, and *n*-propanol.

DEVELOPMENT OF THE ORGANIC ACID ANALYZER

The combination of solid phase pH control, membrane separation of volatile solution constituents, and conductiometric detection was adapted from other instrument designs developed for the determination of ammonia, nitrate, and urea in water (3,4). A first-generation OAAM was developed utilizing these components with the addition of a membrane-based CO_2 re-

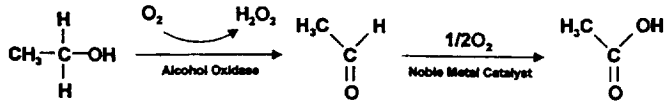

Figure 3. Oxidation of primary alcohols to form the corresponding organic acid.

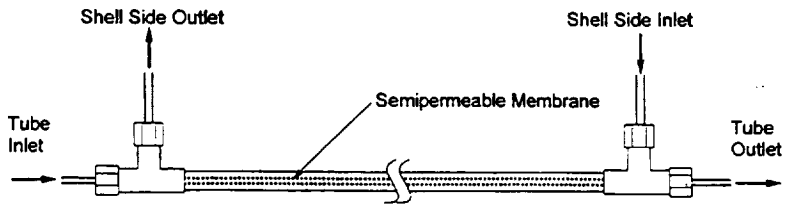

Figure 4. Tube-in-shell countercurrent gas transfer module.

moval process (19). The performance of this early OAAM was limited by poor sensitivity, slow response time, and the inability to discriminate individual organic acids within a mixture. Factors responsible for these performance limitations included the relatively high pH produced by the SPA, the slow removal rate for CO_2 in the presence of organic acids, and the low fractional transfer of organic acids from the sample into the analytical stream. New components were developed to overcome many of these limitations. These include: 1) a composite SPA module capable of lowering the pH of a flow-through stream to 1.75, allowing more efficient transfer of propionic, acetic, and formic acids; 2) a more efficient CDM, which completely removes CO_2 from samples after a contact time of 20 s; and 3) an OATM module with a threefold increase in the transfer rates for organic acids.

The improved SPA module consists of two sequential beds. The first bed contains calcium sulfate, a sparingly soluble salt with a K_{sp} of 9.61×10^{-6}. The second bed contains a strong acid ion exchange resin in the hydrogen ion form. Dissolution of calcium sulfate produces Ca^{2+} ions, which readily displace H^+ from the strong acid ion exchange resin. This composite SPA module produces an effluent pH of 1.75. At this pH, the fraction of volatile, protonated formic acid, the most dissociated organic acid, is 98%. There are two main attractions to use of a SPA module to control pH. The first is the absence of liquid reagents and the elimination of highly corrosive acid solutions. The second is the relatively low level of expendables required to achieve pH control. Assuming a sample flow rate of 0.6 ml/min and a stopped flow time of 10 min, over 100 samples can be analyzed using less than 2 g of calcium sulfate and 10 cm^3 of strong acid IX resin.

Four different membranes were evaluated for use in the CDM. All utilized the tube-in-shell countercurrent design shown in Figure 4. The CO_2-containing sample flows through the central hollow fiber membrane, while the CO_2-free purge gas flows in the opposite direction on the shell side of the CDM. Physical properties of the membranes are given in Table 1. These include: material, length and thickness of the membrane, the maximum diffusion distance for CO_2 to exit the sample, and the surface to volume ratio for the hollow fiber, which indicates the permeable area per unit volume of liquid within the exchange module.

The CDMs were challenged with a solution containing 20 mg/L of inorganic carbon as sodium bicarbonate, which upon acidification yields dissolved CO_2. The nitrogen purge gas flow rate was 26 cm^3/min. The total inorganic carbon (TIC) concentration in the solution was then monitored as a function of flow rate after acidification and passage through the CDM. The flow rates were varied between 0.2 and 2.0 ml/min. For the polyester- and polyimide-based CDMs very low CO_2 per-

Table 1. Various CDM Membrane Properties

CDM Material	CDM Length (cm)	Hollow Fiber Volume (cm^3)	Membrane Wall Thickness (μm)	Maximum Diffusion Distance (μm)	Surface Area/Volume Ratio (cm^2/cm^3)
Polyester	112	0.697	6.4	450	44.9
Polyimide	289	0.111	19	129	180.7
PTFE	500	4.47	52	500	37.5
PDMS	300	0.212	165	315	133.3

meation rates were found. Only 41.8% of the CO_2 was removed after 3.5 min in contact using the polyester membrane, while 37.1% was removed after a 0.6-min contact time with the polyimide membrane. The results for the PTFE and PDMS membranes are shown in Figure 5. At the lowest flow rate tested, 0.2 ml/min corresponding to a contact time of 22.35 min, the PTFE-based CDM removed 90% of the influent CO_2. As the flow rate increased, the fractional CO_2 removal declined rapidly to 50% at 0.7 ml/min. On the other hand, the PDMS membrane removed all CO_2 at flow rates up to 0.6 ml/min, corresponding to a contact time of 22 s. Importantly, the total organic carbon (TOC) retention at this flow rate for formic, acetic, and propionic acids was 94.8%, 97.8%, and 95.2%, respectively. Based on these results, the PDMS-based CDM was selected for incorporation into the OAAM.

The organic acid transfer module (OATM) utilizes a similar design to that of the CDM. In the OATM, the analytical stream is contained within the central microporous polypropylene hollow fiber membrane, while the sample flows through the shell side. The 2-m OATM consists of a central microporous polypropylene hollow fiber membrane with an external diameter of 355 μm and a wall thickness of 28 μm. The membrane surface porosity is 45%, with an average pore size of 0.05 μm, which corresponds to a bubble point of 12.1 atm. The surface to volume ratio for this hollow fiber membrane is 133.7 cm^2/cm^3 with a volume of 0.141 ml. The OATM provides sufficient sensitivity to quantitate organic acid concentrations down to 50 μg/L. Further improvements were made to lower the detection limit. Foremost among these changes was elevation of the OATM operating temperature to ~50°C. Figure 6 shows the transfer efficiency for formic acid as a function of the OATM temperature. Raising the operating temperature from 20°C to 50°C resulted in a threefold improvement in the formic acid transfer rate.

To achieve the highest sensitivity, the OAAM was operated as a stopped flow analyzer. Operated in this manner, sample continuously flows through the CDM and OATM at a flow rate of 0.6 ml/min, while the analytical stream flows through an IX bed, the OATM, and the conductivity detector at a flow rate of 0.4 ml/min. For an analysis, the analytical stream flow is stopped for a specified length of time and then restarted, resulting in a stopped flow conductivity peak at the conductivity detector. The continuous passage of the low pH sample through the OATM creates a volatile organic acid concentration gradient between the sample and analytical streams. Under these conditions, the concentration of organic acids in the analytical stream increases with time as volatile organic acids pass down the concentration gradient through the microporous polypropylene membrane and dissociate in the analytical stream. The organic acids become more concentrated in the analytical stream as contact time increases. To investigate this effect, the conductiometric responses for all three low molecular weight organic acids were determined versus different stopped flow times. These

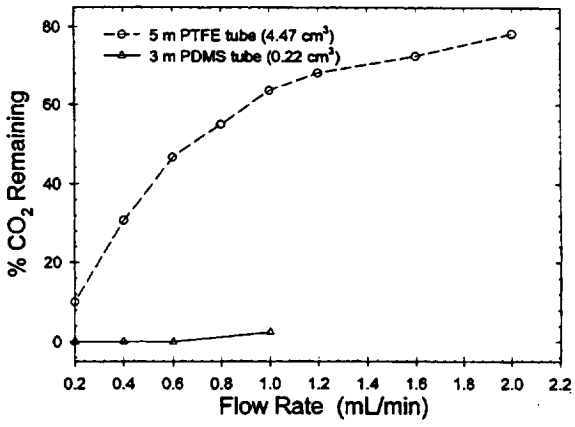

Figure 5. Carbon dioxide degassing for PTFE and PDMS membrane-based CDMs.

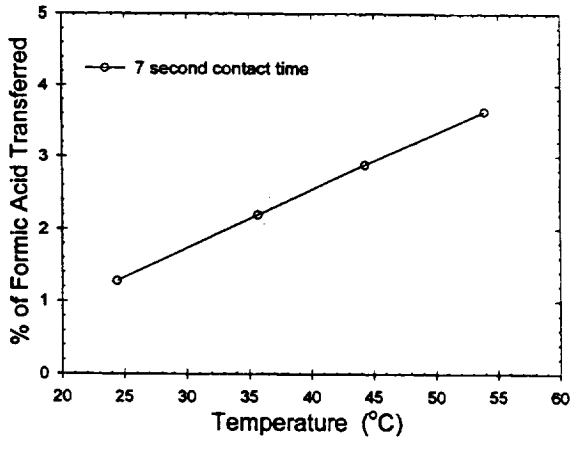

Figure 6. Effect of temperature on OATM transfer efficiency for formic acid.

results are shown in Figure 7. The conductiometric response for a given organic acid concentration increased with stopped flow time asymptotically approaching a limiting value. Although running longer stopped flow times results in great sensitivity, a stopped flow time of 10 min provides both a rapid response and sensitivity.

Preliminary evaluation of detection limits using the stopped flow configuration indicated that organic acids were adsorbed by stainless steel surfaces on the shell side of the OATM. This limited the sensitivity level to 20 μg/L. Evidently, the protective oxide layer on the stainless steel surface becomes positively charged at low pH and adsorbs negatively charged formate, acetate, and propionate ions. To correct this problem, stainless steel within the OATM was replaced by poly ether ether ketone (PEEK), resulting in a significant improvement in the lower limits of detection for organic acids.

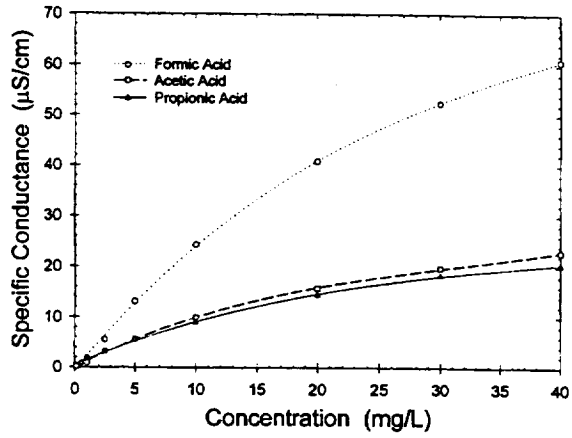

Figure 8. High-level organic acid calibration curves.

ANALYTICAL RESULTS

The OAAM performance was evaluated at the lower pH levels made possible by the improved SPA module, and in combination with the PDMS-based CDM, the PEEK housed OATM operated at 50°C and a 10-min stopped flow time. The flow rates for the sample and analytical streams were 0.6 and 0.4 mL/min, respectively, and the sample pH was 1.75. The conductiometric responses for formic, acetic, and propionic acid solutions with concentrations between 0.1 and 40 mg/L were determined. These results are shown in Figure 8. Analyzer response for concentrations between 0.005 and 1.20 mg/L are shown in Figure 9. Each curve was fit to a third-order polynomial, resulting in correlation coefficients of 0.9993 or better. The nonlinear analytical response occurs because only ionized organic acids are sensed, and as concentration is raised, a decreasing fraction of organic acids become ionized. The fraction ionized after transfer to an essentially deionized water (i.e., the analytical stream) can be determined using the acid dissociation constant, the total concentration of organic acid that was transferred, and assuming that the pH is controlled by the organic acid. Under these conditions,

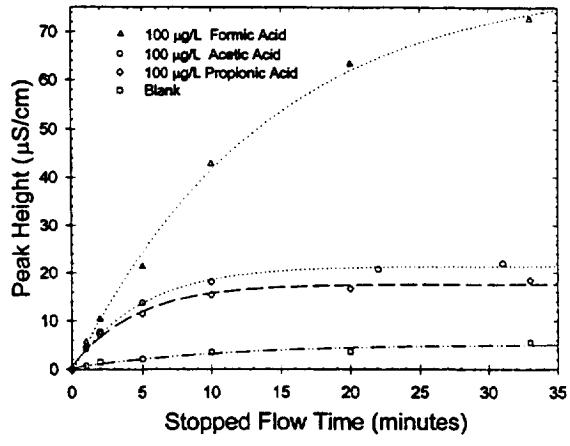

Figure 7. Conductiometric response versus stopped flow time for various organic acids.

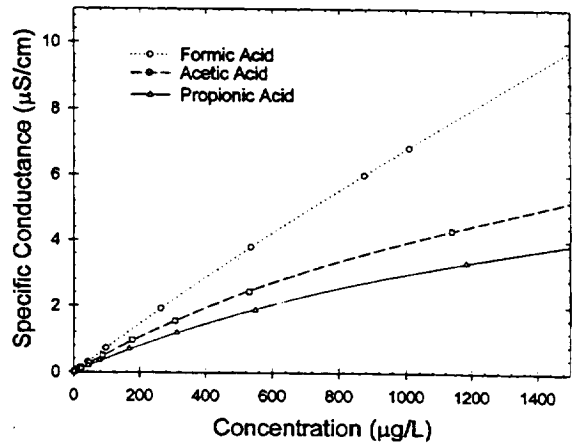

Figure 9. Low-level organic acid calibration curves.

the fraction ionized for formic acid decreases from 0.901 at 40 μg/L to 0.361 at 1 mg/L. Similarly for acetic and propionic acids, the fraction ionized decreases over the same concentration range from 0.627 to 0.150, and from 0.616 to 0.145, respectively. These data show that the relative conductiometric response will decrease as the concentration is raised. The detection limits for this version of the OAAM is on the order of 1–2 μg/L and will provide more than adequate sensitivity for the detection of organic acids at various points within the WRS. These detection limits were achieved without improvements in the conductivity detector sensitivity of 0.01 μS/cm.

The ability to separate organic acids in the analytical stream is a prerequisite for the quantitation of individual organic acids in mixtures. Preliminary work toward this end has yielded positive results. A 200 mg/L mixture of formic, acetic, and propionic acids in unbuffered water was fed to a column containing strong acid cation exchange resin in the hydrogen ion form. The absorbance of the effluent at 204 nm was then monitored versus time in a 1-cm path length cell. The resulting chromatogram, shown in Figure 10, indicates that the three primary organic acids are separable in a low ionic strength aqueous solution using water as the mobile phase. The mobilities roughly correlate with the relative fraction of each species that is ionized in water. For these preliminary experiments, high concentrations were used due to the low sensitivity of absorbance detection. These data demonstrate one method that can be utilized to discriminate between organic acids in mixtures.

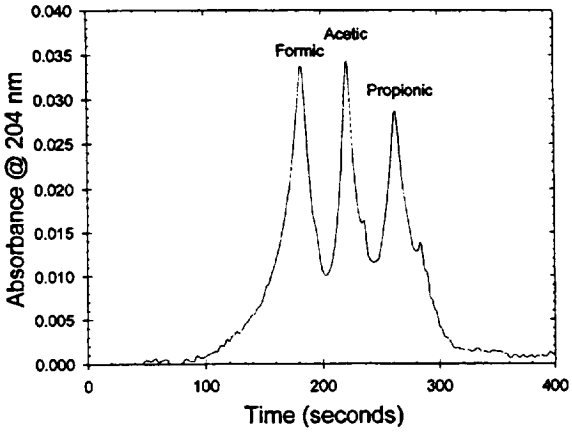

Figure 10. Separation of organic acids on strong acid exchange media in deionized water.

CONCLUSIONS

An organic acid analyzer has been developed that will accurately quantitate formic, acetic, and propionic acids in water over a large dynamic range with high sensitivity. The organic acid analyzer will determine organic acid concentrations between 0.005 and 40 mg/L in less than 15 min using a stopped flow methodology. The lower limit of detection for this instrument is 1–2 μg/L. These low detection limits represent significant improvements over previous analytical instruments, which used the same basic approach. These detection limits were attained by lowering the pH achievable with a SPA bed, raising the CO_2 degassing rates with an improved CDM membrane, and increasing the volatile organic acid transfer rate in the OATM by raising the operation temperature. Such sensitivity exceeds the analytical requirements based on the concentrations of organic acids or their precursors detected during WRS operation (10,11). Importantly, when the sensitivity requirements are relaxed, the response time decreases, as does the sample size, meaning that the SPA lifetime will increase. Integration of an alcohol oxidation reactor with the organic acid analyzer components for an OAAM will represent a significant advancement in analytical instrumentation for use aboard the ISS to monitor WRS performance, because expendables have been reduced to SPA bed consumables, the sample and analytical streams may be directly recycled to the WRS, and the analyzer is capable of semicontinuous on-line analysis. Such instrumentation will improve water quality through enhanced WRS process control, allow early diagnosis of potential problems, and thereby ensure crew health.

Additional work is required to develop a fully functional OAAM with the capability to autonomously determine organic acids and alcohols in spacecraft water. Most importantly, the detection of alcohols must be implemented by incorporating two ambient temperature oxidation reactors prior to entry into the SPA. The first reactor will employ an immobilized enzyme, alcohol oxidase, to oxidize alcohols to aldehydes. This will be followed by a second reactor containing a heterogeneous catalyst to complete the oxidation to the corresponding organic acid. To retain the high sensitivity and large dynamic range of the organic acid analyzer, the kinetics

for these oxidation reactions must be rapid, and following each conversion, the by-products must not be retained on the biocatalyst or catalyst supports.

Other work must be accomplished to bring OAAM concept to completion. First, a detection scheme for the separation of organic acids (and alcohols) in a mixed sample must be fully developed. This work has begun with the chromatographic separation of organic acids using water as the mobile phase. The OATM and CDM must be miniaturized to reduce mass, volume, and power, and improve performance. Miniaturized components will improve performance primarily by reducing sample size and decreasing response time. These components are well suited to microminiaturized lamination fabrication technology in which channels and reservoirs are produced using spin coating and photoresist technology, and membranes are applied as thin sheets between layers.

ACKNOWLEDGMENTS

This work was funded by NASA Grant NAG9-1081 under the Advanced Environmental Monitoring and Control (AEMC) program. The authors would like to thank Dr. Darrell Jan for his support.

James R. Akse, Ph.D., currently serves as Vice President and Director of Research and Development at UMPQUA Research Company. Dr. Akse completed his doctoral work in physical chemistry at Arizona State University, followed by postdoctoral training at the University of Wisconsin, Madison. Prior to joining UMPQUA, Dr. Akse was employed by North American Phillips, with responsibility for the development of novel and improved materials for electronics applications. During the past 10 years, he has provided leadership in the development of novel water reclamation systems using aqueous phase catalytic oxidation–reduction reactions, electrochemical methods, and has developed analytical instrumentation for ammonia and chlorine monitoring.

James E. Atwater, President of UMPQUA Research Company, is a Fellow of the American Institute of Chemists and the Royal Society of Chemistry. He has more than 20 years of research and development experience in the United States and Canada. His research interests include air purification, water reclamation, solid waste treatment, disinfection, sterilization, and the development of analytical instrumentation.

John T. Holtsnider is a senior research chemist who has worked at UMPQUA Research Company since 1989. He received his B.S. in Chemistry from the University of California at Santa Barbara in 1981. John has worked on the Organic Acid and Alcohol Monitor project since 1999. His main research interests lie in microfluidic device fabrication for use in miniaturized chemical systems.

REFERENCES

1. Akse, J. R.; Atwater, J. E. Advanced catalytic methods for the destruction of environmental contaminants. Paper No. 95-LS-70, presented at AIAA Life Sciences and Space Medicine Conference '95, Houston, April 3–5, 1995.
2. Akse, J. R.; Jolly, C.D. Catalytic oxidation for treatment of ECLSS & PMMS waste streams. SAE Technical Paper Series No. 911539. Regenerative Life Support Systems & Processes, SP-873. Warendale, PA: SAE; 1991.
3. Akse, J. R.; Atwater, J. E.; Thompson, J. O.; Sauer, R. L. Reagentless flow injection determination of ammonia and urea using membrane separation and solid phase basification. Microchem. J. 59:372–382; 1998.
4. Akse, J. R.; Atwater, J. E.; Thompson, J. O.; Sauer, R. L. Ammonia monitor. U.S. Patent 5,882,937, 1999.
5. Atwater, J. E. Thermodynamics of the oxidation of dissolved organic contaminants in shuttle Orbiter humidity condensates. J. Environ. Sci. Health A30(4):817–830; 1995.
6. Atwater, J. E.; Akse, J. R.; DeHart, J.; Wheeler, R. R., Jr. Fiber-optic chemiluminescent biosensors for monitoring aqueous alcohols and other water quality parameters. Final Report NASA Contract NAS9-19021, 1994.
7. Atwater, J. E.; Akse, J. R.; DeHart, J.; Wheeler, R. R., Jr.; Verostko, C. E. Fiber-optic chemiluminescent biosensors for monitoring aqueous alcohols and other water quality parameters. U.S. Patent 5,792, 621, 1998.
8. Bagdigian, R.; Parker, D. S.; O'Connor, E. W. ISS water reclamation system design. SAE Technical Paper Series 1999-01-1950, presented at the 29th International Conference on Environmental Systems, Denver, 1999.
9. Carter, D. L.; Holder, D. W.; Alexandre, K.; Shaw, R. G.; Hayase, J. K. Preliminary ECLSS waste water model. SAE Technical Paper Series 951150, presented at the 21st International Conference on Environmental Systems, San Francisco, 1991.
10. Carter, D. L.; Cole, H.; Habercom, M.; Griffith, G.; Slivon, L. Determination of organic carbon and ionic accountability of various waste and product water derived from ECLSS water recovery tests and Spacelab humidity condensate. SAE Technical Paper Series 921313, presented at the 22nd International Conference on Environmental Systems, Seattle, 1992.
11. Carter, D. L.; Bagdigian, R. M. Phase III integrated water recovery testing at MSFC: Single loop test results and lessons learned. SAE Technical Paper Series 932048, presented at the 22nd International Conference on Environmental Systems, Colorado Springs, 1993.
12. Jolly, C. D.; Schussel, L. J.; Carter, L. Advanced development of immobilized enzyme reactors. In: Behrend, A. F.; MacElroy, R. D.; Reysa, R. P., eds. Regenerative life support: Systems & processes. Warrendale, PA: Society of Automotive Engineers; 1991.

13. Jolly, C. D.; Schussel, L. J. Enzymatic catalytic beds for oxidation of alcohols. NASA Tech Briefs, May 1993.
14. Jolly, C. D. Solid phase calibration standards. U.S. Patent 5,559,035, 1996.
15. Jolly, C. D.; DeHart, J. A reagentless separator for removal of inorganic carbon from solution. Final Report Contract NAS8-38460, Marshall Space Flight Center, June 1990.
16. Jolly, C. D. Reagentless separator for removal of acid gases and their hydrolysis products from solutions. U.S. Patent 5,244,478, September, 1993.
17. Sauer, R. L.; Pierre, L. M.; Schultz, J. R.; Sinyak, Y. E.; Skuratov, V. M.; Protasov, N. N.; Bobe, L. S. Chemical analysis of potable water and humidity condensate: Phase one final results and lessons learned. SAE Technical Paper Series 1999-01-2028, presented at the 29th International Conference on Environmental Systems, Denver, 1999.
18. Schussel, L. J.; Atwater, J. E. A continuous alcohol oxidase bioreactor for regenerative life support. Enzyme Microbial Technol. 18:229–235; 1996.
19. Thompson, J. O.; Akse, J. R.; Wheeler, R. R., Jr.; Wisely, M. T.; Atwater, J. E. Microgravity compatible reagentless instrumentation for detection of dissolved organic acids in potable water. Final Report, NASA Contract NAS9-97095, 1997.